The Effect of Applied and Magnetic Fields on the Crystallisation of Hydrocarbons

A Thesis submitted for the degree of Doctor of Philosophy

by

Michele Melanie Rodericks

Centre of Environmental Research

Brunel University

September 2002

This thesis, which is submitted for consideration of an award of Doctor of Philosophy is a record of research work carried out under the supervision of Professor Sue Grimes in the Centre for Environmental Research, Brunel University and, except where due reference is made, has been presented for no other degree.

ABSTRACT

This thesis provides a background on the effects of applied and magnetic fields on crystallisation, and summarises the analytical techniques employed for characterisation and analysis.

The study of applied fields was carried out on the crystallisation of one main system -solid nonadecane. This was then studied further to establish the effects of a solvent and a mixed solid system on the crystallisation of nonadecane.

The systems studied were the crystallisations of: static and dynamic nonadecane, static and dynamic nonadecane in heptane, static and dynamic nonadecane and heneicosane, static and dynamic nonadecane and heneicosane in heptane and static and dynamic nonadecane and crude oil.

The results of these studies showed that the magnetic and applied fields can affect electrostatic forces in molecular solids. It also showed that even the weakest of these forces, Van der Waals forces are affected by applied and magnetic fields.

CONTENTS Page No

CHAPTER 1

CHAPTER 4

CHAPTER 5

To Andrew
and
For Mum, Dad and Sara

Acknowledgments

I must thank my Supervisors Professor Sue Grimes and Professor John Donaldson for their guidance and support during this PhD.
I would like to thank Dr AJ Chaudhary for his invaluable help and input into this thesis.

I would like to thank, Dr Douglas Dick, Dr Sue Woodisse, Professor Peter Hornsby, Professor John Binner, Professor Steve Watts, Dr Alan Beeby, Dr Alan Reynolds, and Maggie Westcott.
I would also like to thank Marina and Helen for their helpful discussions about crystallisation and magnetism.

I would like to say thank you to the wonderful friends I made whilst at Brunel, Bijita, Julie-Anne, Nicola and Rehana.

I would also like to thank my wonderful friends, Dawn, Louise, Molly and Navroop who now know more about magnets than they would have liked to!
I would like to thank Claire and Andy
To Mandy, thank you for all your help and support.

I would also like to thank Nanny and Daphne

I would like to thank my parents and my sister, for all their support throughout my studies, it is very much appreciated.

To Andrew, thank you.

1.0 LITERATURE REVIEW

1.1 Introduction

The work described in this thesis is concerned with the effects of applied fields on the deposition and crystallisation of hydrocarbon waxes. Hydrocarbon wax deposition occurs in oil production operations during the drilling process, and in supply pipelines, when crude oil contains heavier fractions that precipitate out and adhere to the sides of the oil well. This causes a problem because waxy scale on the side of the well reduces the amount of oil that can be extracted and the sides of the well have to be scraped every other day to allow the maximum amount of oil to be recovered. In this study, the effects of applied fields on the mechanism of the deposition is investigated for different configurations and strengths of applied magnetic fields and for different hydrocarbons in a light alkane. The aim of the work is to ascertain whether hydrocarbon crystallisation can be retarded in crude oil to allow the drilling and transport processes to continue uninterrupted.

This chapter provides the background literature for the work described in the thesis including information on the examination of the control of deposition and crystallisation of hydrocarbon waxes, magnetism, the effects of magnets and applied fields on charged species and the effects on molecular solids. This literature review is presented under the following headings

- The Behaviour of Waxes
- Magnetism
- General Effects of Magnetic Fields on Precipitation and Crystallisation
- Magnetic Fields and Molecular Solids

1.2 The Literature Review

1.2.1 The Behaviour of Waxes

Most of the literature published on the behaviour of waxes deals with (i) general discussions on the problems associated with wax deposition, (ii) compositions of waxes and crude oils, (iii) wax precipitation and crystallisation, (iv) predictions of the amount of hydrocarbon precipitation, (v) and crystal morphology. The literature is considered in this section under these headings.

1.2.1.1 Chemistry of Petroleum Waxes

This section is concerned with the general nature and properties of petroleum waxes. Crude oil samples vary in their components including hydrocarbon wax content

1.2.1.2 Polymer Structure

The simplest organic molecule is an alkane, for example CH_4. Paraffins are alkanes and consist of carbon atoms linked by single covalent bonds to hydrogen[1]. The simplest unbranched alkane that is solid at room temperature is nonadecane.

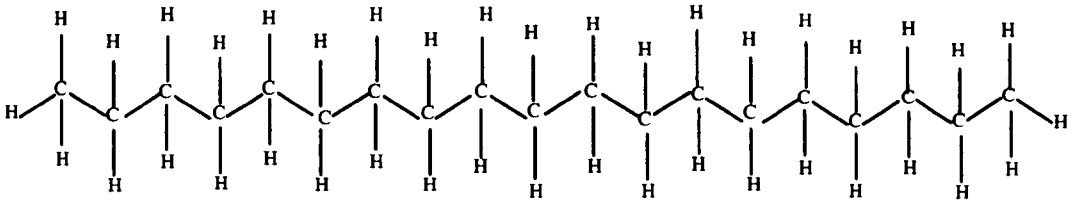

Figure 1.1. The Structure of Nonadecane a long chain alkane.

1.2.1.3 Molecular Interactions

Forces in nature are typically divided into primary bonding forces and secondary bonding forces. Primary bonding forces can be subdivided into ionic, metallic and covalent forces. In hydrocarbons the primary forces are intramolecular covalent bonds. The relevant secondary forces are intermolecular Van der Waals forces, which are weak electrostatic interactions. The strengths of these electrostatic interactions are dependent on the distances between interacting molecules. Van der Waals forces exist between neighbouring molecules in either the liquid or the solid sate and consist of interactions between induced dipoles and are of a relatively short range. This infers that many polymers are dependent on both the configuration and conformation, since both can affect the proximity of one chain relative to another. Therefore, for example, amorphous polypropylene is more flexible than crystalline polypropylene[2].

1.2.1.4 Molecular Solids

A definition of a molecular solid is that it is a collection of distinct molecules held in place only by secondary intermolecular bonding forces. A molecular solid is,

therefore, composed of individual molecules. They often have low melting points(below 100°C) because only a small amount of thermal motion is needed to overcome the relatively weak intermolecular forces holding the solid in place. The ease of breaking Van der Waals forces can also be seen in the ease of solubility in non-polar solvents and iodine I_2 for example is soluble in benzene (0.48 mol/l as compared to 0.00013mol/l in water). The physical properties of molecular solids are dependent on the strengths of their intermolecular forces. Some are as soft as paraffin and others are hard and brittle.

1.2.1.5 Crystallinity

Generally all monomeric and oligomeric substances can be crystallised. The crystallinity of a polymer is dependent on the monomer, i.e. the regularity (chemical, geometrical and spatial) of its macromolecular chains. The more regular the arrangement of the polymer the more likely it is to crystallise. For most polymers the monomers must be arranged in a head to tail sequence to form crystals[2].

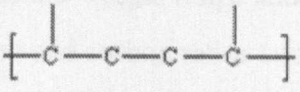

Figure 1.2. A skeletal diagram of a head to tail sequence

It is now recognised that ordered polymers may form plate shaped lamellar crystals, in which the chains are folded back upon themselves. This produces parallel chains perpendicular to the face of the crystals. A study of single crystal patterns obtained from microcrystalline waxes showed that they had bridged lamellar structure[2+3].

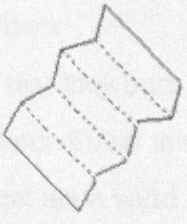

Figure 1.3 A Lamellar structure

This is reminiscent of low weight molecular polyethylene. A parallel study [4] of n-alkyl derivatives of benzene and cyclohexane show that naphthenic components adopt an oblique layer structure. This is different from rectangular layer packing

found in petroleum and branched alkanes[4].

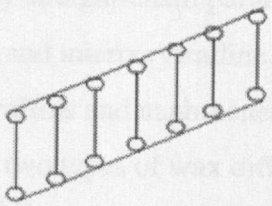

Figure 1.4. An oblique layer structure

1.2.1.6 Microcrystalline and Paraffinic Waxes

A study has been performed on petroleum waxes from sixteen crude oils using a variety of techniques [5]. Two types of petroleum wax were defined, microcrystalline and paraffinic. The microcrystalline waxes are aliphatic hydrocarbon compounds containing a substantial amount of branching and ring structures. They have a large molecular weight range and are gel like in appearance. The rings give rise to low hydrogen and carbon ratios compared to paraffinic waxes. Since there is, in the microcrystalline waxes, a lack of large scale crystallinity a distinct melting regime is not observed. FTIR (Infrared Microscopy) confirms that they consist of fifty five percent straight chained hydrocarbons. Paraffinic waxes consist of carbon chains, which have little to no branching. These waxes have a distinct melting regime and are able to crystallise at low temperatures. They also have a narrow molecular weight range[5].

1.2.1.7 Properties of Petroleum Waxes

An obvious property of alkanes is that they burn and are, in fact, extremely flammable. They have melting points of less than 360°C.

The solubility of waxes is dependent upon solid -solid transitions governed by the melting point. It has been seen that waxes which have melting points less than 47°C display multiple solid-solid transitions. If the wax has a melting point between 47 and 70°C it will have at least one solid- solid transition while waxes with melting points over 70°C do not display any solid -solid transitions[6].

1.2.1.8 Wax Crystallisation

Two types of wax are commonly encountered in crude oils *viz*, macrocrystalline waxes composed on mainly straight-chain paraffins (n-alkanes) of varying chain length (about C20 to C50) and microcrystalline or amorphous waxes also containing a high proportion of isoparaffins and naphthenes (cyclic alkanes) with carbon numbers C30-C60. These two types of wax differ in crystal growth and morphological properties [7-9]. The precipitation of wax which results from the decreased carrying capacity of the fluid solvent (a low molecular weight hydrocarbon) begins when the crude oil is cooled below its cloud point. The crystals formed may develop giving an interlocking 3D structure that can trap the solvating oil, which leads to increased viscosity, gelling and congealing. It is considered that wax precipitation and the low temperature flow properties of crude oils with as little as 2% precipitated wax depend not only on the n-paraffin content; but also the oil matrix, the properties of which are influenced significantly by the presence of aromatic molecules, polar compounds and asphaltenes[7].

1.2.1.9 Problems Associated with Wax Deposition

Numerous publications contain descriptions of the problems associated with deposition of wax in pipelines production equipment and fuels [10-16, 70]. There are two standard measurements of petroleum products, which can be used to determine whether petroleum products are likely to present congealing or deposition problems namely cloud point and pour point measurements. The cloud point is the temperature at which the first evidence of precipitated wax is seen in a system. The pour point is the temperature at which the system becomes a solid mass and because of the deposition of solids the transport of the crude oil becomes a problem [17, 18, 21]. The extent of the problem depends upon the pour point temperature - a crude oil with a pour point above 32°C will congeal under most working conditions while a crude oil with a pour point of 10°C is unlikely to present problems. It can be seen in the case of diesel fuels, that wax deposition can cause engine malfunction [19-24]. In the transportation of crude oil, in pipework however, the low ground temperatures will cause any waxes and asphaltenes present to precipitate out of solution. This will change the fluid flow characteristics of the crude oil from a simple or Newtonian fluid to a non Newtonian fluid [25].

1.2.1.10 Compositions of Waxes and Crude Oils

Crude oils are composed mainly of hydrocarbons but can also contain polar substances such as resins, which are polar fractions and asphaltenes which act as indigenous pour point depressants. An asphaltene is a high molecular weight aggregate occurring in bitumen. [64]. It has a low hydrogen content and a high viscosity in heavy oils is a function of the size and abundance of the asphaltene molecule present [26].

The majority of crude oils contain substantial amounts of hydrocarbon waxes. The composition of the waxes can range from low molecular weight (C20- C60) n-alkanes to solids containing high proportions of high molecular weight branched chain and cyclic hydrocarbons. The n-alkane waxes are generally crystalline depositing as large plates or needles while the branched chain and cyclic hydrocarbon waxes are microcrystalline or amorphous.

The composition of waxes has been discussed by several authors [27], as has the effect of wax composition in response to pour point depressants [27, 66]. Methods used to characterise waxes include Differential Scanning Calorimetry(DSC)[10], cloud point measurement, (even though this is a complicated function of the total wax composition) [10], polarisation microscopy [10], and viscometry [10].

A series of North Sea crude oils has been characterised by determining their wax crystallisation and dissolution temperatures by polarisation microscopy, differential scanning calorimetry and viscometry. The data from polarisation microscopy were said to give the best value for the temperature of the onset of wax deposition on cold surfaces. Activation energies of viscous flow in the Newtonian range for the crude oils were calculated from viscosity data. Light condensates were found to have activation energies of less than 10 kJ/mol, close to those for pure n-alkanes, whereas a highly biodegraded heavy oil had an activation energy of nearly 40 k/mol. There appears to be a correlation between wax precipitation and apparent viscosity and the thermal history of the crude oil. The latter dependence is thought to be due to the presence of indigenous pour point depressants, that from a melt at a temperature of about 80°C and can be built into the wax crystals as they deposit, hence modifying their morphology and surface characteristics. If an oil is heated to lower temperatures, however, the low molecular weight waxes are dissolved preferentially and the indigenous pour point depressants do not build into the precipitating waxes

[10]. Similar effects on wax crystallisation can be achieved in the presence of synthetic pour point depressants (flow improvers, including poly(alkylmethacrylate)-ethylvinylacetate copolymers) [36].

Cloud and pour point measurements have been used to study the composition of waxes in binary n-alkane mixtures [7+40]. N-alkanes crystallise from solutions of their binary mixtures as single n-alkanes and as solid solutions. As the difference in molecular weight of the two n-alkanes increases single phase n-alkane crystallisation predominates.

1.2.1.11 The Role of Pour Point Depressors

In some circumstances the problems of wax deposition can be overcome by addition of crystal growth modifiers (pour point depressants) [28-39, 64]. The purpose of treating crude oils having high pour points[69] with a pour point depressant chemical is to reduce the temperature of congealing and the viscosity of the crude oil. A great deal of research has been undertaken to improve the effectiveness of pour point depressants and to understand the mechanism of their operation [26, 27, 30, 33, 34] and it has been suggested that pour point depression is a function of morphology [36], crystal structure, and crystal growth.

Flow improvers are said to change the morphology of the crystals to thin needles or prisms, which, are not consistent with gelling. The mechanism of pour point depression has been discussed [27, 30]. There are many types of crude oil, some which respond to pour point depressants and others, which do not. The interaction between the wax and the additive is poorly understood. It is therefore difficult to ascertain which additive should be used in specific cases. In one of the studies carried out, twelve crude oils were isolated and it was found that the pour point phenomena is a complex chemical event influenced by the amount of saturates and the chemical composition of the crude oil. Waxes, which precipitate at a temperature above the congealing temperature, contain mainly asphaltenes. Such waxes also contain higher molecular weight species than waxes, which congeal at a lower temperature. Asphaltenes appear to play an important role in the precipitation process. Some waxes are susceptible to chemical additives that interfere with the congealing mechanism. The different high pour point crude oils have differing wax precipitation temperature limits that are associated with the wax-asphaltene ratios.

The maximum precipitation attainable with each crude oil is probably a function of the precipitation temperature, so that asphaltenes are no longer associated with the waxes. A pour point depressant is therefore a chemical which can effectively prevent the formation of a three dimensional wax network.

1.2.1.12 Crystallisation Mechanisms and the Ability to Predict Crystallisation and Deposition

Fundamental issues on crystallisation of waxes have been discussed in a number of papers [40-46, 58-61]. Early work on wax crystallisation [10] suggested that paraffin waxes consisted mainly of n-alkanes with small percentages of branched chain alkanes and cyclic hydrocarbons. Solid n- alkanes with C numbers from 21 to 36 have been reported to show transition points to plastic forms a few degrees below their melting points. The melting points show a linear increase with C number but the relationship with transition temperature shows some anomalies. Branched chain and cyclic hydrocarbons can be precipitated from solution as micro-crystals which are characterised by high plasticity and which, depend on the type of hydrocarbon precipitated and on the ratios of the different hydrocarbons co-deposited in the microcrystalline wax. In any paraffin system, the highest melting n-alkane should be the first to precipitate and this will be followed by deposition of the lower melting components on top of the solid material already formed to give a heterogeneous wax which should have the lower temperature melting hydrocarbons nearer the surface. When two n-alkanes of similar chain length, e.g. C21 and C23, are crystallised from solution they give rise to a continuous series of solid solution waxes [16] and mathematical models have been devised to describe solid solutions of n-alkanes.

N-alkane crystals are thin truncated rhomboids [28] because they show rapid growth in the ab plane and slow growth in c direction. The 3-dimensional interchain molecular bonding energies have been calculated and show the expected much stronger lateral bonding compared with the vertical direction. The nature of the solvent has been shown to have an effect on the nature of the deposited waxes [65]. Although rhombic plates are deposited from both m-xylene and n-heptane solutions, the plates from xylene are thicker and have a different growth rate [28]. Data for crystal growth rates for n-dotriacontane in m-xylene have been reported, and

calculations of the surface roughness of n-dotriacontane from n-heptane and m-xylene have been made. These calculations suggest that differences arise from solvent effects rather than from differences in growth mechanisms.

A number of papers have described studies on the thermal effects of different types of wax [51-54, 77-82], crude oils [50-56, 62, 76] synthetic oils [68] and other petroleum products [57, 58, 67]. In a recent paper, Ronningsen and co-workers [7] report on the characterisation of wax precipitation from crude oils by using differential scanning calorimetry (DSC) to measure glass transition, wax precipitation, wax dissolution temperatures and transition enthalpies. The correlation with wax content was good for wax precipitation and dissolution temperatures but poor for glass transition temperatures. The latter showing better correlation with the concentration of the light components in the oil matrix. Average wax transition enthalpies for precipitation and dissolution were calculated from a combination of DSC and pulsed NMR data.

Work has been carried out to show the effect of growth environment and crystal structure on the crystallisation of n-alkanes. This work provided evidence for the active role played by the solvent.

Saturation temperatures are related to both the alkane structure and molecular length for single n-alkanes. For $C_{20}H_{42}$ and $C_{22}H_{46}$ a clear pattern was established with the reduction in saturation temperatures being related to the formation of solid -solution phase mixing [46].

1.2.1.13 Prediction of Amount of Hydrocarbon Precipitation

Methods of estimating the wax content of crude oils have been discussed [47, 72-75]. Thermodynamic models predicting the onset of crystallisation and the equilibrium amounts of wax precipitated have been based on regular solution theory [47, 49, 54, 73] and polymer solution theory [48]. Models that assume that all the components in a crude oil are capable of precipitating as part of the wax phase tend to over estimate both the amount of wax precipitated and the cloud point temperature [10, 62, 63, 74]. Since the major component of the wax is likely to be formed by the crystallisation of long chain (greater than 6 C- atoms) n-alkanes, only molecules that are compatible with the build up, of solid hydrocarbon crystal molecules will be easily incorporated in the wax. This

would eliminate molecules of branched chain and cyclic hydrocarbon and aromatics as major components of the crystallised hydrocarbon phase. Very little work has been done on the specification of the phases[76] present in wax precipitates and for this reason empirical estimates have been made of the amounts of each type of hydrocarbon present in waxes typically from C7 to C80.

A model has been developed for predicting the amount of wax deposited and the cloud point temperature taking account of the fact that not all components of a crude oil will be capable of inclusion in the solid deposit [71]. The model , which is said to give good agreement between experimental and the calculated parameters, is based on a cubic equation of state and the assumption that the wax forming characteristics of hydrocarbons decrease with their C number. Attempts have been made to relate wax formation temperatures to cloud points or freezing points in diesel fuels [21].

A thermodynamic model has been developed for predicting n- alkane crystallisation and the composition of deposited waxes in diesel fuels, which normally contain C10-C25 components.

Studies on the crystallisation of n-alkanes have suggested that the crystals are deposited in very thin diamond shape plates consisting of layer upon layer of n-alkane molecules. In each layer the n-alkane molecules are stacked side by side with their long axis parallel to the crystallographic c-axis - the vertical axis of the crystal. Stacking faults appear in the crystals because the n-alkane molecules do not line up properly. The effect of these faults is that the crystals are built up of shallow spirals, which can be seen in electron microscopic studies. It has also been suggested that the growth mechanism of packing n-alkane molecules into a crystal leads to the formation of more discrete crystallites being deposited from mixtures of n-alkanes than from single n-alkanes.

Differential scanning calorimetry has been used to identify phase changes in waxes [7] and to measure glass transition temperatures in waxes from North sea crude oils [7]. The glass transition temperatures were found to be in the range -128.5 to -81.5°C and unlike the precipitation and dissolution temperatures did not appear to be correlated with composition. Dissolution temperatures were usually found to be approximately 13°C higher than the precipitation temperatures.

1.2.2 Magnetism

A magnet is a material, which displays a magnetic polarisation either naturally or upon exposure to a magnetic field and can then exert a strong force between it and another permanent magnet (or iron-containing material). In any atom, a positive nucleus is surrounded by negative electrons, and the overall angular momentum is constant. An atom can, therefore be depicted as a small magnet and is described as exhibiting polarity. In general, the greater the alignment of the molecular magnets inside a magnetic material, the stronger the magnetic effect. A material reaches magnetic saturation once all its molecular magnets are aligned and no further increase of its resultant magnetic effect is possible.

Magnetic field strength is measured in terms of Magnetic Flux, which is considered to be the number of magnetic lines emanating from a magnetic substance. Magnetic Flux Density is the amount of flux cutting a small area normal to the direction of the flux and is readily determined by:

$$\text{Magnetic Flux Density, } B = \frac{\text{Magnetic Flux}}{\text{Area of field}}$$

A simple method of classifying magnetic materials is in terms of their magnetic hardness, i.e. hard and soft magnetic materials. The former describes materials which retain their magnetism fairly well after being magnetised, with only a small number of molecular magnets reverting to the random orientations once the magnetising force has been removed. The latter term describes materials, which lose most of their magnetism once the magnetising force has been removed. This category includes the majority of the molecular magnets, which are easily aligned by the applied magnetising force, but readily assume their disorientated and random state in the absence of an applied field. All materials are affected by magnetic fields via induced field (diamagnetic,) interactions. A substance in which atoms and molecules have a zero magnetic moment, is characterised by negative susceptibility.

Paramagnetism, is where the unpaired electrons may be orientated at random on some of the atoms. When the unpaired electrons are aligned so as to be parallel this gives rise to ferromagnetism and a net magnetic moment. If the unpaired electrons are aligned as to be antiparallel this gives rise to a zero overall magnetic moment and antiferromagnetic behaviour. If the alignment of magnetic spin is antiparallel,

but with unequal numbers in the two orientations, there is a net magnetic moment and the material shows ferromagnetic behaviour. [83].

1.2.2.1 Classification of Magnetic Materials

The types of magnetic field used in this work were (1) Permanent magnetic fields, (2) Electromagnetic fields and (3) pulsed magnetic fields and are described in the following sections.

1.2.2.2 Permanent Magnetic Fields

Permanent magnets are possible because magnetism exhibits the phenomenon of hysteresis: when the magnetising force applied to a body is changed and then restored to its original value, the resulting magnetisation of the body does not return to its original condition. A magnetising force (H) is applied to the material and induces a magnetic field (B) to the material.

The classification of permanent magnetic materials can be divided into six categories: (i) Alnico (Fe-Co-Ni-Al), (ii) Ferrites, (iii) Steels, (iv) Precipitation-hardening alloys, (v) Cobalt-rare earth alloys and iron earth alloys, and (vi) Miscellaneous alloys. The range of different permanent-magnetic alloys in each of the above categories makes good provision for an adequate selection of material for a particular application. For the work undertaken in this study the permanent magnetic materials used were ferrites. The stronger, permanent field Iontechnica magnets used were ferrite based.

1.2.2.3 Electromagnetic Fields

An electromagnetic field is produced using a solenoid, which is essentially a wire with current passing through it that is wrapped into a coil. The magnetic field of the individual turns in the coil adds up to give the overall magnetic field of the solenoid. Inside the solenoid, the lines of magnetic flux are closely packed straight and equidistant. Outside the solenoid the lines of magnetic flux open out and then close in a long loop. The magnetic flux density inside the solenoid is thus much greater than on the outside. Furthermore, the internal magnetic field is evenly distributed; and uniform. The end of the solenoid from which the lines of magnetic flux emanate is the north pole (as in the case of a bar magnet) and the end where they re-enter is the south pole. The north and south poles can be readily determined by the clock rule:

If the current flows throughout the solenoid in a clockwise direction, one sees its south pole. If the current flows in a counter-clockwise direction one sees its north pole.

A current carrying solenoid produces a magnetic flux in the same way as a permanent magnet. The magnetic flux of a solenoid can be considerably increased by the insertion of a ferromagnetic core, without having to increase the number of turns on the coil or the current going through it. The reason for this increased magnetic flux is the alignment of the molecular magnets of the core material due to the magnetic field of the solenoid. The molecular magnets assist the solenoid magnetic field and by the correct choice of a suitable core material it is possible to increase the magnetic flux many times over [84].

1.2.2.4 Pulsed Magnetic Fields

Transducers produce complex pulsed electromagnetic waveforms, which can be fed to a ferrite core. This signal is propagated in both an upstream and downstream direction. The version of this unit type used in the present studies was a Hydroflow HS38 pulsed magnet (Supplied by Hydropath) and uses a 5V supply. The sample must be placed in the centre of the magnet to allow propagation of the generated signal into the fluid medium. The frequency of oscillation is between 100 to 160 kHz and a typical waveform is shown in Figure. 1.6.

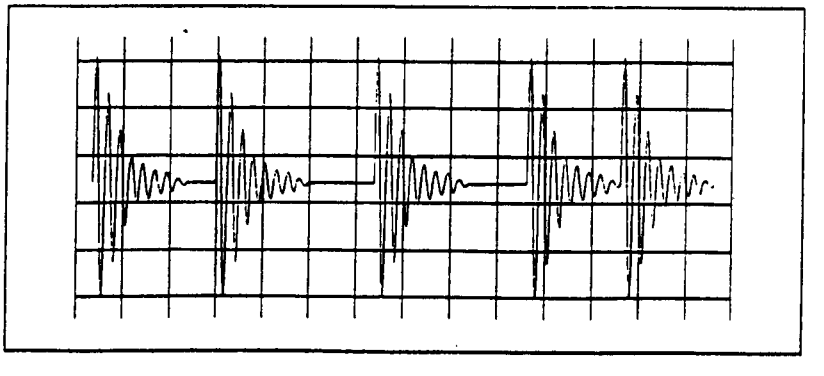

Figure 1.6 Typical waveform of the Hydroflow HS38 pulsed magnet.

1.2.3 General Effects Of Magnetic Fields On Precipitation And Crystallisation

The general aspects of the magnetic treatment of fluids are reviewed in this section.

1.2.3.1 Magnetic Field - Charged Species Interactions

The interactions between applied magnetic fields and many types of charged species in fluids can be shown to change the behaviour of the charged species. Examples of charged species that can be affected by applied magnetic fields include:

- ions
- crystal nuclei
- polar molecules (dipoles)
- ion-pairs
- free radicals
- fine suspensions

The interaction between a charged particle and a magnetic field can be of two types, *viz* (a) direct field charge interactions that affect the entire charged particle, (b) magneto kinetic energy level modification in which the observed effects arise because of interactions between the magnetic field and specific energy levels. Magnetokinetic energy level modification is important in free radical reactions and involves the use of weak magnetic fields (strength 10-100G). Work by Nwang [85] has shown that applied fields can increase the rate of destruction of pollutant organic species by free radical oxidation in the presence of an applied field. Direct interactions require somewhat stronger fields (greater than 500G) and depend upon the nature of the charged species and the strength of the applied fields. An example taken from Grimes *et al* [86] shows that the rate of polymerisation of acrylonitrile can be increased in an applied field. This is an example of a direct field-charge interaction in which, ion-pairs in the fluid are affected by a field of about 1000G. In the process the magnetic field weakens the interaction between the positive and negative parts of the ion-pairs by attempting to set them in helical motion in

opposite directions. This, in turn, makes the active catalyst species more available, and speeds up the action. The polymerisation of acrylonitrile to polyacrylonitrile is an exothermic reaction providing a means of studying the rate of reaction by thermometric titrimetry. Application of a magnetic field results in an increase in the rate of polymerisation as indicated by an increase in heat output. The active catalyst species in the polymerisation is the propan-2-oxide ion (C_3H_5O-) which is added to the monomer solution as a solution of potassium hydroxide in propan-2-oxide. A disadvantage of adding the catalyst in this way is that the activity of the propan-2-oxide ion as a catalyst is reduced by the formation of an ion-pair with potassium ions. The magnetic field on acting to prevent the formation of $RO^-....K^+$ ion pairs thus releases the active catalytic species and favours the polymerisation reaction.

The example of the effects of an applied magnetic field on acrylonitrile polymerisation is only one of many types of field-charge interaction that could be used to demonstrate that the magnetic treatment of fluids is a general phenomenon; involving interactions between the fields and charged species.
For example it has been shown that magnetic fields will interact with the surface charges on fine particles of clays and other dispersed phases and alter their settling properties.

1.2.3.2 Crystallisation and Magnetic Field Effects

The formation of chemical scale, including the deposition of calcium carbonate from hard water is in chemical terms, simply an example of precipitation and crystallisation. The nuclei on which precipitation and crystallisation processes occur in fluids must carry large surface charges that could be affected by applied magnetic fields. There are only two major factors in the growth of precipitates and crystals, and, therefore, in the deposition of chemical scales, namely:

- **the solubility of materials in the fluid**
- **the crystal nucleation process.**

In order to explain the effects of magnetic fields on crystallisation, consideration must be given to how the fields will affect these two major factors.

Laboratory work on the crystallisation process has shown that the magnetic treatment of fluids can result in:

- changes in particle size
- changes in crystallinity
- changes in crystal morphology
- changes in crystal phase
- changes in solubility
- changes in rate of precipitation
- changes in surface charge

These changes are now considered in turn.

Changes in particle size - in the case of calcium carbonate scale, it has been shown that the particle size of the precipitates obtained from hard water increases when the water is passed through a magnetic field. An increase in particle size in this case can have two beneficial effects: (1) the large crystals will not adhere together to form a scale in the same way as smaller crystals which have higher surface charges, (2) the presence of the larger crystals will upset the equilibrium between the fluid and any existing scale because, in general, smaller particles have higher solubility, and hence for larger particles local concentration in solution will be lower. The function of the magnetic units is to alter the nature of the precipitation of calcium carbonate from solution in such a way that scale formation is prevented. The descaling action, therefore, arises as a consequence of this effect and of the resulting changes in scale/fluid equilibria. The increase in particle size of calcium carbonate precipitates, on magnetic treatment, has been confirmed by both electron microscopy and laser-scattering particle size measurement. The difference in particle size is measured by laser scattering, of barium sulphate particles deposited from artificial sea water in zero and applied fields, in which, there is a decrease (from 25 to 5%) in aggregation to give particles greater than 90 micron in the applied field case compared to the zero field case.

Changes in crystallinity - associated with changes in crystal size, in some systems, are changes in the crystallinity of the precipitates obtained. The precipitation of the

amino acid, DL-valine, for example, shows how the magnetic field can alter the crystallinity. In the presence of an applied magnetic field the DL-valine crystals are large and well formed hexagonal platelets while the crystals obtained under the same conditions but in a zero field are much smaller and less well formed.

Changes in crystal morphology - the external faces seen on a crystal are those of the slowest growing faces in the development of the crystal. It is well known that the addition of a chemical can change the growth on one set of crystal planes relative to other planes and hence change the morphology (habit).
Any factor that affects the relative rates of growth of crystals on the various planes of the crystal could alter the crystal habit. An ability to change the crystal habit can be important in determining the nature of precipitation, scale formation and scale prevention. Among the factors that are known to change the morphology of growing crystals under specific circumstances are rate of cooling, nature of solvent, pH, impurities present and degree of supersaturation. There is considerable evidence that the effect of the magnetic field on the growing crystals in magnetically treated fluids also changes the relative rates of growth of the possible external faces of the crystals precipitated. The examples chosen here to illustrate changes in morphology on magnetic treatment are the crystallisations of calcium sulphate dihydrate and anthranilic acid [89]. Changes in the relative intensities of the two strongest lines in the X-ray diffraction powder pattern for calcium sulphate dihydrate on magnetic treatment are consistent with a change in morphology of the crystals. In the case of anthranilic acid, the crystals obtained in a zero field are very large, thin, acicular plates, which contrast markedly with the small, well-formed, three-dimensional rhombic crystals deposited on magnetic treatment.

Changes in crystal phase - When hydrated sodium carbonate is crystallised from aqueous solution, the phase obtained depends upon the temperature[89]. Under normal conditions it is necessary to carry out crystallisation at temperatures above 45°C to obtain sodium carbonate monohydrate ($Na_2CO_3.H_2O$). At temperatures below 35°C the crystal deposited are pure sodium carbonate decahydrate ($Na_2CO_3.10H_2O$). Between 35 and 45°C the product is a mixture of monohydrate, decahydrate and heptahydrate ($Na_2CO_3.7H_2O$). When the sodium carbonate is

crystallised in a magnetic field, however, the phase obtained at temperatures of less than 35°C is the pure monohydrate and not the decahydrate. The thermal analytical data, confirm that the low temperature product crystallised in a field is the monohydrate and that the material precipitated under the same conditions in zero field is a mixture of the three possible hydrates.

Changes in solubility - there is a considerable amount of evidence from the zinc phosphate experiments carried out both in industry and in our laboratories to suggest that treatment of fluids containing zinc phosphate leads to an increase in the solubility or the level of supersaturation of the zinc phosphate in the fluid. This is one aspect of the magnetic treatment of fluids, which could clearly have important implications in scale prevention and removal.

Support for the suggestion that the solubility, or level of supersaturation of phosphates can be altered by magnetic treatment of the fluids comes from a laboratory study on barium sulphate. The solubility data [89]obtained from duplicate experiments with dummy and magnetic units, (Table 1.1), show that more barium sulphate is retained in solution in the magnetically treated fluids.

Barium Sulphate Solubility Ratios		
Value at start of experiment =100		
Time (hours)	Zero Field	Magnetic Field
0	100	100
2	127	189
7	143	233

Table 1.1. Barium Sulphate Solubility Ratios [89]

Changes in rate of precipitation - there is evidence from laboratory studies for changes in rates of precipitation carried out in an applied field in comparison with the rates for the zero field situation. The precipitation of many metal hydroxides, and of calcium oxalate are, for example, delayed in the presence of an applied field. Ellingsen *et al* [87] have shown that a magnetic field can change the rate of precipitation from some solutions. The effects appear to be little or no dependence on the flow velocity. This is in direct contradiction to what has been reported from practical installations, but the explanation may be partly due to turbulence. In cases where little influence is measured initially, a storage time before treatment, may give improvement to the result of magnetically treated water [88, 89]. These general effects of applied fields on precipitation and crystallisation are discussed in more detail in chapter 5 in the interpretation of the experimental results for the present work.

1.2.3.3 Interpretation of Available Data

It has been postulated in earlier work of the Brunel group that [89], three components of a simple precipitation solution will be affected by the field: (a) the charged surface of the growth nuclei, (b) the anions and (c) the cations. The individual anions and cations may increase their available energy by the Lorentz effect as they pass through the field, this extra energy will only be of value if it is dissipated by collision with a growing crystal and this must be a rare occurrence in comparison with normal inter-ionic collisions and collisions between ions and water molecules. It is therefore, at the solid/fluid interface region that explanations of the effects of the magnetic treatment of fluids must be sought.

All of the data that have been obtained on the effects of applied fields on crystallisation and precipitation reactions are consistent with direct interaction between the applied field and the surface charges on growing crystals, crystal nuclei

and pre-nuclear clusters. These direct field charge interactions are significant because they occur at the charged layers of the solid-liquid interface.

In more general terms there are other possible charged species in solutions that could be affected by magnetic fields. These include the water molecules which have a permanent dipole and clusters made up of aggregates of hydrated anions and cations that might have a sufficiently long lifetime to retain the influence of the magnetic field for long enough to have a significant downstream effect.

Donaldson *et al* [89] have developed a method of testing the ability of a solution to form a chemical scale. In addition to tests on hard water, studies were carried out on the propensity of many solutions to form scale, these include calcium phosphate, calcium sulphate, barium sulphate, zinc phosphate and calcium oxalate. The method involves the deliberate deposition of scale in a small bore tube and the measurement of back-pressure as the scale deposit builds up in the tube. The back-pressure thus gives a determination of the rate and extent of scale formation which can conveniently be measured in terms of the time required to build up to a given back-pressure. There was reproducibility in this method, as a series of replicate measurements of calcium carbonate for the scale formation in the two situations, *viz* (i) a control experiment with no unit, (ii) a magnetic experiment in which the water was passed through a magnetic unit. The results show firstly that consistent data can be obtained from replicate experiments. A set of propensity to scale data showed the effect of fluid flow rate on the deposition of calcium carbonate. These data have been obtained under three conditions, *viz* (i) a control experiment with no unit, (ii) a dummy experiment in which the water passed through a non-magnetic unit with exactly the same geometry as the magnetic unit and (iii) applied field situations. The data also shows that, although turbulence in the dummy unit does reduce the time to scale, the application of a magnetic field considerably increases the time required to build up a scale and hence reduces the propensity to form scale. In a similar experiment on calcium sulphate solutions, application of a magnetic field was found to double the time required to deposit gypsum scale.

In view of the wealth of evidence from both laboratory and industrial trials, it is clear that the magnetic treatment of fluids does have a scale preventing effect on many solutions and in particular on hard water. The general acceptability of the technique, however, does depend on the development of an acceptable scientific

explanation for the observed effects.

The research carried out in the Centre for Environmental Research at Brunel University shows that magnetic fields do interact directly with charged species in fluids and that these interactions change the subsequent behaviour of the charged species. The use of applied magnetic fields to control crystal growth, including scale prevention processes, is part of the general phenomenon - the magnetic treatment of fluids.

Work carried out to date in the Brunel group has shown:

- that applied magnetic fields can have a profound effect on the behaviour of charged species in fluids and
- the interactions between applied and hence surface charge materials such as fine precipitates crystal nuclei and prenuclear clusters do change their subsequent behaviour including their growth and aggregation patterns and
- that the scale prevention results achieved with magnetic devices are part of this general phenomenon - the magnetic treatment of fluids.

It has been shown that the above findings can be seen practically by the examples below:

- the scale prevention properties of applied fields are not unique to calcium carbonate scale prevention (the most common application)
- the magnetic interactions can alter the crystallisation patterns of any type of crystal and are not restricted to scale -forming precipitates and
- that these crystal growth control mechanisms, including scale prevention, are part of a general field-charged species phenomenon

Several research groups have carried out experiments on the magnetic treatment of fluids. They have also been monitoring industrial units in the field in a number of different situations. Although many of these monitored studies were concerned with calcium carbonate scaling. They have also shown the commercial success of the technology in monitored trials in the hydrometallurgical sector of the mining industry (calcium sulphate), in metal pre-treatment (calcium, zinc and other phosphates) and in leather treatment (acrylic-based treatment fluids).

Two examples from industrially monitored scale prevention trials carried out by

Donaldson [89] are quoted here:

In duplicate trials with pot heat exchangers [an inner service water stream and an outer hot water circuit], the amount of calcium carbonate deposited was measured after use for the same period of time in a situation where the water supply was hard. Over the period of study the amount of calcium carbonate leached from the heat exchanger when no magnetic unit was used was 40g, in comparison with less than 0.lg. leached when the water was subjected to an applied magnetic field. In a series of experiments with five boiler units of a humidifier system in a hard water area, the life of the boilers was extended from the normal value of l000-l500 hours to well over 2200 hours when the monitored trial was stopped with all five boilers still functioning.

Work carried out [90] shows the effect on calcium carbonate crystals in water, which has been passed through a magnetic field. Calcium carbonate can appear in different shapes.

1.2.3.4 Magnetic Fields and their Effects on Non-metallic/Non magnetic materials

Research carried out by Ko Higashitani looked at the effect of a magnetic field on the stability of non magnetic colloidal particles. For example, ultrafine polystyrene latex and SiO_2 particles in an electrolyte solution. The findings were that the rapid coagulation rate does depend on the magnetic flux density and the duration of magnetic exposure. This is the case even if the magnetic flux density is not high. The degree of magnetic effect depends on the particle size and ions in the medium. The finding which interested the group most, was that the magnetic field effect remained 143 hours after the magnetic exposure was completed and they suggested that effects are attributable to some alteration of the structure of water molecules and ions adsorbed on the particle surface with the magnetic exposure [91].

Experimental studies[92] on the deposition of particles from suspensions subjected to magnetic treatment showed that the action of a static magnetic field on a moving slurry accelerates sedimentation of the suspension. Extensive laboratory and industrial trials showed that under optimum conditions the sedimentation rate, density and consolidation rate increased but the moisture content decreased. These experimental studies suggest that the effects of increased acceleration of coagulation and sedimentation are caused by the action of the magnetic field on the electric

double layer (EDL) around the particles on the aqueous media. It was found that this medium always contains ions. In the literature it has been shown that particle coagulation occurs by surmounting the energy barriers created by the EDL and hydration layers around the particles.

Other researchers[93] looked at the effect of a weak magnetic field under both static (stationary) and dynamic (flowing) conditions. They were particularly interested in the effects on the aggregation and electrophorectic mobility of hematite sol under dynamic conditions. Measurements were made that support the conclusion that aggregation of the hematite sol occurs under dynamic magnetic treatment. From experiments carried out, it is clear that using only flow, or a magnetic treatment without flow, that the observed aggregation requires both flow and orthogonally applied magnetic fields.

The strength of field can be a significant factor A. Maverick *et al* [94] explored the effects of a high magnetic field on chemical bonds. To break a chemical bond using a high magnetic field is dependant on the molecule employed. A quadruply bonded metal dimer is more likely to break if they are based on a small singlet- triplet energy gaps. This was shown after a study of organic aromatic compounds, antiferromagnetic metal dimers and quadruply bonded metal dimers. Other chemical systems show interesting equilibria involving spin state changes. These could be perturbed by the application of magnetic fields.

There are different types of magnetic and applied field that can be employed, in the use of scale prevention.

1.2.4. Magnetic Fields and Molecular Solids

Most of the work that has been carried out on the effects of applied fields on crystallisation has been carried out on inorganic ionic solids in which the close packing of discrete ions is important. Most organic materials are, however, molecular and form solids by packing of the molecules in three dimensions. The forces holding the organic molecules together in a solid are weak electrostatic interactions. These weak forces molecules tend to be slower to orientate themselves at the crystal surface than ions and the strengths of these interactions will vary from Van der Waals forces in hydrocarbons to hydrogen bonding to dipole- dipole interactions in amino acids. It seems likely that these weak interactions could be

modified in the presence of the applied field and this forms the basis of the research presented in this thesis.

Relatively little work has been carried out on the effects of fields on organic compounds, but there is evidence for: (a) changes in the morphology of anthranilic acid, (b) changes in the crystal size of DL-valine[89], (c) the alignment of fibrin fibres [95], (d) alignment of a liquid crystal chromophore in a p-hydrobenzoic acid-poly(ethylene terephthalate) copolymer [96], (e) alignment of benzophenone crystals [97], (f) alignment of dye molecules [98], (g) morphology of sucrose [99], (h) morphology of lactose and [99] (i) change in crystal type of cocoa butter [99].

1.2.4.1 Magnetic Treatment in Oil Wells

There are a number of reports of the use of applied magnetic fields in controlling deposition of waxes in oil pipelines but these reports tend to simply acknowledge the effect without attempting to explain or optimise the mechanism.

There have been some patents filed on the successful treatment of oil wells, for example that of David Stanley [100]. It describes magnetic fluid conditioners consisting of an outer casing with an inner flow sleeve that has a venturi shaped flow slot. The Flow sleeve houses permanent magnets arranged around the flow venturi. This is said to provide disruptive magnetic deflecting forces on a chemical species that flows through the device. A non-magnetic metal material or ceramic magnet material not oriented during the manufacturing process provides the path for the magnetic flux circuits between each bank of permanent magnets. The magnetic deflecting forces alter the growth pattern of paraffin thus inhibiting the build-up of depositional solids in the flowline. Another Patent by Charles Sanderson [101] describes a device for the magnetic treatment of fluids including water, and liquid and gaseous fuels such as gasoline, diesel, gasahol, fuel, propane, natural gas and oil. The device comprises of a magnetic material encased in a non-magnetic material in a long tube.

The scope of this thesis covers the following areas, the effect of applied and magnetic fields on the following systems, static and dynamic solid hydrocarbon set up, static and dynamic solids hydrocarbon with a solvent and static and dynamic on a mixed solid set up. The author then examines the results of the above

experimental set up, and finally describes the effects she believes that the applied and magnetic fields have on the organic system studied.

REFERENCES

1. F. Bettelheim, et al, *General organic and Biochemistry,* **4thEdition**, 1995, 293
2. C. Caraher, *Polymer Chemistry*, **4th Edition**, 1996, 17
3. D. Basset, *Principles of Polymer morphology*, **Cam. Uni. Press**, 1981, 7
4. D. Dorset, *Energy and Fuels*, 2000, **14**, 685
5. B. Musser, *Energy and Fuels*, 1998, **12** 715
6. G.Tiwari, *Petroleum Science and Technology*, 1997, 17
7. H. Ronnigsen, et al, *Energy and Fuels*, 1991, **5**, 914.
8. F. Padgett, et al, *Ind. Chem. Eng*, 1926, **18**, 832.
9. W. Mazee, *J. Inst. Pet.,* 1958, **44**, 401.
10. H. Ronnigsen, et al., *Energy and Fuels*, 1991, **5**, 895.
11. K. Agarwal, *Fuel*, 1989, **68**, 937.
12. T. Bott, et al., *Inst. Pet. Tech*, 1977 **Tech. Paper**. IP-77-077.
13. T. Bott, et al., *Can. J. Chem. Eng*, 1977, **55**, 381.
14. K. Agarwal, *Fuel*, 1990, **69**, 794.
15. P. Bern, et al., *Proc. Eur. Offshore Pet. Conf*, 1980, 571.
16. D. Brownawell et al., *Inst. Pet.*, 1962, **48**, 209.
17. T. Coley, et al., *J. Inst. Pet.*, 1966, **52**, 173.
18. M. McMillan, et al., *SAE Paper* 1983, No. 830594.
19. S. Reddy, *SAE Transactions*, 1984, **93**, 922.
20. J. Zielinski, et al., *Society of Aut. Eng.*, Technical paper series. 1984, No. 841352.
21. D. Schuster, et al., *Polymers as Rheology Modifiers*, 1991, **Ch 18**, 301.
22. W. Matlack, et al., *Proc. SPE Rockey Mount. Reg.* Meet.1983.
23. S. Reddy, *Fuels and Lubs.*, 1986, **65**, 1647.
24. R. Moore ,et al., *Proc. Am. Soc. Testing Mater.* 1932, **32**, 402.
25. E. Barry, *J. Inst. Pet.*, 1971, **57**, 74.
26. C. Irani, *ACS. Div. of Fuel Chem.Preprints.*,1985, **30**, 158
27. G. Holder, et al., *J. Inst. Pet*, 1965, **51**, 243.
28. K. Lewtas, et al., *Adv. Ind Cryst*, 1991, 166
29. S. Reddy, et al., *SAE Transactions*, 1981, **90**, 3598.
30. D. Schuster, et al., *ACS Division of fuel Chemistry Preprints*, 1985, **30**, 169.
31. M. Brod, et al., *J.Inst. Pet*, 1971, **57**, 110.
32. G. Van Engelen, et al., *Proc. Offshore Technol Conf. Houston*, 1979, 1385.

33. J. Tiedje, et al., *Hydrocarbon Processing & Petroleum Refiner*, 1961, **40,** 111.
34. J. Denis, *Revue de Institut Francais du Petrole*, 1987, **42**, 385
35. D. Steere, et al., *Marino Soc. of Aut Eng*, Technical paper series. 1981, No. 810024
36. G. Gavlin, et al., *IEC*, 1953, **45**, 2327.
37. E. Koolvoort, et al., *J. Pet. Technol.*, 1937, **23**, 734.132
38. G. Brown, et al., *Soc. of Aut. Eng.*, Technical paper series, 1988, No. 881652
39. M. Chichakli, et al., *Ind. Eng. Chem.*, 1967, **59**, 86.
40. G. Holder et al., J. *Nature*, 1965, **207**, 719.
41. F. Frank, *Disc Faraday Soc.*1949
42. P. Lovell, et al., *Proc. Oil Shale Symp., Colorado School of Mines,* 1979, 213.
43. S. Dilwar, et al., *Science and Technology*, 1994, 150
44. C. Buchler, et al., *Ind. Eng. Chem.*, 1927, **19**, 718.
45. F. Rhodes, et al., *Ind. Eng. Chem.*, 1927, **19**, 935.
46. G. Holder, et al., *J. Inst. Pet*, 1965, **51**, 228.
47. J. Weingarten, et al., *SPE Paper*, 1986, No. 15654.
48. J. Hansen, et al., *AICHE J.*, 1988, **34**, 1937.
49. K. Won, *Fluid Phase Equilibria*, 1986, **30**, 265.
50. B. Flaherty, *J. Appl. Chem. Biotechn*, 1971, **21**,144.
51. H. Faust, *Thermochimica Acta,* 1978, **26**, 383.
52. R. Miller, et al., *Thermochimica Acta* 1980, **41**, 93.
53. J. Handoo, et al., *Fuel*, 1989, **68**, 1346.
54. K. S. Pedersen,et al., *Energy and Fuels*, 1991, **5**, 924.
55. W. Affens, et al., *Fuel*, 1984, **63**, 543.
56. Wesolowski, *Thermochimica Acta*, 1981, **46**, 21.
57. J. Katz, *Inst.Pet.Tech.*, 1932, 18, 37.
58. R. Edwards, *Ind.Eng.Chem*,.1957, **49,** 750.
59. A. Smith, *J. Chem. Phys.*, 1953, **21** 2229.
60. D. Williams, *J. Chem. Phys*, 1967, **47,** 4680.
61. W. Turner, *Normal Alkanes Ind Eng. Chem. Prod. Res. Develp.*,1971, **10,** 238.
62. T. Perkins, *J. Pet. Technol*, 1971 **March**, 301.
63. C. Irani, *J. Pet. Technol*, 1982 **Feb**, 289.
64. K. North, *Petroleum Geology*, 1985, 31-35
65. J. Carpenter, *Inst.Pet.Tech.*, 1926, **12**, 288.

66. P. Claudy, *Fuel*, 1988, **67**, 58.

67. J. Crine, *IEEE Trans. Electr. Insul.*, 1985, **EI-20**, 419.

68. P. Claudy, *Fuel*, 1986, **65**, 861.

69. T. Shifferman, *J. Pet Technol.*, 1979 **Aug**, 1042.

70. P. Smith, et al., *Eur. Offshore Pet. Conf.*, 1978, 35283.

71. A. Majeed, et al., *Oil. Gas. J.*, 1990, **88**, 63.

72. K. Won, *Fluid Phase Equilibria*, 1989, **53**, 377.

73. A. Majeed, et al., *Proceedings of the 68th GPA Annual Convention.*,1990, **69,** 20.

74. K. Pedersen, *SPE Production & Facilities*, 1995 **Feb**, 46.

75. R. Krishna, et al., *Energy and Fuels*, 1989, **3**, 15.

76. W Pedersen et al. *Energy and Fuels*, 1991, **5**, 908.

77. F. Bosslet, *Thermochimica Acta*, 1983, **70**, 7.

78. F. Bosslet, *Thermochimica Acta*, 1983, **70**, 19.

79. F. Bosslet, *Thermochimica Acta*, 1983, **70**, 35.

80. F. Bosslet, *Thermochimica Acta*, 1983, **70**, 49.

81. F. Noel, *Thermochimica Acta*, 1972, **4**, 377.

82. C. Moynihan, *Thermochimica Acta*, 1982, **52**, 131.

83. J. Donaldson, et al., *Cobalt in Elec. Tech.*, 1988, 13

84. A. Hardcastle, *Ph.D. Thesis, Brunel University, London,* 1996.

85. H. Nwang, *Ph.D. Thesis, Brunel University, London,* 1996.

86. S. Grimes *Tube International*, 1988, 111-118.

87. Ellingsen, et al, *Vatten* 1979, **4**, 309.

88. J. Donaldson, *New Scientist*, 1988, 43-45.

89. J. Donaldson, *Waterline*, 1995, 75-84.

90. A. Thomas *Ph.D. Thesis, The City University, London,* 1986.

91. K. Higashitani, et al., *J. Colloid and Interface Science*, 1992, **152**, 125.

92. N. Gamayunov, *Translated from Zhurnal Prikladnoi Khimii*, 1983, **56(5)**, 1038-1047

93. E. Tombacz, et al., *Colloid Polymer Sci.,* 1991, 269 278.

94. A. Maverick, et al., *Int Journal Quantum Chem.,* 1997, **64,** 607.

95. A. Yamagishi, et al., *J. Phys Soc. Jpn.,* 1989, **58,** 2280.

96. T. Nakai, et al., *Chemistry Letters* 1997, 795.

97. A. Katsuki, et al., *Chemistry Letters* 1996, 607.

98. M. Wei, *Final Report*, 1987.

99. M. Miller, *Ph.D. Thesis*, Brunel University London, 2000.

100. Inventor: Stanley; David (3140 Ambassador Caffery Pkwy., Lafayette, LA 70506) Appl. Number: 97US-779917, Filed: Jan. 7, 1997.

101. Inventor: Sanderson; Charles H. (3717 Fritcha Ave., Fort Wayne, IN 46806) Appl. Number: 80US-167921, Filed: Jul. 14, 1980.

2.0 EXPERIMENTAL PROCEDURES

2.0.1 Aim

The aim of this study is to determine whether applied fields have an effect on the crystallisation of molecular solids.

Studies were carried out on nonadecane alone, and on nonadecane in the presence of heptane, heneicosane, heneicosane and heptane and crude oil, under static and dynamic conditions to identify possible changes in the rate of crystallisation, the melting point, crystallinity and crystal morphology of the solids, obtained.

This chapter contains details of the experimental procedures used for the following studies:

Static and dynamic nonadecane crystallisation,

Static and dynamic nonadecane and heptane crystallisation,

Static and dynamic nonadecane and heneicosane crystallisation,

Static and dynamic nonadecane and heneicosane crystallisation from heptane solution,

Static and dynamic crystallisation of hydrocarbons from crude oil.

The studies were carried out in incubators under controlled temperature conditions.

2.1 Methodology and Experimental Techniques

All of the crystallisation studies were carried out under controlled temperature conditions in incubators. The incubators used were SANYO MIR 152 incubators operated in a range of $\pm 1^0$C to a set temperature. The solid products obtained in the crystallisation studies were stored in a cold room at 4^0C prior to their characterisation by the following techniques:

Powder X-ray Diffraction was deemed to be useful as the information produced could show whether there had been any alterations in the crystal structure and whether the waxes in the study had undergone any phase changes.

Differential Scanning Calorimetry was used to show whether there had been any alterations to the melting regime due to the presence of applied fields.

The melting point measurements were made by hot stage microscopy, using an Electrothermal IA9400 Low Temperature Melting Point Apparatus and recording the onset of melting, through to its completion over a temperature range, determined whilst viewing the sample through the lens piece of the hot stage microscope. A

CRYO Scanning Electron Microscope was used so that a pictorial representation of physical changes to the crystal structure could be observed

2.1.1 Powder X-ray Diffraction

2.1.1.1 A Description of Powder XRD

X-ray powder diffraction is a physical technique used in the characterisation of solids. It is used to determine crystal structures and hence to identify crystalline materials. X-rays are electromagnetic radiation that have a wavelength of approximately 1nm. In the electromagnetic spectrum they lie between gamma and ultra violet rays. They are produced by high energy collisions between charged particles and matter. Usually an energetic beam of electrons is allowed to strike a metal target, such as copper, ionising some of the 1s electrons. An electron from an outer orbital (2p or 3p) immediately drops down to occupy the vacant 1s level. The energy released in the transition appears as X-rays. Since the transition energies have fixed values a characteristic spectrum of X-rays is produced. The Kα transition for copper, the 2p1s has a wavelength of 0.1518nm. The Kβ transition 3p1s is 1.39929Å. The Kα transition is usually used in diffraction as it occurs more frequently and is more intense. To obtain a monochromatic X-ray beam all other wavelengths are filtered out with a nickel filter.

A finely powdered sample which ideally consists of randomly orientated crystals, scatter (diffract) an X-ray beam incident on it. This is because the separation of the planes of atoms in a crystal sample is of the same order of magnitude as the wavelength of X-rays. Crystals consist of layers of atomic planes which when struck by a monochromatic X-ray beam, some of the X-rays are reflected, such that the angle of incidence equals the angle of reflection. The rest are transmitted to be subsequently reflected by succeeding planes. Figure 2.1 shows two x-ray beams 1 and 2 reflected from the adjacent planes, A and B, within the crystal, beam 2′ has to travel the extra distance xyz compared to beam 1′, and for the beams 1′ and 2′ to be in phase, the distance xyz must be equal to a whole number of wavelengths.

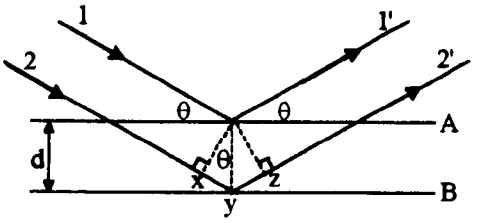

Figure 2.1. Derivation of Bragg's Law for X-ray diffraction

The *d-spacing, d* (the perpendicular distance between pairs of adjacent planes) and the angle of incidence, or *Bragg angle, θ*, are related to the distance *xy* by:

$xy=yz=d\sin\theta$

and

$xyz=2d\sin\theta$

and to be in phase

$xyz=n\lambda$, (where n is an integer)

Therefore

$2d\sin\theta=n\lambda$, Braggs Law

It is only when Bragg's Law is satisfied that the reflected beams are in phase and interfere constructively. At angles of incidence other than the Bragg angle the reflected beams are out of phase and destructive interference occurs. Bragg's Law therefore imposes stringent conditions on the angles at which reflection may occur. Diffracted beams are referred to as reflections and the angle between the incident and the diffracted beam is denoted by 2θ and not simply θ.

In multi-crystalline samples, the various lattices planes are also randomly orientated, and hence will diffract the radiation in an analogous way to the refraction of light by an optical grating. Since no two materials have the same atomic arrangement, every crystalline substance scatters the x-rays in its own unique diffraction pattern, producing a fingerprint of its crystal.

2.1.1.2 Interpretation

The d-spacings and their intensities are the most important features of a powder pattern. The d-spacings (positions) of the line in a powder pattern are governed by the values of the unit cell parameters (cell edges a,b,c, cell angles α,β,γ). The

intensities provide information on the types of atoms present in the sample. In powder X-ray diffraction the intensities are recorded relative to the intensity of the strongest line of the pattern, which is arbitrarily assigned 100. For a particular substance, the line positions are essentially fixed and are characteristic of that substance. Intensities may vary somewhat from sample to sample depending on the method of sample preparation and instrument conditions.

Once the X-ray diffraction pattern has been characterised for a given compound it can be identified by reference to tables of known materials and it can be used to provide a direct comparison between different samples to detect any change in cell dimensions or evidence for changes in morphology.

Powder X-ray diffraction measurements were made using a Philips PW 1710 diffractometer. The samples were crushed using a mortar and pestle, which was surrounded by ice to prevent the wax melting in warm laboratory conditions. And then lightly ground to produce a fine powder, which were used in the XRD analysis.

2.1.2. Differential Scanning Calorimetry (DSC)

2.1.2.1 A Description of DSC

DSC, in this study has been used to measure melting points of wax materials. The model used is of the power -compensated type. It contains two holders, one of which has the sample (Ts), the other a reference (Tr). The DSC is calibrated by running pure metal standards, either indium or lead. This means that the temperature scale can be adjusted so that the two standard points fit on to it.

The DSC holds Ts equal to Tr at all times, whatever the programme conditions, heating, isothermal or cooling. If there is an endothermic reaction in the sample, the DSC, supplies more power to the sample holder. This is so that the temperature does not lag behind Tr. If there is an exothermic reaction then the opposite is true. Therefore the following equation shows the heating/cooling pattern.

$$\frac{dQ}{dt} = mCp\frac{dT}{dt}$$

Where:

$\frac{dQ}{dt}$ = the power

t = the time

T = the temperature

m = the mass

$\frac{dT}{dt}$ = the heating rate

Cp = the capacity

The samples are heated from below, the sample sits in a tripod with the heating mechanism under it. A thin flat sample which has good contact with the base of the holder is therefore required. The system is run in an inert gas atmosphere to prevent reactions with the gas atmosphere. The inert gas is usually either nitrogen or argon. More accurate melting point measurements were made by differential scanning calorimetry using a Perkin Elmer DSC 7.

2.1.3 Scanning Electron Microscopy (Cryo)

The scanning electron microscope was initially constructed by Knoll and Ruska, and is an extremely versatile tool. It is particularly useful for examining the surfaces of materials at high magnification.

2.1.3.1 Resolution

Resolution is probably one of the most important considerations, for a microscope. The increase in resolution over an optical microscope is gained by the use of electrons; resolution is inversely proportional to the (electron) wavelength used. The limit of resolution is defined as the minimum distance between two points that allows for their discrimination as two separate entities. Hence the resolution of a system is defined by the following equation:

$$r = \frac{0.61\lambda}{n \sin \alpha}$$

where r = resolution

0.61 = a constant

λ = wavelength of the medium used (nm)

$\sin\alpha$ = sine of the semiangular aperture of the lens, and,

n = the refractive index of the medium in which the sample lies.

2.1.3.2 Components of the SEM

An SEM is comprised of an evacuated column containing an electron gun, electromagnetic lenses, apertures, electron detector, specimen stage and sometimes other detectors, such as, an X-ray spectrometer. In a modern SEM all of the control functions with the exception of aperture changing are performed electronically. The control column contains all of the control electronics, the camera record tubes, and viewing displays, both of which are cathode ray tubes.

2.1.3.3 The Electron Gun: The SEM produces a coherent beam of virtually monochromatic electrons, this is focused by an electromagnetic lens onto the sample. The most common electron source is the tungsten filament thermionic emission gun. This type of gun is relatively cheap to produce and the filament (cathode) is easy to replace. The gun consists of a bent tungsten filament, with a V shaped tip about 100μm radius. This is surrounded by a metal shield with a central hole, called the Wehnelt cylinder or the cathode shield. The anode is situated below the cathode and is at ground potential. Electrons are emitted from the filament tip if it is heated to above 2700K, the electrons being accelerated away from the gun by applying a high negative voltage between the cathode and the anode. By applying a bias voltage of up to 0-500V between the cathode and the cathode shield, the electrons can be focused to a point below the cathode. To operate successfully the sample chamber must be kept under a vacuum of at least 1H 10^{-5} torr. This helps to reduce the interference of the weakly penetrating electron beam by gaseous particles. It also reduces the oxidation of the tungsten filament, therefore prolonging the guns' working life.

2.1.3.4 The Electron Lens: Electron microscopes use electromagnetic lenses that are designed to provide a magnetic field almost parallel to the direction of travel of the electrons. The strength of the magnetic field is proportional to the number of windings of the lens multiplied by the current through the windings, whilst the effect of the lens is inversely proportional to the accelerating voltage applied to the gun. The function of an electron lens is to bring the beam of electrons produced by the gun to a focus at the focal point of the lens, the latter being inversely proportional to the strength of the magnetic field. Electron microscopes also contain

small electromagnetic coils that are used to correct astigmatism, deflect the beam for alignment and to scan the beam into its characteristic raster.

2.1.3.5 Specimen Stage: The samples are mounted onto a specimen stage, which is within the vacuum system, therefore the samples have to be dry and able to withstand the vacuum. To enable the examination of the sample, the stage has x, y, and z translation, tilt and rotate facilities. The stage is electronically grounded to the microscope to provide a conducting pathway for the electrons.

2.1.3.6 Construction and Image Formation: After the electron beam has been generated by the tungsten filament thermionic electron gun and accelerated by the accelerating voltage, it enters the condenser system where it is demagnified. It is then focused onto a sample by an objective lens as described above. Between the objective lens and the sample are a set of coils that cause the beam to scan across the sample in a series of parallel line. This is known as rastering.
The fine beam of electrons interacts with the specimen to produce a variety of different signals: high energy backscattered electrons, low energy secondary electrons, absorbed electrons, X-rays and cathodoluminescence. All interaction products can be collected and amplified to produce a signal, which can be used to control brightness to the cathode ray tube. The nature of the interaction of the electron beam will be affected by topography, composition, magnetic and electric character of the specimen.
Scanning Electron Microscopy (CRYOSEM) was carried out using a JEOL 35 cryo-electron microscope with the sample being freeze fractured inside the microscope before analysis.

2.2 Wax Crystallisation Basic Experimental Set Up

All the experiments performed on wax crystallisation were carried out under both static and dynamic conditions. The solid test materials were melted at 50^0C and then crystallised in sample tubes within incubators set at a given temperature for each experiment type. Crystallisation experiments were performed on solutions of the solid waxes in the light hydrocarbon solvent heptane.

2.2.1 Static Experiments

The nonadecane was obtained in a crystalline solid form. The bottle containing the solid nonadecane was placed in the incubator set at 50^0C. It was stored in the incubator and left to become fully molten before use in experiments. The molten nonadecane was stored in the incubator, which was set at 50^0C for use in further experiments.

In each case, test material to make up 5ml in a cylindrical sample tube was extracted from the melt or the stock solution. The time taken for the wax to crystallise was then measured (defined as the point at which no liquid wax remained in the sample tube). Each experiment was repeated 3 times and samples were removed from each experiment for analysis.

Samples were obtained from crystallisation in a zero field (control) conditions (set up 1) and for the following crystallisations in applied fields:

(ii) 500G	(set up 2)
(iii) 2500G	(set up 3)
(iv) Pulsed	(set up 4)
(v) AC	(set up 5)
(vi) 6 Volt DC (6V DC)	(set up 6)
(vii) 12 Volt DC (12V DC)	(set up 7)

2.2.2 Experimental Procedures

The following is a description of each set of experiments used under static and dynamic conditions.

2.2.2.1 Set Up 1 – Control

The test material was placed in the incubator and the time taken to crystallise under both static and dynamic conditions was measured. This sample was used to determine whether the other experimental conditions affected the crystallisation time.

2.2.2.2 Set Up 2 - 500G Permanent Magnet

The sample was placed within the centre of the 500 Gauss permanent magnets. The magnet was N-S facing (figure 2.2.).

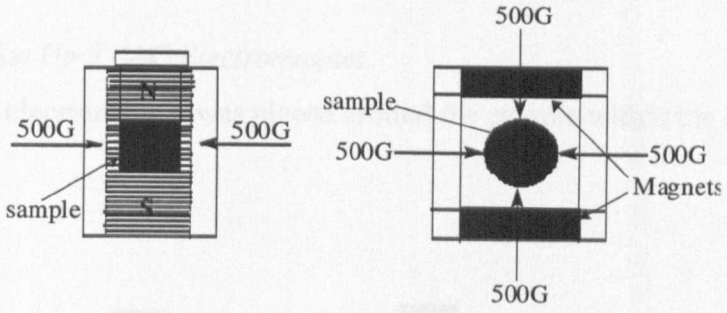

Figure 2.2. The Permanent 500G magnet

2.2.2.3 Set Up 3 - 2500G Permanent Magnet

The 2500 Gauss permanent magnets were placed around the sample with a N-S configuration (figure 2.3).

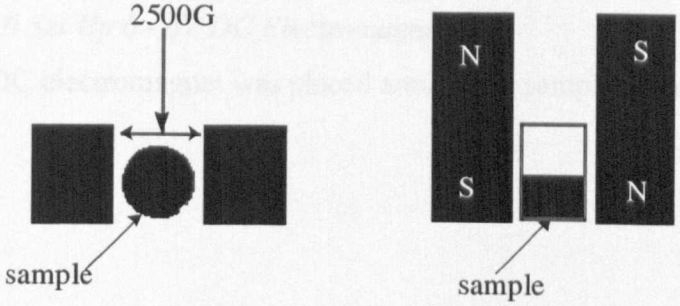

Figure 2.3. The 2500G Permanent magnet

2.2.2.4 Set Up 4 - Pulsed Magnet

The sample was placed within the pulsed magnet device (figure 2.4).

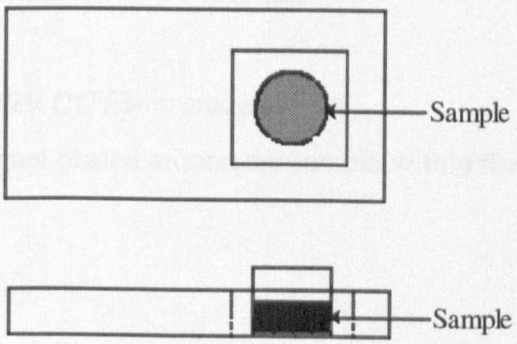

Figure 2.4. The Pulsed applied field

2.2.2.5 Set Up 5 - AC Electromagnet

The AC electromagnet was placed around the sample within the incubators (figure 2.5).

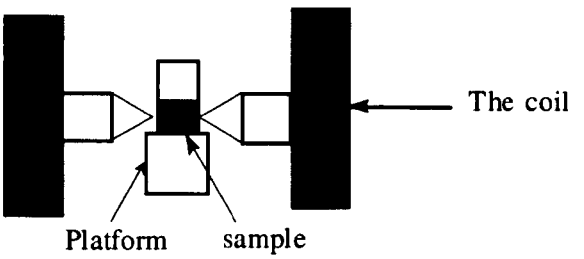

Figure 2.5. The AC Electromagnetic field

2.2.2.6 Set Up 6 - 6V DC Electromagnet

The DC electromagnet was placed around the sample within the incubators (figure 2.6).

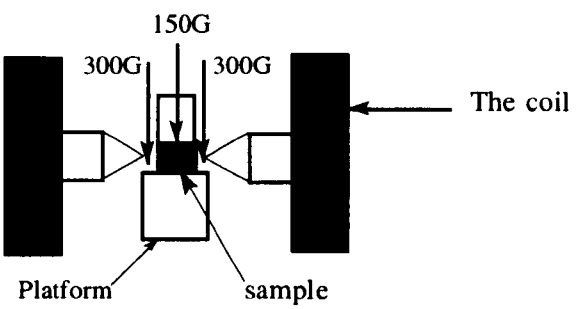

Figure 2.6. The 6V DC field

2.2.2.7 Set Up 7 - 12V DC Electromagnet

The DC electromagnet placed around the sample within the incubators (figure 2.7).

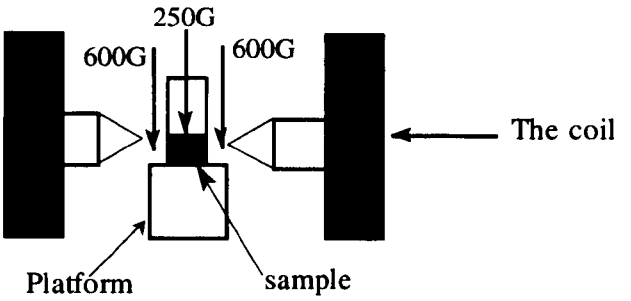

Figure 2.7. The 12V DC field

2.2.3 Dynamic Experiments

In dynamic experiments (fig 2.8) 100ml of the test material contained in a glass delivery vessel (A), in the incubator at 50^0C, is siphoned via silicone tubing (diameter 4mm) into a (B) second storage bottle (the receiving vessel) and two 4ml aliquots removed from (B) and labelled Sample 1a, 1b. The receiving vessel was then exchanged with the delivery vessel and the procedure repeated. Again 4ml aliquots were removed to give samples 2a, 2b. This was carried out a total of eight times resulting in 8 samples each containing 4ml aliquots of test material. The time taken to perform the procedure was 16 minutes.

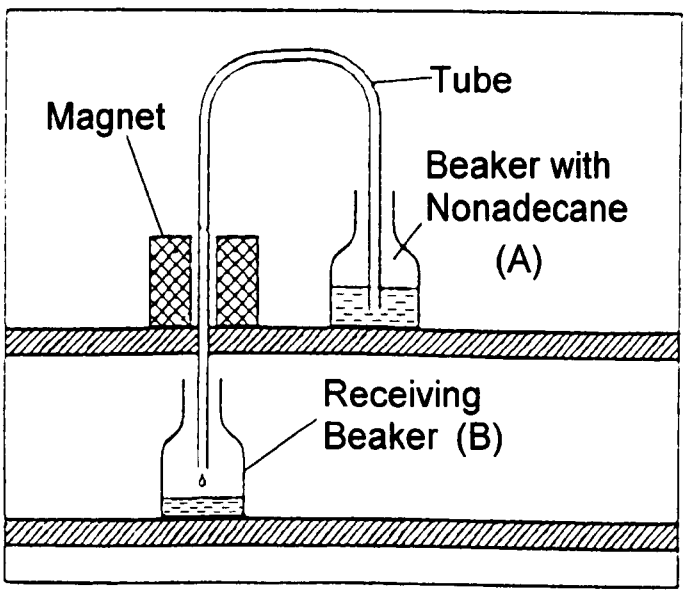

Figure 2.8. Dynamic Set Up

Samples were obtained from crystallisation in a zero field (control) conditions (set up 1) and for the following crystallisations in applied fields:

(ii) 500G (set up 2)

(iii) 2500G (set up 3)

(iv) Pulsed (set up 4)

(v) AC (set up 5)

(vi) 6V DC (set up 6)

(vii)12V DC (set up 7)

2.3 Experiments Performed

The following experiments were carried out to determine whether applied fields affected the crystallisation of the test material.

2.3.1 Static and Dynamic Nonadecane.

These experiments were performed to determine the affect of an applied field on a simple wax, i.e. a solid alkane. The dynamic studies were performed to simulate field conditions in oil transport pipelines.

2.3.2 Static and Dynamic Nonadecane in Heptane

These experiments were performed to determine whether the solvent added to the hydrocarbon system changed the effect of an applied field. The nonadecane and heptane mixture was crystallised under controlled temperature conditions in incubators. The nonadecane wax in 5g aliquots was mixed with 5ml of heptane to achieve complete dissolution. Each 5g portion was added separately, so as to allow the previous portion to dissolve completely. Four stock solutions of nonadecane/heptane at different saturation levels were produced and crystallised at an optimum working temperature. The following temperatures were chosen as a result of the nonadecane study whereby the length of time to crystallise could be monitored within a reasonable time frame. These were 20g/5ml crystallised at 25^0C, 15g/5ml crystallised at 20^0C, 10g/5ml crystallised at 20^0C and 5g/5ml crystallised at 15^0C. The saturation point was determined by adding small quantities of nonadecane to 5 ml of heptane. The subsequent mixture was stirred continuously and the temperature monitored. When the mixture had reached a constant

temperature and wax remained at the base of the sample vessel, the saturation point had been reached.

For nonadecane/heptane this was found to be 20g/5ml at room temperature.

2.3.3 Static and Dynamic Nonadecane and Heneicosane

These experiments were carried out to determine the effect of an applied field on a mixed hydrocarbon system. The nonadecane and heneicosane mixture was crystallised under controlled temperature conditions in incubators. The nonadecane wax (20g) was added to (20g) of heneicosane. The temperature used was chosen as a result of the nonadecane and nonadecane and heptane studies, to achieve crystallisation within a reasonable time frame. A stock melt of the nonadecane and heneicosane was produced, by placing the solid mixture in the incubator at 50^0C. The mixture was crystallised at the optimum working temperature, which was found to be 22.5^0C.

2.3.4 Static and Dynamic Nonadecane and Heneicosane in Heptane

These experiments were performed to determine the effect of an applied field on a mixed hydrocarbon system, to which a solvent has been added. A saturated mixture of equal quantities of nonadecane and heneicosane was required to carry out the following experiments. The saturation point was determined by adding small measured quantities of nonadecane and heneicosane to 5 ml of heptane. The subsequent mixture was stirred continuously and the temperature monitored. When the mixture had reached a constant temperature and the wax formed at the base of the sample vessel, the saturation point had been reached. This was found to be 20g/5ml, 10g of nonadecane and 10 g of heneicosane at room temperature. The experiments performed were based on the maximum level of saturation obtained in heptane. The temperature used was chosen as a result of the nonadecane, nonadecane and heptane, nonadecane and heneicosane studies, so that the length of time to crystallise could be monitored within a reasonable time frame.

A stock solution of the nonadecane and heneicosane in heptane was produced and crystallised at an optimum working temperature, which was found to be 10^0C

2.3.5 Static and Dynamic Nonadecane and Crude Oil.

These experiments were carried out using a crude oil supplied by a sponsoring company. The crude oil was amorphous, and so was saturated with the simple alkane (nonadecane) to provide a system that give crystallisation in a reasonable time period. This work was carried out to determine whether an applied field had an effect on a complex hydrocarbon system.

A saturated mixture of nonadecane and crude oil was required to carry out the following experiments. The saturation point was determined by adding small measured quantities of nonadecane to 1ml of crude oil. The subsequent mixture was stirred continuously and the temperature monitored. When the mixture had reached a constant temperature and the wax formed at the base of the sample vessel, the saturation point had been reached. The saturation of crude oil with nonadecane was found to be 5g/4ml at room temperature. The experiments performed were based on the maximum level of saturation obtained in the crude oil. The following temperature was chosen as a result of the nonadecane, nonadecane and heptane, nonadecane and heneicosane and nonadecane and heneicosane in heptane studies, to gave a time to crystallise that could be monitored within a reasonable time frame. A stock solution of the nonadecane and crude oil was produced and crystallised at the optimum working temperature, which was found to be 22.5^{0}C.

3.0 RESULTS AND DISCUSSION

3.1 Crystallisation Time Measurements

The time in minutes to achieve crystallisation of a wax is an easily measured parameter. To determine the statistical significance of the results, standard deviations (σ) were calculated from sets of data involving at least 12 measurements for each type of experiment. A change in the time of crystallisation in an experiment was regarded as statistically significant only if the average value in an applied field differed from the control by more than 2(σ). Table 3.1 lists the standard deviations for each type of crystallisation experiment.

Experiment type	Standard Deviation in minutes
Nonadecane static at 20^0C,	2.4
Nonadecane static at 22.5^0C	1.9
Nonadecane static at 25^0C	2.0
Nonadecane dynamic at 25^0C	1.5
Nonadecane in Heptane static 20g/5ml at 25^0C	3.0
Nonadecane in Heptane static 15g/5ml at 20^0C	3.0
Nonadecane in Heptane static 10g/5ml at 20^0C	3.0
Nonadecane in Heptane static 5g/5ml at 15^0C	3.0
Nonadecane in Heptane dynamic 20g/5ml at 25^0C	3.0
Nonadecane in Heptane dynamic 15g/5ml at 20^0C	3.0
Nonadecane in Heptane dynamic 10g/5ml at 20^0C	3.0
Nonadecane in Heptane dynamic 5g/5ml at 15^0C	3.0
Nonadecane and Heneicosane 50:50 static at 10^0C	3.0
Nonadecane and Heneicosane 50: 50 dynamic at 10^0C	3.0
Nonadecane and Heneicosane in Heptane static at 10^0C	3.0
Nonadecane and Heneicosane in Heptane dynamic at 10^0C	3.0
Nonadecane and Crude oil static at 22.5^0C	3.0
Nonadecane and Crude oil dynamic at 22.5^0C	3.0

Table 3.1. Standard deviations of all the experimental types performed

3.2 Experimental Results Data

3.2.1 Static Nonadecane

3.2.1.1 Crystallisation Times of Nonadecane Under Static Conditions

The data for the crystallisation for nonadecane experiments under static conditions in different applied fields and at different temperatures are in table 3.2.-3.4. Standard deviation calculations were carried out to determine whether any of the differences obtained are significant. Data for the melting points of the crystals obtained are in table 3.5 and their X-ray powder diffraction data are in tables 3.37-3.43.

The standard deviation calculation for a series of static nonadecane crystallisation experiments in minutes gave σ =2.4 at 20^{0}C, σ =1.9 at 22.5^{0}C, σ =2.0 at 25^{0}C

In this study on nonadecane crystallisation, the effects of applied fields are carried out by measuring the time taken for nonadecane to solidify under different temperature conditions. The replicate measurements show good reproducibility. Any delay in crystallisation appears to be temperature dependent. The statistically significant results in this set of experiments are the AC field at 20^{0}C, the 2500G, pulsed fields at 22.5^{0}C and the 2500G and pulsed fields at 25^{0}C. All these field conditions show a significant lengthening of the crystallisation time as compared to the control experiments. The results obtained at 20^{0}C are in table 3.2. The average value for the control is 24.2 minutes and the spread of the results covered by 2σ for table 3.2. is 23-31minutes.

Crystallisation time in minutes						
Replicates at 20^{0}C						
		1	2	3	Average	Statistically significant
Control	**(Set up 1)**	24.0	24.5	24.3	24.2	No
500G	**(Set up 2)**	25.5	26.2	27.5	26.4	No
2500G	**(Set up 3)**	24.3	24.4	24.5	24.4	Yes
Pulsed	**(Set up 4)**	24.4	25.2	26.3	25.3	Yes
AC	**(Set up 5)**	28.5	28.4	29.3	28.7	Yes
6V DC	**(Set up 6)**	25.4	26.1	25.8	25.7	No
12V DC	**(Set up 7)**	22.4	23.5	23.1	23.0	No

Table 3.2. Crystallisation times in minutes of Static Nonadecane under varying field conditions at 20^{0}C

The results obtained at 22.5^{0}C are in table 3.3. The average value for the control is 29.1 minutes and the spread of the results covered by 2σ for table 3.3 is 27-35.

Crystallisation time in minutes					
Replicates at 22.5^{0}C					
	1	2	3	Average	Statistically significant
Control	31.0	28.3	28.2	29.1	No
500G	28.5	29.2	29.0	28.9	No
2500G	33.4	31.5	31.3	32.0	No
Pulsed	34.1	31.4	33.3	32.9	No
AC	29.2	30.4	31.2	30.2	No
6V DC	31.0	29.4	31.4	30.6	No
12V DC	34.1	32.2	32.4	32.9	No

Table 3.3 Crystallisation times in minutes of Static Nonadecane under varying field conditions at 22.5^{0}C

The results obtained at 25^{0}C are in table 3.4. The average value for the control is 40.5 minutes and the spread of the results covered by 2σ for table 3.4 is 35-47.

Crystallisation time in minutes					
Replicates at 25^{0}C					
	1	2	3	Average	Statistically significant
Control	40.5	40.0	41.2	40.5	No
500G	39.0	40.5	40.0	39.8	No
2500G	51.2	50.5	50.0	50.5	Yes
Pulsed	75.0	75.1	75.3	75.1	Yes
AC	45.4	44.4	45.5	45.1	No
6V DC	44.2	37.3	38.4	39.9	No
12V DC	34.4	45.1	46.0	41.8	No

Table 3.4 Crystallisation times in minutes of Static Nonadecane under varying field conditions at 25^{0}C

3.2.1.2 Melting Points Static Nonadecane

The melting points of the nonadecane samples crystallised in applied fields were unaffected except for those carried out in the DC electromagnetic fields. The melting point temperatures were elevated in the case of the stronger DC field at 20^{0}C and the weaker DC field at 22.5 and 25^{0}C.

Melting Points (^{0}C)												
	20^{0}C				22.5^{0}C				25^{0}C			
	1	2	3	Av	1	2	3	Av	1	2	3	Av
Control	32.5-33.5	32.5-33.9	32.5-33.6	32.5-33.6	32.4-33.6	32.3-33.4	32.4-34.0	32.4 -33.6	32.4 -33.6	32.6 -34.2	32.5 -33.9	32.5 -33.9
500G	32.4-33.5	32.5-33.8	32.7-33.6	32.5-33.6	32.6-33.8	32.4-33.6	32.5-33.8	32.5-33.7	32.3-33.6	32.6-34.0	32.3-33.5	32.4-33.7
2500G	32.7-34.3	32.3-33.7	32.4-33.9	32.5-34.0	32.7-33.8	32.8-33.8	32.6-34.0	32.7-33.8	32.8-33.8	32.5-33.5	32.6-33.7	32.6-33.6
Pulsed	32.2-34.4	32.6-34.0	32.4-33.9	32.4-33.1	32.5-34.3	32.4-33.9	32.5-33.1	32.5-33.8	32.1-33.4	32.3-33.6	32.4-33.5	32.4-33.5
AC	32.7-33.6	32.8-33.2	32.9-33.7	32.8-33.5	32.9-34.1	33.2-34.3	32.8-34.0	32.9-31.1	32.6-34.1	32.7-34.4	32.4-33.8	32.6-34.1
6V DC	32.2-34.4	32.4-34.0	32.1-34.3	32.2-34.2	33.3-35.5	32.2-35.3	32.5-35.4	32.6-35.4	33.3-35.5	32.2-35.3	32.5-35.4	32.6-35.4
12V DC	33.3-35.5	32.2-35.3	32.5-35.4	32.6-35.4	32.2-33.5	32.4-33.7	32.1-33.4	32.2-33.5	32.6-34.1	32.5-33.9	32.5-34.1	32.6-34.0

Table 3.5 Melting Points, of Static Nonadecane crystallised at different temperatures under varying field conditions.

3.2.1.3 Powder XRDs Static Nonadecane

Powder X-ray diffraction was used as a means of determining whether the final crystalline state of the nonadecane wax had altered as a result of the presence of applied fields. See Tables 3.37-3.43 at the end of the chapter.

3.2.1.3.1 Further Powder XRDs Static Nonadecane

The results from the nonadecane studies were further analysed. For systems that showed an effect on the XRD, data were collected from slow X-ray scan to give more accurate values of d-spacing. See Table 3.44 at the end of the chapter

3.2.1.4 Scanning Electron Micrographs

Scanning Electron Micrographs were used as a visual means to determine whether there had been any changes in appearance of the crystalline solid as a result of an applied field.

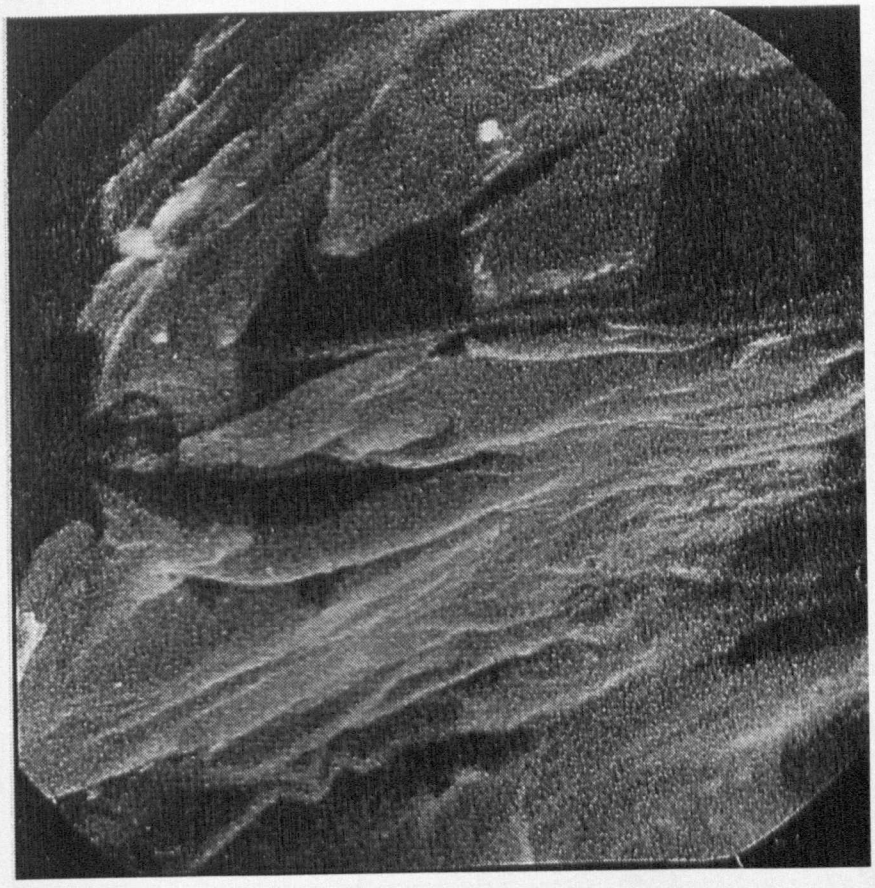

Figure 3.1 Static Nonadecane at 25^0C

3.2.2 Dynamic Nonadecane

3.2.2.1 Crystallisation Times of Nonadecane Under Dynamic Conditions

The data for the crystallisation for nonadecane experiments under dynamic conditions in different applied fields at 25^0C are in table 3.6. Standard deviation calculations were carried out to determine whether any of the differences obtained are significant. Data for the melting points of the crystals obtained are in table 3.7 and the X-ray powder diffraction data are in table 3.45. The standard deviation

calculation, for a series of dynamic nonadecane crystallisation experiments σ =1.5 minutes.

In this study on nonadecane crystallisation, the effects of applied fields were measured by the time required to crystallise the wax. Under the following dynamic field conditions used, (2500G, Pulsed, AC, and 12VDC) produced a significant lengthening of crystallisation time at 25^{0}C. The results obtained at 25^{0}C are in table 3.6. The average value for the control is 41 minutes and the spread of the results covered by 2σ for table 3.6. is 38-44 minutes (as a doubling of the standard deviation gives range).

Crystallisation time in minutes				
Replicates at 25^{0}C				
	1	2	Average	Statistically significant
Control	40.0	42.1	41.0	No
500G	47.5	49.1	48.3	No
2500G	60.4	61.3	60.5	Yes
Pulsed	67.0	68.0	67.3	Yes
AC	47.2	47.2	47.2	Yes
6V DC	43.2	43.3	43.2	No
12V DC	46.5	45.4	46.0	Yes

Table 3.6 Crystallisation times in minutes of Dynamic Nonadecane at 25^{0}C under varying field conditions

3.2.2.2 Melting Points of Dynamic Nonadecane

The melting points of the nonadecane samples crystallised in applied fields were unaffected. All the melting points were reproducible and in good agreement.

Melting Points (^{0}C)			
	No. of the run		
	1	2	Average
Control	32.1 - 32.2	32.3 - 33.9	32.2 - 33.1
500G	32.4 - 32.6	32.5 - 33.1	32.5 - 32.9
2500G	32.0 - 33.0	32.4 - 34.2	32.2 - 33.6
Pulsed)	32.3 - 32.9	32.1 - 32.6	32.2 - 32.8
AC	32.1 - 32.6	32.2 - 33.0	32.2 - 32.8
6V DC	32.3 - 33.1	32.3 - 33.2	32.3 - 33.1
12V DC	32.5 - 33.2	32.4 - 33.2	32.5 - 33.2

Table 3.7 Melting Points, of Dynamic Nonadecane crystallised at 25^{0}C under varying field conditions.

3.2.2.3 Powder XRDs Dynamic Nonadecane

Powder X-ray diffraction was used as a means of determining whether the final crystalline state of the nonadecane wax had altered as a result of the presence of applied fields. See Table 3.45 at the end of the chapter.

3.2.3 Static Nonadecane in Heptane, 20g/5ml

3.2.3.1 Crystallisation Times of Static Nonadecane and Heptane 20g/5ml

The data for the crystallisation for nonadecane in heptane 20g/5ml experiments under static conditions in different applied fields at 25^0C are in table 3.8. Standard deviation calculations were carried out to determine whether any of the differences obtained are significant. Data for the melting points of the crystals obtained are in table 3.9 and the X-ray powder diffraction data are in table 3.46. The standard deviation calculation for a series of static nonadecane in heptane 20mg/5ml crystallisation experiments gave σ =3.0 minutes.

In this study on nonadecane crystallisation, from heptane the effects of applied fields are measured by the time taken for nonadecane to solidify at 25^0C. The replicate measurements show good reproducibility. The presence of the solvent heptane appears to have considerably prolonged the crystallisation time period especially when compared to the nonadecane experiments described in the previous section (3.2.1.1). The field conditions where the crystallisation times were significantly extended in an applied field are for the 2500G, Pulsed, 12VDC and 6VDC field to a lesser extent. A field condition where the crystallisation time was significantly reduced was the AC field. The results obtained at 25^0C are in table 3.8. The average value for the control is 50.2 minutes and the spread of the results covered by 2σ for table 3.8 is 47.2-53.2 minutes.

Crystallisation time in minutes					
	Replicates at 25^0C				
	1	2	3	Average	Statistically significant
Control	50.0	50.0	51.4	50.2	No
500G	70.0	71.0	70.3	70.2	Yes
2500G	90.0	92.0	90.1	90.2	Yes
Pulsed	105.0	103.4	102.2	103.3	Yes
AC	30.0	30.4	30.3	30.3	Yes
6V DC	87.0	90.0	87.2	88.0	Yes
12V DC	120.0	120.5	121.0	120.3	Yes

Table 3.8 Crystallisation times in minutes of Static Nonadecane in Heptane 20g/5ml at 25^0C under varying field conditions.

3.2.3.2 Melting Points Static Nonadecane and Heptane 20g/5ml

Applied fields had little effect on the melting points of the Nonadecane samples crystallised from solutions of nonadecane in heptane 20g/5ml at 25^{0}C under all field conditions.

Melting Points (^{0}C)				
Replicates at 25^{0}C				
	1	2	3	Average
Control	31.8 – 33.8	32.1 - 33.4	32.0 - 33.6	31.6 - 33.5
500G	32.1 – 33.4	31.8 - 33.5	32.1 - 33.5	32.0 - 33.5
2500G	32.1 – 33.2	32.4 - 33.8	32.2 - 33.5	32.2 - 33.5
Pulsed	31.8 – 33.0	29.5 - 32.6	30.7 - 32.8	30.6 - 32.8
AC	32.1 – 33.1	32.3 - 33.7	32.1 - 33.4	32.2 - 33.4
6V DC	32.7 - 34.6	29.8 - 32.5	30.5 - 33.9	31.0 - 33.7
12V DC	32.5 - 33.2	31.9 - 33.7	32.5 - 33.7	32.3 - 33.5

Table 3.9 Melting Points, of Static Nonadecane and Heptane 20g/5ml, crystallised at 25^{0}C under varying field conditions.

3.2.3.3 Powder XRDs Static Nonadecane and Heptane 20g/5ml

Powder X-ray diffraction was used as a means of determining whether the final crystalline state of the nonadecane wax had altered as a result of the presence of applied fields. See Table 3.46 at the end of the chapter.

3.2.4 Static Nonadecane in Heptane 15g/5ml

3.2.4.1 Crystallisation Times of Static Nonadecane in Heptane 15g/5ml

The data for the crystallisation for nonadecane in heptane 15g/5ml experiments under static conditions in different applied fields at 20^{0}C are in table 3.10. Standard deviation calculations were carried out to determine whether any of the differences obtained are significant. Data for the melting points of the crystals obtained are in table 3.11 and the X-ray powder diffraction data are in table 3.47. The standard deviation calculation for a series of static nonadecane in heptane 15g/5ml crystallisation experiments gave σ =3.0 minutes.

In this study on nonadecane crystallisation the effects of applied fields are measured by the time taken for nonadecane to solidify at 20^{0}C. The replicate measurements show good reproducibility. The field conditions under which, the crystallisation times were significantly extended were the, 500G, 2500G, Pulsed and 12V DC fields. Field conditions under which the crystallisation times were significantly

reduced were the AC and 6VDC field by a small margin. The results obtained at 20^{0}C are in table 3.10. The average value for the control is 33.1minutes and the spread of the results covered by 2σ for table 3.10 is 27-39 minutes.

Crystallisation time in minutes					
Replicates at 20^{0}C					
	1	2	3	Average	Statistically significant
Control	32.0	32.0	37.0	33.1	No
500G	45.0	46.0	47.1	46.1	Yes
2500G	55.0	55.0	55.0	55.0	Yes
Pulsed	60.0	55.4	60.0	58.2	Yes
AC	26.1	27.0	27.0	26.2	Yes
6V DC	27.0	25.0	30.3	28.2	Yes
12V DC	43.0	41.5	42.5	42.3	Yes

Table 3.10 Crystallisation times in minutes of Static Nonadecane in Heptane 15g/5ml in varying field conditions at 20^{0}C.

3.2.4.2 Melting Points Static Nonadecane and Heptane 15g/5ml

Applied fields had little effect on the melting points of the nonadecane samples crystallised from solutions of nonadecane in heptane (15g/5ml) at 20^{0}C.

Melting Points (^{0}C)				
Replicates at 20^{0}C				
	1	2	3	Average
Control	32.0 - 32.6	27.4 - 30.4	29.6 - 31.7	29.9 - 31.5
500G	28.1 - 29.2	28.0 - 30.9	27.2 - 29.2	27.8 - 29.8
2500G	27.4 - 29.2	34.7 - 36.6	29.7 - 33.3	30.6 - 33.0
Pulsed	29.7 - 32.7	29.3 - 32.7	31.8 - 33.1	30.3 - 32.8
AC	32.0 - 33.9	31.1 - 31.9	31.9 - 32.9	31.6 - 32.9
6V DC	31.3 - 33.7	32.6 - 34.0	31.6 - 32.4	31.8 - 33.4
12V DC	32.2 - 33.9	32.8 - 33.8	31.8 - 32.6	32.3 - 33.4

Table 3.11 Melting Points of Static Nonadecane and Heptane 15g/5ml, crystallised at 20^{0}C under differing field conditions.

3.2.4.3 Powder XRDs Static Nonadecane and Heptane 15g/5mg

Powder X-ray diffraction was used as a means of determining whether the final crystalline state of the nonadecane wax had altered as a result of the presence of applied fields. See Table 3.47 at the end of the chapter.

3.2.5 Static Nonadecane and Heptane 10g/5ml

3.2.5.1 Crystallisation Times of Static Nonadecane in Heptane 10g/5ml

The data for the crystallisation of nonadecane from heptane 10g/5ml experiments under static conditions in different applied fields at 20^0C are in table 3.12. Standard deviation calculations were carried out to determine whether any of the differences obtained are significant. Data for the melting points of the crystals obtained are in table 3.14 and the X-ray powder diffraction data are in table 3.48. The standard deviation calculation, for a series of static nonadecane in heptane 10g/5ml crystallisation experiments gave σ =3.0 minutes.

In this study on nonadecane crystallisation the effects of applied fields are measured by the time taken for nonadecane to solidify at 20^0C. The replicate measurements show good reproducibility. The field conditions did not show a significant increase in their crystallisation. This particular data set, for 10g/5ml nonadecane and heptane, shows under all field conditions a reduction in crystallisation time. The results obtained at 20^0C are in table 3.12. The average value for the control is 41.0minutes and the spread of the results covered by 2σ for table 3.12 is 35-47minutes.

Crystallisation time in minutes					
	Replicates at 20^0C				
	1	2	3	Average	Statistically significant
Control	41.0	41.0	41.0	41.0	No
500G	35.5	35.4	35.4	35.5	No
2500G	35.5	35.4	35.5	36.0	Yes
Pulsed	30.3	27.5	29.4	28.0	Yes
AC	30.2	30.5	31.2	30.4	Yes
6V DC	31.1	30.1	31.0	30.3	Yes
12V DC	29.2	33.5	29.3	30.5	Yes

Table 3.12 Crystallisation times in minutes of Static Nonadecane in Heptane 10g/5ml in varying field conditions at 20^0C

The nonadecane in heptane 10g/5ml experiment was repeated due to the nature of the results. The results from further experimentation can be seen in Table 3.13.

Crystallisation time in minutes					
Replicates at 20^{0}C					
	1	2	3	Average	Statistically significant
Control	43.00	43.00	43.00	43.00	No
500G	38.50	37.16	40.00	38.42	No
2500G	38.00	34.45	35.31	36.20	Yes
Pulsed	34.50	37.00	37.43	36.31	Yes
AC	35.00	36.20	37.43	36.21	Yes
6V DC	32.20	31.43	36.25	33.29	Yes
12V DC	35.40	40.29	40.50	39.00	No

Table 3.13 Crystallisation times in minutes of Static Nonadecane in Heptane 10g/5ml in varying field conditions at 20^{0}C

3.2.5.2 Melting Points Static Nonadecane and Heptane 10g/5ml

Applied fields had little effect on the melting points of the nonadecane samples crystallised from solutions of nonadecane in heptane (10g/5ml) at 20^{0}C under all field conditions.

Melting Points (^{0}C)				
Replicates at 20^{0}C				
	1	2	3	Average
Control	32.0 - 33.7	31.9 - 33.9	32.1 - 33.9	32.0 - 33.8
500G	32.4 - 33.5	32.5 - 33.5	32.5 - 33.5	32.5 - 33.5
2500G	32.1 - 33.6	32.1 - 33.4	32.1 - 33.4	32.1 - 33.5
Pulsed	32.0 - 33.7	32.1 - 33.4	32.1 - 33.6	32.1 - 33.5
AC	29.5 - 32.2	29.1 - 31.5	29.6 - 31.6	29.4 - 31.8
6V DC	32.3 - 33.4	32.3 - 33.3	32.4 - 33.4	32.3 - 33.4
12V DC	32.2 - 33.2	29.0 - 31.2	30.6 - 32.0	30.6 - 32.1

Table 3.14 Melting Points, of Static Nonadecane in Heptane with 10g/5ml, crystallised at 20^{0}C under varying field conditions.

3.2.5.3 Powder XRDs Static Nonadecane in Heptane 10g/5ml

Powder X-ray diffraction was used as a means of determining whether the final crystalline state of the nonadecane wax had altered as a result of the presence of applied fields. See Table 3.48 at the end of the chapter.

3.2.6 Static Nonadecane and Heptane 5g/5ml

3.2.6.1 Crystallisation of Static Nonadecane in Heptane 5g/5ml

The data for the crystallisation of nonadecane in heptane 5g/5ml experiments under static conditions in different applied fields at 15^0C are in table 3.15. Standard deviation calculations were carried out to determine whether any of the differences obtained are significant. Data for the melting points of the crystals obtained are in table 3.16 and the X-ray powder diffraction data are in table 3.49. The standard deviation calculation for a series of static nonadecane in heptane 5g/5ml crystallisation experiments gave σ =1.5 minutes. In this study of nonadecane crystallisation, the effects of applied fields are measured by the time taken for nonadecane to solidify at 15^0C. The replicate measurements show good reproducibility. The field condition under which the crystallisation time is significantly extended is the Pulsed field by a small margin. The results obtained at 15^0C are in table 3.15. The average value for the control is 34.5 minutes and the spread of the results covered by 2σ for table 3.15 is 31-42minutes.

Crystallisation time in minutes					
Replicates at 15^0C					
	1	2	3	Av	Statistically significant
Control	34.3	36.3	34.4	34.5	No
500G	37.0	42.4	38.5	39.2	No
2500G	50.0	53.0	52.0	51.2	Yes
Pulsed	68.0	63.0	62.1	64.1	Yes
AC	56.0	56.3	57.0	56.4	Yes
6V DC	57.5	57.4	58.0	57.2	Yes
12V DC	66.0	53.0	53.0	57.2	Yes

Table 3.15 Crystallisation times in minutes of Static Nonadecane in Heptane 5g/5ml under varying field conditions

3.2.6.2. Melting Points Static Nonadecane and Heptane 5g/5ml

Applied fields had little effect on the melting points of the nonadecane samples crystallised from solutions of nonadecane in heptane (5g/5ml) under all field conditions.

Melting Points (^{0}C)				
Replicates at 15^{0}C				
	1	2	3	Av
Control	32.0 - 33.7	31.9 - 33.9	32.1 - 33.9	32.0 - 33.8
500G	32.4 - 33.5	32.5 - 33.5	32.5 - 33.5	32.5 - 33.5
2500G	32.1 - 33.6	32.1 - 33.4	32.1 - 33.4	32.1 - 33.5
Pulsed	32.0 - 33.7	32.1 - 33.4	32.1 - 33.6	32.1 - 33.5
AC	29.5 - 32.2	29.1 - 31.5	29.6 - 31.6	29.4 - 31.8
6V DC	32.3 - 33.4	32.3 - 33.3	32.4 - 33.4	32.3 - 33.4
12V DC	32.2 - 33.2	29.0 - 31.2	30.6 - 32.0	30.6 - 32.1

Table 3.16 Melting points, of Static Nonadecane and Heptane with 5g/5ml, crystallised at 15^{0}C under varying field conditions.

3.2.6.3 Powder XRDs Static Nonadecane in Heptane 5g/5ml

Powder X-ray diffraction was used as a means of determining whether the final crystalline state of the nonadecane wax had altered as a result of the presence of applied fields. See Table 3.49 at the end of the chapter.

3.2.7 Dynamic Studies Nonadecane in Heptane 20g/5ml

3.2.7.1 Crystallisation Times of Dynamic Nonadecane in Heptane 20g/5ml

The data for the crystallisation for nonadecane in heptane 20g/5ml experiments under dynamic conditions in different applied fields at 25^{0}C are in table 3.17. Standard deviation calculations were carried out to determine whether any of the differences obtained are significant. Data for the melting points of the crystals obtained are in table 3.18 and the X-ray powder diffraction data are in table 3.50. The standard deviation calculation for a series of dynamic nonadecane in heptane 20g/5ml crystallisation experiments gave σ =3.0 minutes.

In this study of nonadecane in heptane under dynamic conditions at 25 ^{0}C the results produced were of good reproducibility. The field conditions where crystallisation times were significantly extended were the pulsed and AC fields. The results obtained at 25^{0}C are in table 3.17. The average value for the control is 43.5 minutes and the spread of the results covered by 2σ for table 3.17 is 38-50 minutes.

Crystallisation time in minutes				
	Replicates at 25^{0}C			
	1	2	Av	Statistically significant
Control	43.5	43.5	43.5	No
500G	47.0	47.0	47.0	No
2500G	51.3	51.3	51.3	Yes
Pulsed	75.2	75.2	75.2	Yes
AC	68.4	68.4	68.4	Yes
6V DC	22.1	22.1	22.1	Yes
12V DC	28.4	28.4	28.4	Yes

Table 3.17 Crystallisation times in minutes of Dynamic Nonadecane in Heptane 20g/5ml under varying field conditions at 25^{0}C.

3.2.7.2 Melting Points Dynamic Nonadecane and Heptane 20g/5ml

The melting points of the nonadecane samples crystallised in applied fields were unaffected. All the melting points were reproducible and in good agreement.

Melting Points (^{0}C)					
	No. of the run				
	1	2	3	4	5
Control	32.3	33.3	32.3	32.6	32.5
500G	33.2	32.8	32.9	33.1	33.0
2500G	32.4	32.2	33.0	32.5	33.3
Pulsed	32.5	32.9	33.4	33.0	33.3
AC	33.1	32.6	33.2	32.4	32.5
6V DC	33.1	32.1	33.4	33.8	32.8
12V DC	32.7	33.0	33.6	33.3	33.3

Table 3.18 Melting Points, of Nonadecane and Heptane 20g/5ml crystallised at 25^{0}C under varying field conditions.

3.2.7.3 Powder XRDs Dynamic Nonadecane in Heptane 20g/5ml

Powder X-ray diffraction was used as a means of determining whether the final crystalline state of the nonadecane wax had altered as a result of the presence of applied fields. See Table 3.50 at the end of the chapter.

3.2.8 Dynamic Nonadecane in Heptane 15g/5ml

3.2.8.1 Crystallisation Times of Dynamic Nonadecane in Heptane 15g/5ml

The data for the crystallisation for nonadecane in heptane 15g/5ml experiments under dynamic conditions in different applied fields at 20^{0}C in table 3.2.8.1. Standard deviation calculations were carried out to determine whether any of the

differences obtained are significant. Data for the melting points of the crystals obtained are in table 3.20 and the X-ray powder diffraction data are in table 3.51. The standard deviation calculation for a series of dynamic nonadecane in heptane 15g/5ml crystallisation experiments gave σ =3.0 minutes.

In this study of nonadecane in heptane under dynamic conditions at 20 ^{0}C the results produced were of good reproducibility. The field conditions under which the crystallisation times were extended significantly were the pulsed and 12VDC fields. The results obtained at 20^{0}C are in table 3.19. The average value for the control is 23.5 minutes and the spread of the results covered by 2σ for table 3.19 is 18-30 minutes.

Crystallisation time in minutes				
Replicates at 20^{0}C				
	1	2	Av	Statistically significant
Control	23.5	23.5	23.5	No
500G	29.4	29.4	29.4	No
2500G	26.1	26.1	26.1	No
Pulsed	33.5	33.5	33.5	Yes
AC	25.0	25.0	25.0	No
6V DC	26.0	26.0	26.0	No
12V DC	44.0	44.0	44.0	Yes

Table 3.19 Crystallisation times in minutes of Dynamic Nonadecane in Heptane 15g/5ml under varying field conditions at 20^{0}C

3.2.8.2 Melting Points Dynamic Nonadecane and Heptane 15g/5ml

The melting points of the Nonadecane samples crystallised in applied fields were unaffected. All the melting points were reproducible and in good agreement.

Melting Points (^{0}C)					
	No. of the run				
	1	2	3	4	5
Control	33.0	31.9	32.2	33.1	32.6
500G	32.5	32.1	32.3	32.1	32.8
2500G	32.6	32.7	32.2	32.5	32.9
Pulsed	32.7	32.7	32.8	32.5	32.8
AC	32.7	32.7	32.8	32.5	32.8
6V DC	33.4	32.8	32.9	32.9	33.0
12V DC	32.3	32.9	32.7	33.0	32.8

Table 3.20 Melting Points, of Nonadecane and Heptane 15g/5ml crystallised at 20^{0}C under varying field conditions.

3.2.8.3 Powder XRDs Dynamic Nonadecane in Heptane 15g/5ml

Powder X-ray diffraction was used as a means of determining whether the final crystalline state of the nonadecane wax had altered as a result of the presence of applied fields. See Table 3.51 at the end of the chapter.

3.2.9 Dynamic Nonadecane in Heptane 10g/5ml

3.2.9.1 Crystallisation Times of Dynamic Nonadecane in Heptane 10g/5ml

The data for the crystallisation for nonadecane in heptane 10g/5ml experiments under Dynamic conditions in different applied fields at 20^0C are in table 3.21. Standard deviation calculations were carried out to determine whether any of the differences obtained are significant. Data for the melting points of the crystals obtained are in table 3.22 and the X-ray powder diffraction data are in table 3.52. The standard deviation calculation for the dynamic nonadecane in heptane 10g/5ml crystallisation experiments gave σ =3.0 minutes

The study of nonadecane in heptane at 20^0C showed good reproducibility. The field condition under which the crystallisation times were significantly extended was the pulsed field. Under dynamic conditions with a decreasing saturation level it can be seen that the pulsed field is the only applied field able to affect the crystallisation times. The results obtained at 20^0C are in table 3.21. The average value for the control is 23.5 minutes and the spread of the results covered by 2σ for table 3.21 is 18-30 minutes.

Crystallisation time in minutes				
	Replicates at 20^0C			
	1	2	Av	Statistically significant
Control	23.5	23.5	23.5	No
500G	25.0	25.0	25.0	No
2500G	29.3	29.3	29.3	No
Pulsed	34.5	34.5	34.5	Yes
AC	20.0	20.0	20.0	No
6V DC	20.4	20.4	20.4	No
12V DC	22.3	22.3	22.3	No

Table 3.21 Crystallisation times in minutes of Dynamic Nonadecane in Heptane 10g/5ml in varying field conditions at 20^0C.

3.2.9.2 Melting Points Dynamic Nonadecane and Heptane 10g/5ml

The melting points of the nonadecane samples crystallised in applied fields were unaffected. All the melting points were reproducible and in good agreement.

Melting Points (^{0}C)					
	No. of the run				
	1	2	3	4	5
Control	33.1	32.6	32.3	32.7	32.6
500G	32.5	33.1	32.9	32.5	32.5
2500G	32.5	33.0	32.3	32.9	32.8
Pulsed	32.4	33.2	32.8	32.7	32.6
AC	33.4	32.6	32.7	33.2	32.5
6V DC	32.7	32.7	32.7	32.4	32.7
12V DC	33.9	33.7	33.9	32.8	32.4

Table 3.22 Melting Points, of Nonadecane and Heptane 10g/5ml crystallised at 20^{0}C under varying field conditions.

3.2.9.3 Powder XRDs Dynamic Nonadecane in Heptane 10g/5ml

Powder X-ray diffraction was used as a means of determining whether the final crystalline state of the nonadecane wax had altered as a result of the presence of applied fields. See Table 3.52 at the end of the chapter.

3.2.10 Dynamic Studies Nonadecane in Heptane 5g/5ml

3.2.10.1 Crystallisation Times of Dynamic Nonadecane in Heptane 5g/5ml

The data for the crystallisation for nonadecane in heptane 5g/5ml experiments under dynamic conditions in different applied fields at 15^{0}C are in table 3.23. Standard deviation calculations were carried out to determine whether any of the differences obtained are significant. Data for the melting points of the crystals obtained are in table 3.24 and the X-ray powder diffraction data are in table 3.53. The standard deviation calculation for a series of dynamic nonadecane in heptane 5g/5ml crystallisation experiments gave σ =3.0 minutes

The results from the crystallisation of nonadecane in heptane at 15^{0}C, produces results with good reproducibility. The field conditions under which the crystallisation times are marginally extended but are statistically significant are the 2500G and the Pulsed fields. The field condition, under which the crystallisation time is most significantly reduced, is the AC field. The results obtained at 15^{0}C are in table 3.23. The average value for the control is 28.1 minutes and the spread of the results covered by 2σ for table 3.23 is 22-34 minutes.

Crystallisation time in minutes				
Replicates at 15^{0}C				
	1	2	Av	Statistically significant
Control	28.1	28.1	28.1	No
500G	28.2	28.2	28.2	No
2500G	33.1	33.1	33.1	No
Pulsed	33.4	33.4	33.4	No
AC	17.0	17.0	17.0	Yes
6V DC	23.3	23.3	23.3	No
12V DC	21.2	21.2	21.2	No

Table 3.23 Crystallisation times in minutes of Dynamic Nonadecane in Heptane 5g/5ml in varying field conditions at 15^{0}C.

3.2.10.2 Melting Points Dynamic Nonadecane and Heptane 5g/5ml

The melting points of the nonadecane samples crystallised in applied fields were unaffected. All the melting points were reproducible and in good agreement.

Melting Points (^{0}C)					
	No. of the run				
	1	2	3	4	5
Control	32.4	32.1	33.3	33.3	33.0
500G	32.1	32.3	32.9	32.6	33.6
2500G	33.6	33.4	33.0	33.2	33.7
Pulsed	32.4	33.2	32.8	32.7	32.6
AC	33.1	33.0	33.0	33.5	33.2
6V DC	32.4	32.9	32.2	33.0	32.7
12V DC	32.4	33.0	32.9	32.8	32.7

Table 3.24 Melting Points, of Nonadecane and Heptane 5g/5ml crystallised at 15^{0}C under varying field conditions.

3.2.10.3 Powder XRDs Static Nonadecane in Heptane 5g/5ml

Powder X-ray diffraction was used as a means of determining whether the final crystalline state of the nonadecane wax had altered as a result of the presence of applied fields. See Table 3.53 at the end of the chapter.

3.2.11 Static Nonadecane and Heneicosane 50:50

3.2.11.1 Crystallisation Times of Static Nonadecane and Heneicosane 50:50

The data from the crystallisation of nonadecane and heneicosane systems for experiments under static conditions in different applied fields at 10^{0}C are in table 3.25. Standard deviation calculations were carried out to determine whether any of

the differences obtained are significant. Data for the melting points of the crystals obtained are in table 3.26 and the X-ray powder diffraction data are in table 3.54. The standard deviation calculation for the static of nonadecane and heneicosane crystallisation experiments gave σ =3.0 minutes.

In this study of nonadecane and heneicosane combined at 10^0C, the effect of applied fields is considered on a complex system. The field condition under which the crystallisation time is extended is the pulsed field. The field condition under which the crystallisation time is significantly reduced is the AC field. The results obtained at 20^0C are in table 3.25. The average value for the control is 33.5 minutes and the spread of the results covered by 2σ for table 3.25 is 28-40minutes.

Crystallisation time in minutes					
Replicates at 10^0C					
	1	2	3	Av	Statistically significant
Control	33.5	33.5	33.5	33.5	No
500G	29.0	28.2	29.4	28.4	No
2500G	27.1	27.4	28.0	27.3	No
Pulsed	48.0	44.0	48.2	46.2	Yes
AC	22.0	22.5	23.3	22.2	Yes
6V DC	30.2	31.5	32.5	31.4	No
12V DC	29.3	33.1	25.1	29.2	No

Table 3.25 Crystallisation times in minutes of Static Nonadecane and Heneicosane 50:50 in varying field conditions at 10^0C.

3.2.11.2 Melting points of Static Nonadecane and Heneicosane 50:50

Applied fields had little effect on the melting points of the nonadecane and heneicosane samples crystallised under all field conditions.

Melting Points (^{0}C)			
	No. of the run		
	1	2	Av
Control	36.0	36.6	36.3
500G	37.4	37.1	37.3
2500G	36.0	36.1	36.1
Pulsed	36.5	35.7	36.1
AC	-	-	-
6V DC	36.2	36.3	36.3
12V DC	36.1	36.0	36.0

Table 3.26. Melting points, of Nonadecane and Heneicosane crystallised at 10^0C under varying field conditions.

3.2.11.3 Powder XRDs Static Nonadecane and Heneicosane 50:50

Powder X-ray diffraction was used as a means of determining whether the final crystalline state of the nonadecane wax had altered as a result of the presence of applied fields. See Table 3.54 at the end of the chapter

3.2.12 Dynamic Nonadecane and Heneicosane

3.2.12.1 Crystallisation Times of Dynamic Nonadecane and Heneicosane 50:50

The data for the crystallisation for of nonadecane and heneicosane experiments under dynamic conditions in different applied fields at 10^0C are in table 3.27. Standard deviation calculations were carried out to determine whether any of the differences obtained are significant. Data for the melting points of the crystals obtained are in table 3.28 and the X-ray powder diffraction data is in table 3.55. The standard deviation calculation for a series of dynamic of nonadecane and heneicosane crystallisation experiments gave σ =3.0 minutes

This study examines how a complex system such as nonadecane and heneicosane performs under dynamic conditions. The field condition under which the crystallisation time is significantly extended is the pulsed field. The results obtained at 10^0C are in table 3.27. The average value for the control is 22.0 minutes and the spread of the results covered by 2σ for table 3.27 is 16-28 minutes.

Crystallisation time in minutes				
Replicates at 10^0C				
	1	2	Av	Statistically significant
Control	22.0	22.0	22.0	No
500G	27.3	27.3	27.3	No
2500G	30.2	30.2	30.2	Yes
Pulsed	66.0	66.0	66.0	Yes
AC	35.1	35.1	35.1	Yes
6V DC	32.1	32.1	32.1	Yes
12V DC	41.3	41.3	41.3	Yes

Table 3.27 Crystallisation times of Dynamic Nonadecane and Heneicosane 50:50 in varying field conditions at 10^0C

3.2.12.2 Melting Points of Dynamic Nonadecane and Heneicosane 50:50

The melting points of the Nonadecane samples crystallised in applied fields were unaffected. All the melting points were reproducible and in good agreement.

Melting Points (^{0}C)					
	No. of the run				
	1	2	3	4	5
Control	36.0	36.1	35.4	35.7	36.0
500G	37.3	35.8	36.3	35.5	36.6
2500G	36.3	35.7	35.7	35.5	35.0
Pulsed	36.2	6.3	38.2	38.6	38.7
AC	37.4	37.8	37.2	38.0	37.4
6V DC	38.6	37.6	37.1	37.1	37.5
12V DC	35.9	36.1	36.1	36.2	36.0

Table 3.28 Melting Points, of Dynamic Nonadecane and Heneicosane crystallised at 10^0C under varying field conditions.

3.2.12.3 Powder XRDs Dynamic Nonadecane and Heneicosane 50:50

Powder X-ray diffraction was used as a means of determining whether the final crystalline state of the nonadecane wax had altered as a result of the presence of applied fields. See Table 3.55 at the end of the chapter.

3.2.13 Static Nonadecane and Heneicosane in Heptane

3.2.13.1 Crystallisation Times of Static Nonadecane and Heneicosane in Heptane

The data for the crystallisation for of nonadecane and heneicosane in heptane experiments under static conditions in different applied fields at 10^0C are in table 3.29. Standard deviation calculations were carried out to determine whether any of the differences obtained are significant. Data for the melting points of the crystals obtained are in table 3.30 and the X-ray powder diffraction data are in table 3.56. The standard deviation calculation for a series of static of nonadecane and heneicosane in heptane crystallisation experiments gave σ =3.0 minutes.

In this study the effect of applied fields on a complex system in a solvent is measured using crystallisation times. The field conditions under which the crystallisation times are significant are 2500G, Pulsed, AC, 6V DC and 12V DC. The results obtained at 10^0C are in table 3.29. The average value for the control is 20.3 minutes and the spread of the results covered by 2σ for table 3.29 is 14-26 minutes.

Crystallisation time in minutes					
Replicates at 10^0C					
	1	2	3	Av	Statistically significant
Control	20.2	20.4	21.1	20.3	No
500G	24.3	25.1	24.2	24.3	No
2500G	33.3	35.2	29.4	32.4	Yes
Pulsed	33.1	32.3	33.0	32.3	Yes
AC	30.0	29.2	29.4	29.3	Yes
6V DC	28.2	30.1	31.0	29.2	Yes
12V DC	34.0	26.3	27.0	29.1	Yes

Table 3.29 Crystallisation times in minutes of Static Nonadecane and Heneicosane in Heptane in varying field conditions at 10^0C.

3.2.13.2 Melting Points of Static Nonadecane, Heneicosane in Heptane

Applied fields had little effect on the melting points of the nonadecane and heneicosane samples crystallised under all field conditions.

Melting Points (^{0}C)			
	No. of the run		
	1	2	Av
Control	36.0	36.6	36.3
500G	35.8	35.8	35.8
2500G	35.9	36.2	36.0
Pulsed	35.9	36.0	36.0
AC	35.7	36.4	36.0
6V DC	35.9	36.5	36.7
12V DC	35.9	36.6	36.2

Table 3.30 Melting Points of Static Nonadecane and Heneicosane in Heptane at 10^0C under varying field conditions.

3.2.13.3 Powder XRDs of Static Nonadecane, Heneicosane in Heptane

Powder X-ray diffraction was used as a means of determining whether the final crystalline state of the nonadecane wax had altered as a result of the presence of applied fields. See Table 3.56 at the end of the chapter.

3.2.14 Dynamic Studies Nonadecane and Heneicosane in Heptane

3.2.14.1 Crystallisation Times of Dynamic Nonadecane and Heneicosane in Heptane

The data for the crystallisation for of nonadecane and heneicosane in heptane experiments under dynamic conditions in different applied fields at 10^0C are in table 3.31. Standard deviation calculations were carried out to determine whether any of the differences obtained are significant. Data for the melting points of the crystals obtained are in table 3.32 and the X-ray powder diffraction data is in table 3.57. The standard deviation calculation for the series of static nonadecane and heneicosane in heptane crystallisation experiments gave $\sigma = 3.0$ minutes

The results of this study show that the field conditions under which the crystallisation time is significantly extended is the pulsed fields by a small margin. The results obtained at 10^0C are in table 3.31. The average value for the control is 22.4 minutes and the spread of the results covered by 2σ for table 3.31 is 16-28 minutes.

Crystallisation time in minutes				
Replicates at 10^0C				
	1	2	Av	Statistically significant
Control	22.4	22.4	22.4	Yes
500G	25.2	25.2	25.2	No
2500G	32.1	32.1	32.1	Yes
Pulsed	33.0	33.0	33.0	Yes
AC	21.5	21.5	21.5	No
6V DC	29.1	29.1	29.1	Yes
12V DC	29.4	29.43	29.4	Yes

Table 3.31 Crystallisation times in minutes of Dynamic Nonadecane and Heneicosane in Heptane in varying field conditions at 10^0C.

3.2.14.2 Melting Points of Dynamic Nonadecane and Heneicosane in Heptane

The melting points of the nonadecane samples crystallised in applied fields were unaffected. All the melting points were reproducible and in good agreement.

	Melting Points (^{0}C)				
	No. of the run				
	1	2	3	4	5
Control	36.8	36.2	35.7	36.5	36.3
500G	35.7	35.6	35.9	36.4	36.0
2500G	36.6	36.3	36.3	36.6	36.0
Pulsed	36.8	36.1	36.5	35.8	36.7
AC	36.0	36.9	35.8	36.9	35.6
6V DC	35.6	36.2	35.7	35.8	36.7
12V DC	36.7	35.9	36.5	36.2	36.0

Table 3.32 Melting Points of Nonadecane and Heneicosane in Heptane crystallised at 10^{0}C under varying field conditions

3.2.14.3 Powder XRDs of Dynamic Nonadecane and Heneicosane in Heptane

Powder X-ray diffraction was used as a means of determining whether the final crystalline state of the nonadecane wax had altered as a result of the presence of applied fields. See Table 3.57 at the end of the chapter.

3.2.15 Static Nonadecane and Crude Oil Studies

3.2.15.1 Crystallisation Times of Static Nonadecane Crude Oil

The data for the crystallisation of nonadecane from crude oil in experiments under static conditions in different applied fields at 10^{0}C are in table 3.33. Standard deviation calculations were carried out to determine whether any of the differences obtained are significant. Data for the melting points of the crystals obtained are in table 3.34 and the X-ray powder diffraction data are in table 3.58. The standard deviation calculation for a series of static crude oil and nonadecane crystallisation experiments gave σ =3.0 minutes. In this study the effect of applied fields on a crude oil system was investigated. The field conditions under which the crystallisation times are most significantly extended are the 2500G and the pulsed fields. The results obtained at 10^{0}C are in table 3.33. The average value for the control is 52.2 minutes and the spread of the results covered by 2σ for table 3.33 is 46-58 minutes.

Crystallisation times in minutes					
Replicates at 22.5^{0}C					
	1	2	3	Av	Statistically significant
Control	41.1	57.3	58.0	52.2	No
500G	47.5	50.2	52.5	49.5	No
2500G	62.0	90.0	82.1	78.1	Yes
Pulsed	152.0	156.2	165.0	157.2	Yes
AC	66.2	52.2	56.2	58.3	No
6V DC	58.1	59.1	63.0	60.1	Yes
12V DC	54.1	54.3	55.1	54.3	No

Table 3.33 Crystallisation times in minutes of Static Nonadecane and Crude oil in varying field conditions at 22.5^{0}C.

3.2.15.2 Melting Points of Static Nonadecane and Crude Oil

Applied fields had little effect on the melting points of the nonadecane and heneicosane samples crystallised under all field conditions.

Melting Points (^{0}C)			
	No. of the run		
	1	2	Av
Control	36.2	31.3	33.8
500G	30.7	29.3	30.1
2500G	29.8	30.1	30.0
Pulsed	30.7	29.4	30.1
AC	29.6	28.4	29.1
6V DC	29.6	29.1	29.5
12V DC	29.6	29.0	29.3

Table 3.34 Melting Points of Static Nonadecane and Crude oil crystallised at 22.5^{0}C under varying field conditions.

3.2.15.3 Powder XRDs Static Nonadecane and Crude oil

Powder X-ray diffraction was used as a means of determining whether the final crystalline state of the nonadecane wax had altered as a result of the presence of applied fields. See Table 3.58 at the end of the chapter.

3.2.16 Dynamic Nonadecane and Crude oil

3.2.16.1 Crystallisation Times of Dynamic Nonadecane and Crude oil

The data for the crystallisation of crude oil and nonadecane experiments under dynamic conditions in different applied fields at 22.5^{0}C are in table 3.35. Standard

deviation calculations were carried out to determine whether any of the differences obtained are significant. Data for the melting points of the crystals obtained are in table 3.36 and the X-ray powder diffraction data are in table 3.59. The standard deviation calculation for a series of dynamic crude oil and nonadecane crystallisation experiments gave σ =3.0 minutes

In this study the field condition under which the crystallisation time is most significantly extended is the pulsed field. The results obtained at 22.5^{0}C are in table 3.33. The average value for the control is 32.0 minutes and the spread of the results covered by 2σ for table 3.33 is 26-38 minutes

	Replicates at 22.5^{0}C			
	1	2	Av	Statistically significant
Control	32.0	32.0	32.0	Yes
500G	33.2	33.2	33.2	No
2500G	42.5	42.5	42.5	Yes
Pulsed	65.0	65.0	65.0	Yes
AC	42.2	42.2	42.2	Yes
6V DC	55.3	55.3	55.3	Yes
12V DC	47.0	47.0	47.0	Yes

Table 3.35 Crystallisation times in minutes of Dynamic Nonadecane and Crude oil at varying field conditions at 22.5^{0}C.

3.2.16.2 Melting Points of Dynamic Nonadecane and Crude oil

The melting points of the Nonadecane samples crystallised in applied fields were unaffected. All the melting points were reproducible and in good agreement.

	Melting Points (^{0}C)				
	No. of the run				
	1	2	3	4	5
Control	30.6	25.6	24.4	29.5	27.6
500G	28.3	27.7	27.8	28.8	26.7
2500G	27.1	29.1	29.7	27.9	28.4
Pulsed	30.0	28.2	24.0	30.3	29.5
AC	29.5	28.8	30.2	28.3	25.2
6V DC	28.4	28.9	27.4	29.4	30.2
12V DC	30.0	28.2	24.0	30.3	29.5

Table 3.36 Melting Points of Dynamic Nonadecane and Crude oil crystallised at 22.5^{0}C under varying field conditions.

3.2.16.3 Powder XRDs Dynamic Nonadecane and Crude Oil

Powder X-ray diffraction was used as a means of determining whether the final crystalline state of the nonadecane wax had altered as a result of the presence of applied fields. See Table 3.59 at the end of the chapter. The results described in this chapter are discussed in chapter 4

Tables of X-ray Diffraction Data For All Experimental Set-Ups.

Table 3.37 Powder XRDs Static Nonadecane Experiment 1

Reference		Sample no.	Control 20^{0}C		Control 22.5^{0}C		Control 25^{0}C	
d (i) Å	I/I (i)		d (i) Å	I/I (i)	d (i) Å	I/I (i)	d (i) Å	I/I (i)
8.630	16	1	8.531	13	8.774	7	8.528	7
		2	8.549	14	8.427	9	8.334	7
		3	8.503	8	8.526	9	8.325	5
6.482	24	1	6.429	4	6.399	5	6.308	4
		2	6.440	8	6.377	44	6.306	4
		3	6.455	6	6.243	6	6.302	3
5.197	21	1	5.162	5	5.106	3	4.942	5
		2	5.161	5	5.340	4	5.203	5
		3	5.015	4	5.164	4	5.443	6
4.103	100	1	4.107	100	4.105	100	4.097	100
		2	4.116	100	4.095	100	4.043	100
		3	4.126	100	4.046	100	4.100	100
3.699	49	1	3.646	64	3.715	26	3.703	39
		2	3.714	38	3.708	32	3.646	25
		3	3.664	61	3.689	57	3.705	30

Table 3.37 Powder X-ray Diffraction data on the samples obtained from Static Nonadecane Experiment 1.

Table 3.38 Powder XRDs Static Nonadecane Experiment 2

Reference		Sample no.	500G at 20^{0}C		500G at 22.5^{0}C		500G at 25^{0}C	
d (i) Å	I/I (i)		d (i) Å	I/I (i)	D (i) Å	I/I (i)	d (i) Å	I/I (i)
8.630	16	1	8.505	10	8.535	16	8.661	29
		2	8.506	6	8.637	25	8.715	42
		3	8.482	6	8.603	14	8.250	15
6.482	24	1	6.334	6	6.446	9	6.622	11
		2	6.440	4	6.489	14	6.643	15
		3	-	-	6.481	8	6.598	10
5.197	21	1	5.178	4	5.153	6	5.215	7
		2	4.607	3	5.179	9	5.221	5
		3	5.247	7	5.186	5	5.244	7
4.103	100	1	4.100	100	4.153	100	4.167	100
		2	4.116	100	4.153	100	4.300	100
		3	4.104	100	4.171	100	4.189	100
3.699	49	1	3.717	46	3.719	40	3.757	37
		2	3.678	27	3.769	60	3.954	30
		3	3.772	43	3.773	47	3.784	38

Table 3.38 Powder X-ray Diffraction data on samples obtained from static Nonadecane Experiment 2

Table 3.39 Powder XRDs Static Nonadecane Experiment 3

Reference		Sample no	2500G at 20^0C		2500G at 22.5^0C		2500G at 25^0C	
d (i) Å	I/I (i)		d (i) Å	I/I (i)	d (i) Å	I/I (i)	d (i) Å	I/I (i)
8.630	16	1	8.881	10	8.864	40	8.618	11
		2	8.703	26	8.693	21	8.347	15
		3	8.500	20	8.676	22	8.543	12
6.482	24	1	6.627	14	6.520	20	6.417	8
		2	6.527	13	6.584	9	6.474	6
		3	6.408	1	6.504	13	6.417	8
5.197	21	1	5.275	8	5.215	10	5.149	6
		2	5.210	8	5.261	5	5.106	6
		3	5.157	8	5.204	7	5.148	5
4.103	100	1	4.192	100	4.259	100	4.126	10
		2	4.153	100	4.210	100	4.121	100
		3	4.091	100	4.152	100	4.136	100
3.699	49	1	3.760	37	3.841	46	3.713	50
		2	3.731	37	3.829	26	3.703	58
		3	3.732	29	3.707	48	3.710	51

Table 3.39 Powder X-ray Diffraction data on samples obtained from static Nonadecane Experiment 3

Table 3.40 Powder XRDs Static Nonadecane Experiment 4

Reference		Sample. no.	Pulsed at 20^0C		Pulsed at 22.5^0C		Pulsed at 25^0C	
d (i) Å	I/I (i)		d (i) Å	I/I (i)	d (i) Å	I/I (i)	d (i) Å	I/I (i)
8.630	16	1	8.582	18	8.323	6	8.755	28
		2	8.662	24	8.665	11	8.804	60
		3	8.796	29	8.715	26	.909	89
6.482	24	1	6.472	11	6.295	5	6.556	17
		2	6.504	13	6.515	6	6.594	38
		3	6.572	18	6.500	10	6.639	78
5.197	21	1	5.169	6	5.149	3	5.231	9
		2	5.210	7	5.163	3	5.254	18
		3	5.181	8	5.189	9	5.291	34
4.103	100	1	4.146	100	4.109	100	4.913	100
		2	4.160	100	4.132	100	4.174	100
		3	4.127	100	4.182	100	4.199	100
3.699	49	1	3.731	35	3.732	29	3.740	28
		2	3.727	18	3.734	25	3.747	20
		3	3.777	22	3.760	46	3.765	40

Table 3.40 Powder X-ray Diffraction data on samples obtained from static Nonadecane Experiment 4

Table 3.41 Powder XRDs Static Nonadecane Experiment 5

Reference		Sample no.	AC at 20^0C		AC at 22.5^0C		AC at 25^0C	
d (i) Å	I/I (i)		d (i) Å	I/I (i)	d (i) Å	I/I (i)	d (i) Å	I/I (i)
8.630	16	1	8.811	11	8.651	11	7.692	10
		2	8.821	10	8.537	9	8.716	11
		3	8.822	15	8.590	11	8.543	13
6.482	24	1	6.551	10	6.507	7	6.542	7
		2	6.505	10	6.462	5	6.490	8
		3	6.581	9	6.502	6	6.436	9
5.197	21	1	5.181	5	5.203	5	5.162	5
		2	5.206	6	5.176	4	5.147	6
		3	5.152	4	5.205	4	5.163	5
4.103	100	1	4.150	100	4.129	100	4.143	100
		2	4.151	100	4.115	100	4.124	100
		3	4.170	100	4.104	100	4.135	100
3.699	49	1	3.731	40	3.727	37	3.734	43
		2	3.728	38	3.729	35	3.735	36
		3	3.749	56	3.699	47	3.735	26

Table 3.41 Powder X-ray Diffraction data on samples obtained from static Nonadecane Experiment 5

Table 3.42 Powder XRDs Static Nonadecane Experiment 6

Reference		Sample no.	6V DC at 20^0C		6V DC at 22.5^0C		6V DC at 25^0C	
d (i) Å	I/I (i)		d (i) Å	I/I (i)	d (i) Å	I/I (i)	d (i) Å	I/I (i)
8.630	16	1	.811	47	8.620	24	8.619	8
		2	8.821	70	8.863	27	8.767	3
		3	8.822	15	8.604	25	8.644	35
6.482	24	1	6.551	28	6.479	18	6.476	10
		2	6.505	54	6.633	16	6.565	12
		3	6.581	10	6.532	18	6.478	21
5.197	21	1	5.181	16	5.264	7	5.189	6
		2	5.206	35	5.310	5	5.250	
		3	5.152	6	5.244	7	5.199	1
4.103	100	1	4.150	100	4.173	100	4.180	100
		2	4.151	100	4.195	100	4.189	100
		3	4.170	100	4.194	100	4.161	100
3.699	49	1	3.731	32	3.782	38	3.758	40
		2	3.728	37	3.772	51	3.766	28
		3	3.749	30	3.775	42	3.759	37

Table 3.42 Powder X-ray Diffraction data on samples obtained from static Nonadecane Experiment 6

Table 3.43 Powder XRDs Static Nonadecane Experiment 7

Reference		Sample no.	12V DC at 20^{0}C		12V DC at 22.5^{0}C		12V DC at 25^{0}C	
d (i) Å	I/I (i)		d (i) Å	I/I (i)	d (i) Å	I/I (i)	d (i) Å	I/I (i)
8.630	16	1	8.466	6	8.461	10	8.533	16
		2	8.778	6	8.963	21	8.806	41
		3	9.021	13	8.469	11	8.864	73
6.482	24	1	6.401	4	6.375	5	6.427	16
		2	6.651	4	6.370	18	6.606	23
		3	6.702	8	6.342	6	6.599	46
5.197	21	1	5.142	4	-	-	5.172	6
		2	5.289	3	5.359	12	5.262	13
		3	5.336	7	5.341	14	5.258	30
4.103	100	1	4.100	100	4.129	100	4.138	100
		2	4.127	100	4.210	100	4.189	100
		3	4.219	100	4.126	100	4.196	100
3.699	49	1	3.630	11	3.762	41	3.742	37
		2	3.771	17	3.773	46	3.753	40
		3	3.810	53	3.769	42	3.770	57

Table 3.43 Powder X-ray Diffraction data on samples obtained from static Nonadecane Experiment 7

Table 3.44 Powder XRDs Static Nonadecane Further Analysis

	Control			Pulsed	
	2θ	d space	Index	d space	2θ
1	6.72	13.139	004	13.475	6.55
2	10.1	8.748	006	8.896	9.94
3	13.51	6.551	008	6.633	13.34
4			0010	5.292	16.74
5	20.98	4.231	110	4.295	20.67
6	22.96	3.871	0014,200	3.903	22.77

Table 3.44 Powder X-ray Diffraction data on samples obtained from static Nonadecane Experiments, which were further analysed.

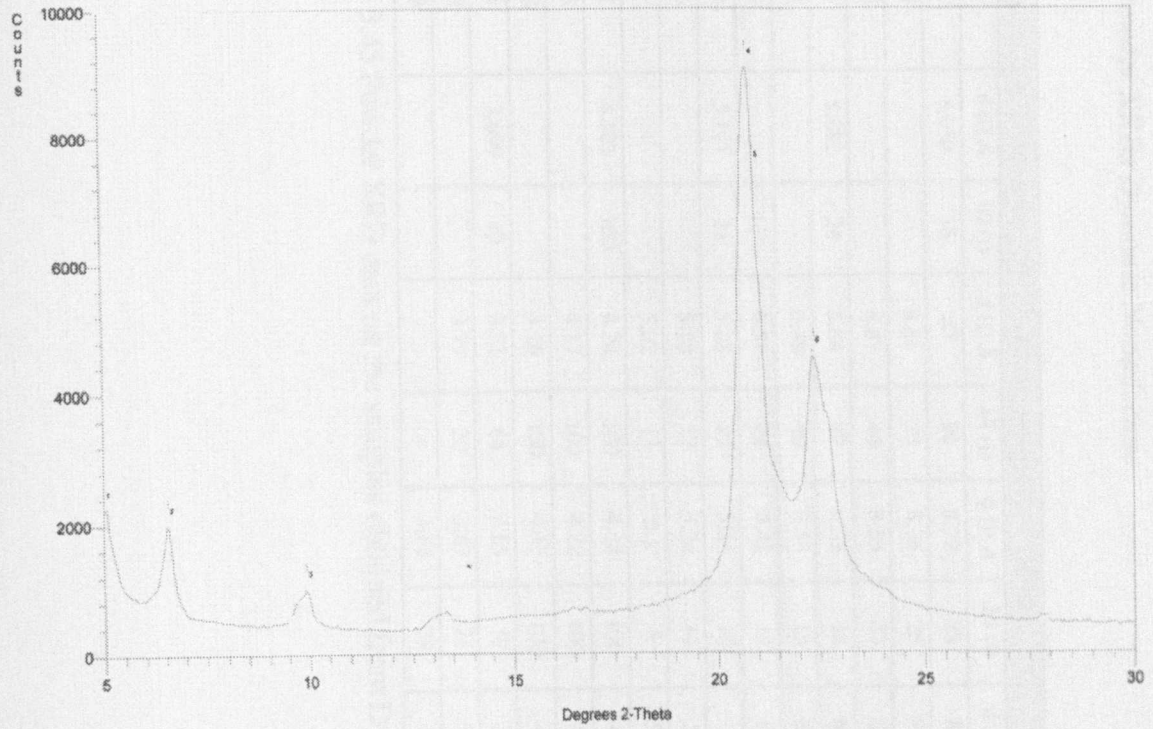

Figure 3.2 Powder X-ray Diffraction data on samples obtained from Static Pulsed Nonadecane Experiments

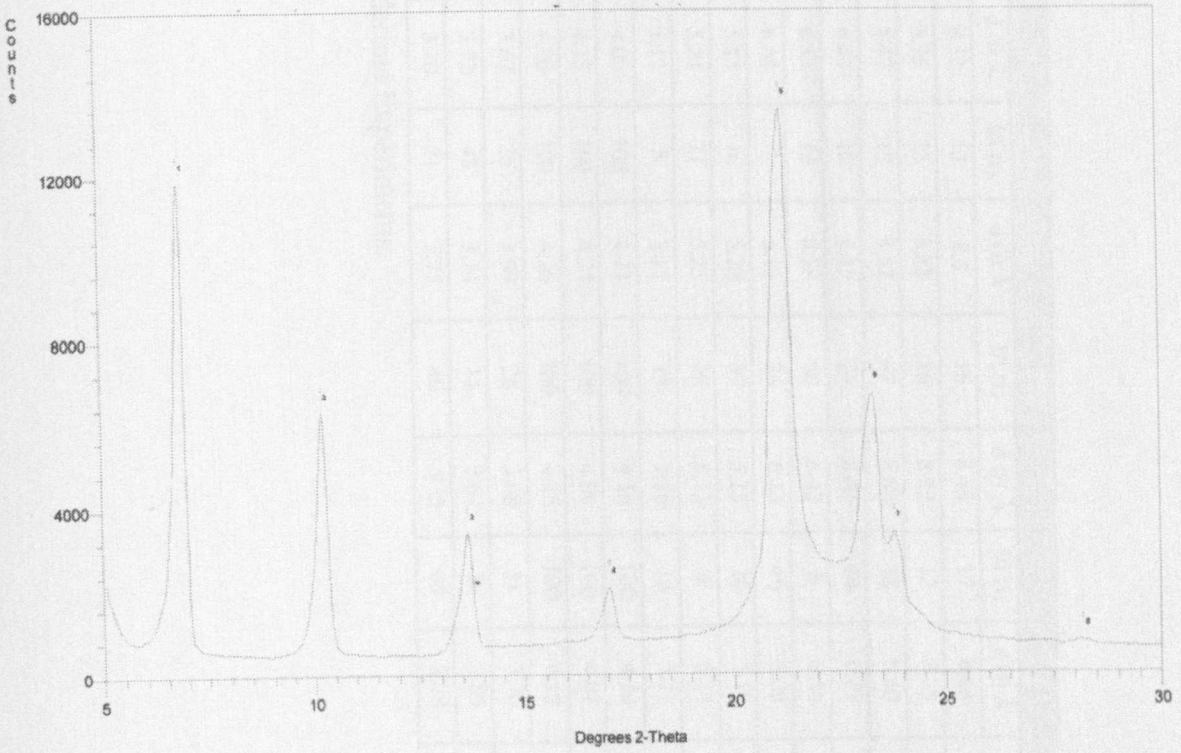

Figure 3.3 Powder X-ray Diffraction data on samples obtained from Static Control Nonadecane Experiments

3.45 Powder XRDs Dynamic Nonadecane

Sample no.	Nonadecane		Control		500G		2500G		Pulsed		AC Magnet		6V DC		12V DC	
	d (i) Å	I/I (i)	d (i) Å	I/I (i)	d (i) Å	I/I (i)	d (i) Å	I/I (i)	d (i) Å	I/I (i)	d (i) Å	I/I (i)	d (i) Å	I/I (i)	d (i) Å	I/I (i)
1	8.630	16	87	91	8.72	28	8.60	20	8.52	12	8.8	16	8.48	17	8.64	100
5			8.61	55	8.76	25	8.73	17	8.75	25	8.82	16	8.52	12	8.75	100
8			8.67	44	8.53	23	8.57	39	8.47	17	8.57	47	8.64	18	8.60	58
1	6.482	24	6.64	47	6.53	18	6.61	12	6.42	10	6.43	24	6.41	44	6.49	49
5			6.48	40	6.55	15	6.53	10	6.53	16	6.58	60	6.42	8	6.56	44
7			6.51	24	6.43	12	6.45	24	6.44	7	6.46	26	6.43	40	6.38	40
8	5.197	21	5.28	23	5.21	12	5.2	8	5.13	16	5.23	37	5.15	20	5.19	24
5			5.18	27	5.24	11	5.22	8	5.24	21	5.25	28	5.13	6	5.24	18
			5.22	13	5.1	8	5.21	14	5.12	5	5.17	15	5.16	18	5.11	29
1	4.103	100	4.24	100	4.14	100	4.21	100	4.09	100	4.21	100	4.16	100	4.19	54
5			4.17	100	4.22	100	4.20	100	4.15	100	4.24	100	4.09	100	4.01	19
8			4.16	100	4.15	100	4.13	100	4.08	100	4.16	100	4.15	100	4.18	51
1	3.699	49	3.71	64	3.65	17	3.69	4	3.67	36	3.69	26	3.68	31	3.70	10
5			3.77	20	3.67	21	3.75	25	3.72	48	3.74	14	3.67	36	3.85	50
8					3.81	39	3.72	46	3.70	21	3.75	40	3.73	40	3.73	40

Table 3.45 Powder XRD data on the samples obtained from Dynamic Nonadecane Experiments.

3.46 Powder XRDs Static Nonadecane and Heptane 20g/5ml

Sample no.	Nonadecane		Control		500G		2500G		Pulsed		AC Magnet		6V DC		12V DC	
	d (i) Å	I/I (i)	d (i) Å	I/I (i)	d (i) Å	I/I (i)	d (i) Å	I/I (i)	d (i) Å	I/I (i)	d (i) Å	I/I (i)	d (i) Å	I/I (i)	d (i) Å	I/I (i)
1	8.630	16	8.561	14	8.550	16	8.628	27	8.747	16	8.324	15	8.678	35	8.912	2
2			8.646	11	8.754	12	8.517	17	8.433	21	8.648	11	8.507	15	8.615	15
3			8.646	12	8.937	7	8.884	22	8.703	26	8.340	7	8.701	17	8.830	27
1	6.482	24	6.450	7	6.245	19	6.485	15	6.544	10	6.306	7	6.497	23	6.732	17
2			6.492	7	6.554	7	6.512	8	6.521	13	6.299	5	6.666	13	6.481	12
3			6.812	6	6.637	5	6.633	12	6.521	16	6.593	14	6.633	9	6.595	18
1	5.197	21	5.172	5	5.035	12	5.187	10	5.232	7	5.174	4	5.204	16	5.352	14
2			5.193	5	5.269	5	5.192	6	5.133	8	5.072	4	5.157	12	5.192	10
3			5.190	5	5..286	4	5.202	8	5.209	13	5.256	9	5.167	7	5.291	11
1	4.103	100	4.132	100	4.148	100	4.157	100	4.136	100	4.187	100	4.192	100	4.189	100
2			4.170	100	4.131	100	4.200	100	4.157	100	4.116	100	4.168	100	4.192	100
3			4.235	100	4.230	100	4.251	100	4.273	100	4.223	100	4.224	100	4.252	100
1	3.699	49	3.764	37	3.744	28	3.677	73	3.768	45	3.759	90	3.224	55	3.750	44
2			3.791	19	3.757	25	3.731	34	3.746	23	3.681	22	3.747	34	3.762	49
3			3.876	15	3.792	44	3.765	46	3.781	1	3.688	38	3.875	41	3.795	32

Table 3.46 Powder XRD data on the samples obtained from Static Nonadecane and Heptane Experiments

3.47 Powder XRDs Static Nonadecane in Heptane 15g/5ml

Sample no.	Nonadecane		Control		500G		2500G		Pulsed		AC Magnet		6V DC		12V DC	
	d (i) Å	I/I (i)	d (i) Å	I/I (i)	d (i) Å	I/I (i)	d (i) Å	I/I (i)	d (i) Å	I/I (i)	d (i) Å	I/I (i)	d (i) Å	I/I (i)	d (i) Å	I/I (i)
1	8.630	16	8.832	12	9.374	12	8.545	15	8.746	14	8.637	7	8.859	13	8.887	6
2			8.913	83	8.874	33	8.835	12	8.856	10	8.756	21	8.587	13	8.848	35
3			8.894	83	8.940	29	8.766	23	9.090	31	8.838	13	8.721	12	8.773	32
1	6.482	24	6.602	8	-	-	6.438	8	-	-	6.714	4	6.607	7	6.645	4
2			6.642	48	6.614	21	6.558	7	6.638	7	-	-	6.452	8	6.630	23
3			6.619	2	6.652	21	6.563	13	6.776	25	6.576		6.591	7	6.581	23
1	5.197	21	5.226	6	-	-	5.186	6	-	-	-	-	5.276	6	5.302	3
2			5.295	30	-	-	5.241	5	5.296	4	-	-	5.176	3	5.287	16
3			5.268	34	-	-	5.248	9	5.279	5	-	-	5.198		5.246	12
1	4.103	100	4.139	100	4.235	100	4.177	100	4.133	100	4.078	100	4.210	100	4.146	100
2			4.224	100	4.241	100	4.231	100	4.183	100	4.129	100	4.167	100	.214	100
3			4.243	100	4.305	100	4.170	100	4.348	100	4.180	100	4.188	100	4.779	100
1	3.699	49	3.763	29	3.746	37	3.763	34	3.813	40	3.728	35	3.737	39	3.742	24
2			3.791	19	3.375	52	3.769	35	3.741	36	3.763	34	3.743	32	3.773	55
3			3.876	15	3.858	68	3.780	39	3.927	39	3.789	24	3.739	35	3.820	41

Table 3.47 Powder X-ray Diffraction data on the samples obtained from Nonadecane in Heptane Experiments carried out at 20^0C

3.48 Powder XRDs Static Nonadecane in Heptane 10g/5ml

Sample no.	Nonadecane		Control		500G		2500G		Pulsed		AC Magnet		6V DC		12V DC	
	d (i) Å	I/I (i)	d (i) Å	I/I (i)	d (i) Å	I/I (i)	d (i) Å	I/I (i)	d (i) Å	I/I (i)	d (i) Å	I/I (i)	d (i) Å	I/I (i)	d (i) Å	I/I (i)
1	8.630	16	8.869	30	8.630	11	8.797	9	8.841	16	9.373	9	8.750	12	8.293	14
2			8.755	28	8.629	16	8.812	24	9.041	63	8.824	12	8.664	13	8.672	24
3			8.904	19	9.339	20	8.938	15	8.718	26	9.337	19	8.776	11	8.387	15
1	6.482	24	6.607	20	6.550	6	6.548	7	6.613	9	6.402		-	-	6.613	18
2			6.557	7	6.491	10	6.602	24	6.703	50	-	-	6.567	16	6.475	10
3			6.040	1	-	-	6.732	16	6.629	14	6.723	19	6.541	18	6.532	1
1	5.197	21	5.218	17		-	5.237	6	-	-	5.120	5	5.315		-	
2			5.239	2	-	-	5.274	21	5.341	27	-	-	5.205	10	5.192	6
3			5.225	15	5.365	16	-	-	5.352	20	5.357	16	5.252	7	5.197	
1	4.103	100	4.151	100	4.187	100	4.158	100	4.190	100	4.121	100	4.223	100	4.234	10
2			4.118	100	4.136	100	4.259	100	.207	100	4.193	100	4.164	100	4.157	10
3			4.251	100	4.248	100	4.223	100	4.173	100	4.260	100	4.153	100	4.134	10
1	3.699	49	3.751	49	3.757	33	3.746	40	3.755	32	.736	29	3.775	32	3.816	3
2			3.748	42	3.705	36	3.781	52	.812	36	3.784	42	3.713	36	3.753	5
3			3.864	35	3.833	44	3.769	48	3.761	48	3.828	34	3.715	37	3.732	34

Table 3.48 Powder XRD data on the samples obtained from Static Nonadecane in Heptane Experiments.

3.49 Powder XRDs Static Nonadecane in Heptane 5g/5ml

Sample no	Nonadecane		Control		500G		2500G		Pulsed		AC Magnet		6V DC		12V DC	
	D (i) Å	I/I (i)	d (i) Å	I/I (i)	d (i) Å	I/I (i)	d (i) Å	I/I (i)	d (i) Å	I/I (i)	d (i) Å	I/I (i)	d (i) Å	I/I (i)	d (i) Å	I/I (i)
1	8.630	16	8.503	6	8.665	11	8.661	7	8.667	13	8.712	8	8.656	9	8.678	9
2			8.964	5	8.834	7	.748	10	8.783	7	8.792	6	8.689	10	8.910	7
3			8.707	12	9.331	13	8.761	15	8.639	7	8.724	8	8.721	6	8.847	7
1	6.482	24	-	-	6.402	6	6.624	11	6.498	7	6.56	5	6.503	6	6.511	5
2			6.567	3	6.616	5	6.641	6	-	-	6.497	4	.512	5	-	-
3			-	-	-	-	6.643	5	6.359	6	-	-	6.269	6	-	-
1	5.197	21	-	-	5.151	5	-		5.194	5	-	-	5.220	4	5.231	4
2			-		5.297	4	5.185	5	5.849	4	5.259	4	5.210	3	-	-
3			-	-	-	-	-	-	5.729		-	-	5.218	4		-
1	4.103	100	4.125	100	4.117	100	4.221	100	4.147	100	4.091	100	4.112	100	4.154	100
2			4.156	100	4175	100	4.122	100	4.173	100	4.132	100	4.176	100	.161	100
3			4.119	100	.218	100	4.203	100	4.163	100	4.182	100	4.168	100	4.052	100
1	3.699	49	3.732	4	3757	36	3.746	35	3.770	34	3.706	44	3.752	48	3.765	36
2			3.802	34	.780	29	3.693	20	3.747	38	3.727	35	3.769	28	3.754	36
3			3.790	39	3.748	38	3.758	52	3.748	37	3.753	41	3.709	36	3.747	33

Table 3.49 Powder X-ray Diffraction data on the samples obtained from Nonadecane in Heptane Experiments.

3.50 Powder XRDs Dynamic Nonadecane in Heptane 20g/5ml

Sample no.	Nonadecane		Control		500G		2500G		Pulsed		AC Magnet		6V DC		12V DC	
	d (i) Å	I/I (i)	d (i) Å	I/I(i)	d (i) Å	I/I (i)	d (i) Å	I/I (i)	d (i) Å	I/I (i)	d (i) Å	I/I (i)	d (i) Å	I/I (i)	d (i) Å	I/I (i)
1	8.630	16	8.496	11	8.481	20	8.790	28	8.856	19	8.826	18	9.076	20	8.873	13
3			8.733	19	8.996	3	859	8	8.792	24	8.796	8	9.029	23	9.124	10
5			8.911	9	8.615	14	9.055	17	8.843	23	8.911	16	8.796	16	9.007	20
7			8.894	15	8.632	13	8.811	25	8.469	22	8.569	8	9.024	12	.760	7
8			8.966	11	9.048	15	8.795	17	8.816	33	.942	17	8.939	0	8.829	12
1	6.482	24	6.428	7	6.738	15	6.837	3	6.621	16	6.587	9	6.734	13	6.629	8
3			6.573	12		-	-	-	6.603	12	-	-	6.680	15	6.774	5
5			-	-	6.567	9	6.727	11	6.613	18	6.659	7	6.590	14	-	-
7			-		-	-	6.728	12.5	6.495	12	6.452	8	6.715	8	6.579	10
8			6.634	7	-	-	6.731	11	6.578	6	6.690	16	6.665	19	-	-
1	5.197	21	4.986	6	5.361	9	5.697	19	-	-	-	-	-	-	5.339	6
3			5.243	8	-	-	-	-	-	-		-	5.324		-	-
5			5.302		5.512	8	-	-	-	-	-	-	5.332	10	-	-
7			5.299	10	-	-	-	-	5.201	7	5.176	6	5.333	6	5.274	6
8			-	-	-	-	5.835	8	5.251	11	-	-	5.174	9	-	-
1	4.103	100	4.185	100	4.257	10	4.303	100	4.260	100	4.186	100	4.226	100	4.11	10
3			41.76	100	4.295	100	4.230	100	4.273	100	4.237	100	4.182	100	4.224	100
5			.215	00	4.238	100	4.231	100	4.273	100	4.265	00	4.159	100	.241	100
7			.242	100	4.321	100	4.244	100	4.173	100	.232	100	4.174	100	4.156	100
8			4.247	100	4.341	100	4.205	100	4.224	100	4.163	100	.201	100	4.164	100
1	3.699	49	3.572	44	3.849	49	.871	47	3.782	3	3.811	47	.821	40	3.759	55
3			3.779	32	3.813	5	3.798	30	3.847	53	3.825	45	3.792	39	3.805	34
5			3.793	32	3.818	36	.812	39	.820	44	3.836	43	3.795	41	.800	8
7			3.850	52	3.950	33	.790	43	56	3	3.879	46	3.753	37	3.748	
8			3.863	42	3.950	40	3.797	33	3.861	3		42	3.750	20	3.760	41

Table 3.50 Powder XRD data on the samples obtained from Dynamic Nonadecane in Heptane 20g/5ml Experiments.

3.51 Powder XRDs Dynamic Nonadecane and Heptane 15g/5ml

Sample no.	Nonadecane		Control		500G		2500G		Pulsed		AC Magnet		6V DC		12V DC	
	d (i) Å	I/I (i)	d (i) Å	I/I (i)	d (i) Å	I/I (i)	d (i) Å	I/I (i)	d (i) Å	I/I (i)	d (i) Å	I/I (i)	d (i) Å	I/I (i)	d (i) Å	I/I (i)
1	8.630	16	8.883	17	8.937	24	9.411	23	8.950	22	8.745	16	8.806	10	8.798	16
3			8.965	16	8.704	15	8.733	42	8.980	28	8.668	11	8.832	9	8.836	32
5			8.796	22	8.798	26	8.829	19	8.804	23	8.827	13	8.556	15	8.936	29
7			8.832	17	8.831	13	8.768	17	8.826	25	8.786	12	8.881	20	8.913	26
8			8.785	33	8.646	14	9.006	58	8.849	38	8.644	12	8.812	14	8.854	31
1	6.482	24	6.665	11	6.654	12	6.663	11	6.675	10	-	-	6.605	6	-	-
3			6.671	9	6.532	12	6.795	21	6.690	14	6.409	6	6.608	9	6.621	16
5			6.788	19	6.517	17	6.747	16	6.582	10	6.594	6	-	-	6.635	12
7			6.639	7	6.914	7	6.714	11	6.597	12	6.553	9	6.646	10	6.672	12
8			6.571	1	6.432	7	6.693	33	6.638	18	-	-	6.583	7	6.654	15
1	5.197	21	5.341	6	-	-	-	-	5.313	7	5.239		5.234	4	-	-
3			5.320	6	5.232	4	-	-	-	-	-	-	5.271	5	-	-
5			5.379	12	-	-	5.5364	9	5.128	7	-	-	-	-	-	-
7			-	-	-	-	5.154	7	-	-	5.158	8	-	-	5.141	7
8			5.243	11	5.137	5	5.292	2	5.292	10	-	-	-	-	-	-
1	4.103	100	4.217	100	4.239	100	4.302	10	4.250	100	4.227	100	4.150	100	4.413	100
3			4.211	100	4.234	100	4.262	100	4.292	100	4.410	100	4.211	100	4.184	100
5			4.252	100	4.208	100	4.228	100	4.246	100	4.254	100	4.189	100	4.136	100
7			4.218	100	4.300	100	.192	100	4.247	100	4.249	100	4.285	100	4.207	100
8			.218	00	4.206	100	.363	100	4.250	100	4.201	100	4.193	100	4.226	100
1	3.699	49	3.825	32	3.829	37	3.824	32	3.773	30	3.776	43	3.741	35	3.751	34
3			3.80	35	3.782	34	3.861	36	3.933	38	3.739	38	3.772	40	3.790	41
5			3.841	32	3.763	38	3.814	35	3.843	38	3.892	44	3.774	36	3.798	45
7			3.868	29	3.936	39	3.698	42	3.884	44	3.870	48	3.871	34	3.723	38
8			3.744	8	3.743	27	3.867	54	3.867	56	3.881	48	3.831	39	3.783	41

Table 3.51 Powder XRD data on the samples obtained from Dynamic Nonadecane in Heptane 15g/5ml Experiments

3.52 Powder XRDs Dynamic Nonadecane and Heptane 10g/5ml

Sample no.	Nonadecane		Control		500G		2500G		Pulsed		AC Magnet		6V DC		12V DC	
	d (i) Å	I/I (i)	d (i) Å	I/I (i)	d (i) Å	I/I (i)	d (i) Å	I/I (i)	d (i) Å	I/I (i)	d (i) Å	I/I (i)	d (i) Å	I/I (i)	d (i) Å	I/I (i)
1	8.630	16	8.823	19	8.848	9	8.833	17	9.031	17	8.853	17	8.967	21	8.820	17
3			8.8637	20	8.869	15	8.884	4	8.904	30	8.883	8	8.880	27	9.057	13
5			8.567	22	8.647	13	8.984	29	8.872	29	8.794	9	9.009	22	8.898	23
7			8.808	18	8.751	9	.997	24	8.969	33	8.880	11	8.882	23	9.111	3
8			8.937	20	8.819	19	8.940	44	8.699	30	9.109	15	8.828	20	8.874	20
1	6.482	24	6.582	0	6.594	5	-	-	6.669	10	6.487	6	6.688	10	6.625	9
3			6.503	12	6.631	7	6.617	11	6.619	20	6.621	4	6.602	15	6.729	8
5			6.452	12	6.484	7	6.649	15	6.623	13	6.633	4	6.744	13	6.663	13
7			6.631	10	6.583	4	6.619	12	6.678	22	6.586	6	6.621	11	6.799	8
8			6.677	13	6.607	13	6.649	24	6.543	17	6.640	9	6.596	10	6.639	12
1	5.197	21	5.271	6	5.240	3	5.033	3	5.293	6	.212	4	5.266	6	280	5
3			5.212	9	5.250	4	5.295	6	5.274	9	5.270	2	5.254	9	5.329	5
5			5.176	6	5.177	4	5.326	9	5.275	7	-	-	-	-	5.315	8
7			.260	7	-	-	-	-	5.317	13	-	-	-	-	-	-
8			5.250	8	5.258	6	5.326	15	5.218	9	5.307	5	5.245	7	5.284	8
1	4.103	100	4.175	100	4.900	100	4.221	100	4.173	100	4.152	100	4.161	100	4.153	100
3			4.166	100	4.107	100	4.208	100	4.191	100	4.199	100	4.164	100	4.187	100
5			4.136	100	4.165	100	4.203	100	4.191	100	4.158	100	4.173	100	4.200	100
7			4.162	100	4.189	100	4.261	100	4.223	100	4.168	87	4.181	100	4.206	100
8			4.178	100	4.122	100	4.259	100	4.150	100	4.200	100	4.130	100	4.168	100
1	3.699	49	3.751	37	3.765	37	3.730	34	3.765	36	3.745	39	3.730	39	3.756	32
3			3.748	47	3.725	24	3.795	38	3.775	36	3.769	35	3.764	26	3.818	33
5			3.739	43	3.793	38	3.776	43	3.794	50	3.710	46	3.792	25	3.779	32
7			3.758	9	3.804	33	3.820	37	3.779	40	3.767	100	3.798	41	3.789	32
8			3.779	45	3.734	33	3.867	41	3.743	34	3.786	40	3.740	42	3.757	30

Table 3.52 Powder XRD data on the samples obtained from Dynamic Nonadecane in Heptane 10g/5ml Experiments

3.53 Powder XRD s Dynamic Nonadecane in Heptane 5g/5ml

Sample no.	Nonadecane		Control		500G		2500G		Pulsed		AC Magnet		6V DC		12V DC	
	d (i) Å	I/I (i)	d (i) Å	I/I (i)	d (i) Å	I/I (i)	d (i) Å	I/I (i)	d (i) Å	I/I (i)	d (i) Å	I/I (i)	d (i) Å	I/I (i)	d (i) Å	I/I (i)
1	8.630	16	8.761	8	8.779	12	8.902	14	8.674	26	8.581	8	8.834	27	9.179	26
3			8.495	16	8.857	23	8.868	20	9.032	30	8.820	16	8.971	21	8.943	2
5			8.580	11	8.851	21	8.827	20	8.819	22	9.123	11	8.814	48	8.928	29
7			8.821	14	8.817	28	8.888	18	8.910	32	8.942	14	.44	23	9.015	47
8			8.822	11	-	-	8.893		8.971	0	8.825	1	9.189		8.858	13
1	6.482	24	6.554	5	6.588	8	6.633	7	6.520	11	6.572	5	6.587	12	.792	20
3			6.411	9	6.627	13	6.656	11	6.729	6	6.502	9	6.690	19	6.712	11
5			6.526	5	6.466	10	6.593	9	6.593	8	6.769	5	6.730	21	6.682	12
1			6.601	8	6.602	16	6.773	10	6.643	8	6.615	8	6.615	10	6.742	23
8			6.590	6	-	-	6.661		.576	10	6.590	6	6.699	18	6.826	5
1	5.197	21	-	-	-	-	-	-	-	-	5.235	-	5.011	6	-	-
3			5.417	6	5.283	8	-	-	-	-	-	6	-	-	-	-
5			5.195	4	5.161	6	-		-	-	5.361	4	-	-	5.330	5
7			5.268	5	-	-	-	-	5.293		-		-	-	-	-
8			5.252	4	-	-	-	-	5.328	6	-	4	5.401	13	-	-
1	4.103	100	4.149	100	4.175	100	4.197	100	4.231	100	4.132	100	4.232	100	4.233	100
3			4.152	100	4.146	100	4.414	100	4.286	100	4.181	100	4.238	100	4.252	100
5			4.153	100	4.182	100	4.216	100	4.172	100	4.255	100	4.232	100	4.289	100
7			4.163	100	4.180	100	3.941	100	4.156	100	4.193	100	4.165	100	4.196	100
8			4.163	100	-	-	4.273	100	4.152	100	4.235	100	4.149	100	4.242	100
1	3.699	49	3.748	33	3.752	35	3.801	30	3.888	30	3.744	30	3.863	45	3.823	46
3			3.731	39	3.758	6	3.854	28	3.853	36	3.692	36	3.887	46	3.804	33
5			7.35	40	3.780	40	3.845	38	3.848	44	3.895	44	3.851	38	3.869	45
7			3.732	41	3.804	40	3.723	4	3.765	44	3.786	44	3.741	40	3.757	35
8			3.693	41	-	-	3.900	36	3.744	36	3.891	36	3.739	24	3.833	18

Table 3.53. Powder XRD data on the samples obtained from Dynamic Nonadecane in Heptane 5g/5ml Experiments

3.54 Powder XRDs Static Nonadecane and Heneicosane 50:50

Sample no.	Nonadecane		Heneicosane		Control		500G		2500G		Pulsed		AC Magnet		6V DC		12V DC	
	d (i) Å	I/I (i)	d (i) Å	I/I (i)	d (i) Å	I/I (i)	d (i) Å	I/I (i)	d (i) Å	I/I (i)	d (i) Å	I/I (i)	d (i) Å	I/I (i)	d (i) Å	I/I (i)	d (i) Å	I/I (i)
1	8.630	16	14.14		8.800	7	-	-	-	-	9.081	6	-	-	-	-	-	-
2					-	-	-	-	-	-	8.772	7	-	-	9.132	7	-	-
1	6.482	24	9.612		-	-	-	-	-	-	-	-	-	-		-	-	-
2					-	-	-	-	-	-	-	-	-	-	-	-	-	-
1	5.197	21	7.186		-	-		-	-	-	-	-	-	-	-	-	-	-
2					-	-	-	-	-	-	-	-	-	-	-	-	-	-
1	4.103	100	4.142	100	4.173	100	4.209	100	4.208	100	4.200	100	-	-	4.192	100	4.188	100
2					4.131	100	4.233	100	4.192	100	4.213	100	-	-	4.167	100	4.134	100
1	3.699	49	3.752		3.770	35	3.859	43	3.802	35	3.748	41	-	-	3.890	40	3.877	40
2					3.839	39	3.914	40	3.869	40	3.899	42	-	-	3.833	43	3.828	45

Table 3.54 Powder XRD data on the samples obtained from static Nonadecane and heneicosane Experiments

3.55 Powder XRDs Dynamic Nonadecane and Heneicosane 50:50

Sample no.	Nonadecane		Heneicosane		Control		500G		2500G		Pulsed		AC Magnet		6V DC		12V DC	
	d (i) Å	I/I (i)	d (i) Å	I/I (i)	d (i) Å	I/I (i)	d (i) Å	I/I (i)	d (i) Å	I/I (i)	d (i) Å	I/I (i)	d (i) Å	I/I (i)	d (i) Å	I/I (i)	d (i)Å	I/I (i)
1	8.630	16	14.14				-	-	-	-			-	-		-		-
3																		
5																		
7																		
8					-	-		-	-	-								
1	6.482	24	9.612		9.801	100	9.745	31	9.572	36	9.929	-7	9.633	88	9.326	75	9.783	28
3					9.933	95	9.923	3	9.943	46	9.534		9.619	48	9.615	29	9.353	41
5					9.535	76	9.541	12	9.437	60	9.555	50	9.719	44	9.872	43	9.790	100
7					9.55	88	9.544	7	9.924	38	9.529	54	9.888	51	9.489	100	9.649	55
8					9.634	36			9.481	66	9.462	8	9.505		9.685	27	9.728	30
1	5.197	21	7.186		5.743	33	5.069	3	7.337	18-	5.799	5	5.687	17	5.757	8	5.793	8
					7.253	61	7.199	11			7.325	10-	7.153	42	6.984	26	7.241	20
3					5.817	33			5.795	19	5.655	3	7.156	25	5.832	7	5.846	16
					7.348	71	7.31	3	7.332	3	7.111	9			7.365	20	7.406	37
5					7.283	29	7.371	8	7.03	25	5.786	17	7.222	26	5.739	13	5.747	20
											7.351	35			7.234	34	7.237	28
7					-	-	7.359	4	5.788	10	5.812	11	5.777	15	7.066	43	7.177	30
									7.306	25	7.353	25	7.287	30				
8					7.411	24	5.761	19	5.763	18	7.06	10-	7.233	37	7.329	19	5.833	10
							7.269	42	7.272	42-							7.379	23
1	4.103	100	4.142	100	-	-	4.399	92	4.274	100	4.328	100	4.312	100	4.295	100	4.277	100
3					4.348	100	4.338	84	4.305	100	4.275	100	4.236	100	4.371	100	4.36	100
5					4.340	100	4.275	100	4.245	100	4.257	100	4.303	100	4.318	100	4.283	32
7					4.325	100	4.241	100	4.216	100	4.349	100	4.262	100	4.272	100	4.304	100
8					4.302	100	4.341	100	4.344	100	4.278	100	4.376	100	4.319	100	4.359	100
1	3.699	49	3.752		3.854	47	3.970	100	3.949	81	3.939	80	3.923	45	3.294	73	3.9	46
3					3.954	61	3.947	100	3.790	57	3.893	72	3.935	54	3.940	74	3.962	95
5					3.958	76	3.968	78	3.875	68	3.871	53	3.192	55	3.943	53	3.92	36
7					3.942	55	3.966	68	3.915	57	3.957	85	3.889	66	3.913	43	3.915	75
8					3.939	72	3.937	80	3.959	70	3.855	71	3.978	68	3.95	61	3.981	65

Table 3.55 Powder XRD data on the samples obtained from Dynamic Nonadecane and Heneicosane Experiments

3.56 Powder XRDs Static Nonadecane and Heneicosane in heptane 50:50

Sample no	Nonadecane		Heneicosanin		Control		500G		2500G		Pulsed		AC Magnet		6V DC		12V DC	
	d (i) Å	I/I (i)	d (i) Å	I/I (i)	d (i) Å	I/I (i)	d (i) Å	I/I (i)	d (i) Å	I/I (i)	d (i) Å	I/I (i)	d (i) Å	I/I (i)	d (i) Å	I/I (i)	d (i)Å	I/I (i)
1	8.630	16	14.14		8.950	5	8.376	7									8.785	-13
2																	-	-
1	6.482	24	9.612														-	-
2																	-	-
1	5.197	21	7.186								5.614	12					-	-
2																	-	-
1	4.103	100	4.142	100	4.191	100	4.212	100	4.180	100	4.252	100	4.281	100	4.305	100	4.217	100
2					4.189	100	4.140	100	4.169	100	4.276	100	4.3	100	4.225	100	4.269	100
1	3.699	49	3.752		3.894	41	3.869	36	3.818	44	3.919	75	3.899	47	3.926	50	3.823	49
2					3.846	43	3.794	45	3.863	53	3.959	57	3.909	45	3.849	44	3.888	34

Table 3.56 Powder XRDs Nonadecane and Heneicosane in heptane static 50:50

3.57 Powder XRDs Dynamic Nonadecane and Heneicosane in Heptane 50:50

Sample no	Nonadecane		Heneicosane		Control		500G		2500G		Pulsed		AC Magnet		6V DC		12V DC	
	d (i) Å	I/I (i)	d (i) Å	I/I (i)	d (i) Å	I/I (i)	d (i) Å	I/I (i)	d (i) Å	I/I (i)	d (i) Å	I/I (i)	d (i) Å	I/I (i)	d (i) Å	I/I (i)	d (i)Å	I/I (i)
1	8.630	16	14.14				-	-	-	-		6	11.524	100				
3																		
5																		
7											11.601	100					13.889	86
8					-	-		-	-	-		7					13.545	100
1	6.482	24	9.612		9.222	16-	9.531	39	9.725	37	9.839	100-	9.535	100	9.505	75	9.495	27
3					9.542	6	9.646	100	9.770	45	9.918	100	9.491	53	9.792	100	9.694	60
5					9.580	24	9.665	95	9.421	38	9.895	100	9.504	46	9.495	45	9.495	83
7					9.279	22	9.499	66	9.481	25	9.572	54	9.523	100	9.492	71	9.306	53
8					9.570	-13	9.573	24	9.446	50	10.008	71	9.957	100	9.482	12	9.117	40
1	5.197	21	7.186		6.950	-5	7.187	16	5.745	9	5.755	11	7.440	38	5.857	50	5.877	14
									7.288	17	7.283	39			7.418	100	7.448	64
3					7.208	3	5.708	12	7.268	18	5.799	16	5.879	26	5.761	22	-	-
							7.176	40			7.318	52	7.439	40	7.240	66		
5					6.982	10	5.703	15	5.838	9	5.180	21	-	-	5.925	27	5.908	33
							7.169	35	7.385	21	7.167	52					7.483	33
7					6.971	8	7.336	25	5.693	9	5.912	24	5.924	22	5.912	28	5.031	38
									7.344	17	7.487	56	7.120	36	7.505	28	6.996	36
8					7.261	-6	7.185	10	7.066	18	5.829	31	5.834	21	-	-	5.464	25
											7.362	100	7.376	75			6.881	13
1	4.103	100	4.142	100	4.239	100	4.262	100	4.307	100	4.332	44	4.182	61	4.364	87	4.382	100
3					4.238	100	4.319	40	4.260	100	4.345	47	4.217	100	4.312	88	4.314	100
5					4.220	100	4.280	100	4.255	100	4.357	60	4.297	100	4.312	100	4.255	100
7					4.222	100	4.323	100	4.257	100	4.448	47	4.249	66	4.399	100	4.224	100
8					4.298	100	4.253	100	4.333	100	4.369	31	4.361	31	4.287	100	4.186	52
1	3.699	49	3.752		3.867	42	3.916	51	3.961	50	3.958	23	-	-	-	-	3.993	35
3					-	-	3.952	35	3.911	34	3.974	27	3.991	40	3.944	38	3.946	65
5					3.877	41	3.919	62	3.822	63	-	-	3.966	38	3.966	54	-	-
7					3.859	64	3.973	62	3.889	41	-	-	-	-	-	-	3.86	79
8					3.94	43	3.902	51	3.933	48	3.996	19	3.988	18	3.932	53	3.852	23

Table 3.57 Powder XRDs Nonadecane and Heneicosane heptane dynamic 50:50

3.58 Powder XRDs Static Nonadecane and Crude oil

Sample no.	Nonadecane		Control		500G		2500G		Pulsed		AC Magnet		6V DC		12V DC	
	d (i) Å	I/I (i)	d (i) Å	I/I (i)	d (i) Å	I/I (i)	d (i) Å	I/I (i)	d (i) Å	I/I (i)	d (i) Å	I/I (i)	d (i) Å	I/I (i)	d (i) Å	I/I (i)
1	8.630	16	-	-	-	-	-	-	-	-	-	-	-	-	-	-
2			-	-	-	-	-	-	-	-	-	-	-	-	-	-
1	6.482	24	-	-	-	-	-	-	-	-	-	-	-	-	-	-
2			-	-	-	-	-	-	-	-	-	-	-	-	-	-
1	5.197	21	-	-	-	-	-	-	-	-	5.527	58	-	-	-	-
2			-	-	-	-	-	-	-	-	5.488	62	-	-	-	-
1	4.103	100	4.239	100	4.241	100	4.251	100	4.298	100	4.270	100	4.254	100	4.223	100
2			4.247	100	4.270	100	4.337	100	4.241	100	4.237	100	4.259	100	4.228	100
1	3.699	49	3.844	44	3.867	40	3.861	41	3.844	39	3.893	43	3.859	40	3.850	39
2			3.880	39	3.851	38	-	-	3.857	40	3.859	43	3.843	39	3.835	39

Table 3.58 Powder XRDs Static Nonadecane and Crude oil

3.59 Powder XRDs Dynamic Nonadecane and Crude oil

Sample no.	Nonadecane		Control		500G		2500G		Pulsed		AC Magnet		6V DC		12V DC	
	d (i) Å	I/I (i)	d (i) Å	I/I (i)	d (i) Å	I/I (i)	d (i) Å	I/I (i)	d (i) Å	I/I (i)	d (i) Å	I/I (i)	d (i) Å	I/I (i)	d (i) Å	I/I (i)
1	8.630	16	-	-	-	-	-	-	-	-	-	-	-	-	-	-
3			-	-	-	-	-	-	-	-	-	-	-	-	-	-
5			-	-	-	-	-	-	-	-	-	-	-	-	-	-
7			-	-	-	-	-	-	-	-	-	-	-	-	-	-
8				-	-	-	-	-	-	-	-	-	-	-	-	-
1	6.482	24	-	-	-	-	-	-	-	-	-	-	-	-	-	-
3			-	-	-	-	-	-	-	-	-	-	-	-	-	-
5			-	-	-	-	-	-	-	-	-	-	-	-	-	-
7			-	-	-	-	-	-	-	-	-	-	-	-	-	-
8			-	-	-	-	-	-	-	-	-	-	-		--	-
1	5.197	21	-	-	-	-	5.528	35	-	-	-	-	-	-	-	-
3			-	-	-	-	-	-	-	-	-	-	-		-	-
5				-	-	-	-	-	-	-	-	-	-	-	-	-
7			-	-	-	-	-	-	-	-	-	-	-	-	-	-
8			-	-	-	-	-	-	-	-	-	-	-	-	-	-
1	4.103	100	4.159	100	4.212	100	4.149	100	4.234	100	4.288	100	4.292	100	4.345	100
3			4.193	100	4.331	100	4.213	100	4.212	100	4.324	100	4.354	100	4.264	100
5			4.170	100	4.237	100	4.227	100	4.223	100	4.371	100	4.228	100	4.196	100
7			4.238	100	4.211	100	3.269	100	4.146	100	4.231	100	4.312	100	4.247	100
8			4.183	100	-	-	4.188	100	4.230	100	4.225	100	4.239	100	4.251	100
1	3.699	49	3.795	40	3.822	40	3.718	38	3.875	40	3.932	51	3.863	39	3.939	43
3			3.879	38	3.929	42	3.832	8	3.835	41	-	-	3.945	43	3.827	38
5			3.813	42	3.859	37	3.839	36	3.840	39	3.947	43	3.839	39	3.813	42
7			3.869	37	-	-	3.875	37	.796	39	3.801	40	3.919	40	3.889	38
8			3.859	42	3.842	39	3.855	40	3.856	48	3.847	37	3.873	54	3.872	44

Table 3.59 Powder XRDs Dynamic Nonadecane and Crude oil

4.0 RESULTS AND INTERPRETATION

4.1 Results

For each of the systems studied the following measurements were carried out:

- Melting points of solid products
- Time to crystallise the hydrocarbon
- Powder X-ray Diffraction of solid products
- Scanning Electron Micrographs of solvent products

4.2 Melting Points

There were no significant changes in any of the melting points for the hydrocarbons crystallised in a magnetic field compared to those crystallised in a zero field.

4.3 Crystallisation Times

4.3.1 Static Nonadecane Systems

Statistically significant increases in the time to crystallise the hydrocarbons in applied fields were found for the following static systems:

- Nonadecane at 25^0C, a permanent 2500G field.
- Nonadecane at 25^0C, a pulsed field.
- Nonadecane in Heptane 20g/5ml at 25^0C, a permanent 500G field.
- Nonadecane in Heptane 20g/5ml at 25^0C, a permanent 2500G field
- Nonadecane in Heptane 20g/5ml at 25^0C, a pulsed field.
- Nonadecane in Heptane 20g/5ml at 25^0C, an electromagnetic, AC field
- Nonadecane in Heptane 20g/5ml at 25^0C, an electromagnetic 6V DC field
- Nonadecane in Heptane 20g/5ml at 25^0C, a electromagnetic 12V DC field
- Nonadecane in Heptane experiments 15g/5ml at 20^0C, a permanent 500G field
- Nonadecane in Heptane experiments 15g/5ml at 20^0C, a permanent 2500G field.
- Nonadecane in Heptane experiments 15g/5ml at 20^0C, a pulsed field
- Nonadecane in Heptane experiments 15g/5ml at 20^0C, an electromagnetic 12V DC field.
- Nonadecane in Heptane experiments 5g/5ml at 15^0C, a permanent 2500G field
- Nonadecane in Heptane experiments 5g/5ml at 15^0C, a pulsed field
- Nonadecane in Heptane experiments 5g/5ml at 15^0C, an electromagnetic, AC field

- Nonadecane in Heptane experiments 5g/5ml at 15^0C, an electromagnetic, 6V DC field.
- Nonadecane in Heptane experiments 5g/5ml at 15^0C, an electromagnetic 12V DC fields.
- Nonadecane and heneicosane at 10^0C, the pulsed field.
- Nonadecane and heneicosane in heptane at 10^0C the, permanent 2500G field.
- Nonadecane and heneicosane in heptane at 10^0C,a pulsed field.
- Nonadecane and heneicosane in heptane at 10^0C, an electromagnetic AC field
- Nonadecane and heneicosane in heptane at 10^0C, an electromagnetic, 6V DC field.
- Nonadecane and heneicosane in heptane at 10^0C, an electromagnetic 12V DC field.
- Nonadecane and crude oil at 22.5^0C, a permanent 2500G field.
- Nonadecane and crude oil at 22.5^0C, a pulsed field.
- Nonadecane and crude oil at 22.5^0C, an electromagnetic AC field
- Nonadecane and crude oil at 22.5^0C, an electromagnetic 6V DC field.
- Nonadecane and crude oil at 22.5^0C, an electromagnetic 12V DC field.

4.3.2 Dynamic Nonadecane Systems

Statistically significant increases in the time to crystallise the hydrocarbons in applied fields were found for the following dynamic systems:

- Nonadecane at 25^0C, a permanent 2500G field
- Nonadecane at 25^0C, a pulsed field.
- Nonadecane at 25^0C, an electromagnetic AC field
- Nonadecane at 25^0C, an electromagnetic 12V DC field
- Nonadecane in Heptane 20g/5ml at 25^0C, a permanent 500G field.
- Nonadecane in Heptane 20g/5ml at 25^0C, a permanent 2500G field,
- Nonadecane in Heptane 20g/5ml at 25^0C, a pulsed field
- Nonadecane in Heptane 20g/5ml at 25^0C, an electromagnetic AC field
- Nonadecane in Heptane 15g/5ml at 20^0C, a pulsed field
- Nonadecane in Heptane 15g/5ml at 20^0C, an electromagnetic 12V DC field.
- Nonadecane in Heptane 10g/5ml at 20^0C, a pulsed field.
- Nonadecane in Heptane 5g/5ml at 15^0C, an electromagnetic AC field.

- Nonadecane and heneicosane at 10^0C, a permanent 2500G field
- Nonadecane and heneicosane at 10^0C, a pulsed field
- Nonadecane and heneicosane at 10^0C, an electromagnetic AC field
- Nonadecane and heneicosane at 10^0C, an electromagnetic 6V DC field
- Nonadecane and heneicosane at 10^0C, an electromagnetic 12V DC field.
- Nonadecane and heneicosane in heptane 10^0C, a permanent 2500G field
- Nonadecane and heneicosane in heptane 10^0C, a pulsed field
- Nonadecane and heneicosane in heptane 10^0C, an electromagnetic 6V DC field
- Nonadecane and heneicosane in heptane 10^0C, an electromagnetic 12V DC field.
- Nonadecane and crude oil at 22.5^0C, a permanent 2500G field.
- Nonadecane and crude oil at 22.5^0C, pulsed field
- Nonadecane and crude oil at 22.5^0C, an electromagnetic AC field
- Nonadecane and crude oil at 22.5^0C, an electromagnetic 6V DC field
- Nonadecane and crude oil at 22.5^0C, an electromagnetic 12V DC field.

4.3.3 Nonadecane Systems

Statistically significant decreases in the time to crystallise the hydrocarbons in applied fields were found for the following systems:

- Static Nonadecane in heptane 15g/5ml, an electromagnetic, AC field
- Static Nonadecane in heptane 15g/5ml, an electromagnetic 6V DC field.
- Static Nonadecane in heptane 10g/5ml, a pulsed, field.
- Static Nonadecane in heptane 10g/5ml, an electromagnetic 6V DC field.
- Dynamic Nonadecane in heptane 20g/5ml, an electromagnetic 6V DC field.
- Dynamic Nonadecane in heptane 20g/5ml, an electromagnetic 12V DC field.
- Static Nonadecane and Heneicosane 50:50, an electromagnetic AC field.

4.4 Powder X-ray Diffraction

The Powder X-ray diffraction studies were apparently not significant at first sight, but detailed studies of the situations with major changes in the time to crystallise showed that this is not always the case.

4.4.1 Static Nonadecane

The crystallites for static nonadecane experiments were further analysed and X-ray studies showed a shift in the peaks from left to right that is to higher 2 θ values and increased unit cell size.

The changes in the cell dimensions are small but are consistent in the direction of increased unit cell size. For example the details of an accurate scan of a static nonadecane crystallisation in a pulsed field are compared in table 3.44

4.5 Scanning Electron Micrographs of Solvent Products

The scanning electron micrographs showed differences between the control samples at 25^0C and nonadecane samples at 25^0C, which had been exposed to an applied field.

4.6 Results Explained

The aim of the work described in this thesis was to determine whether applied fields could affect the crystallisation of solid hydrocarbons under different conditions. For two types of applied field, a 2500G permanent magnetic field and a pulsed field there was a statistically significant increase in the time taken to crystallise nonadecane in a static crystallisation situation at 25^0C.
In dynamic experiments designed to model the flow of hydrocarbons, the time to crystallise nonadecane at 25^0C showed a statistically significant increase in the time to crystallise for most types of applied field *viz.*, 2500G, pulsed, AC and 12V DC.

The melting points of the solid product nonadecane and X-ray diffraction data shows that there is no change in the phase of the solid products obtained by crystallisation in an applied field.

Electron micrographs of nonadecane crystallised in a static situation in an applied field show that the particles are smaller consisting of more distinct crystallites than those obtained in a zero field. This suggests that changes in particle size and morphology occur in the presence of an applied field.

A detailed study of the X-ray diffraction powder patterns of one of the samples showing a large change in time to crystallise (static nonadecane in a pulsed field at 25^0C) shows that there is a small but significant shift in the diffraction pattern indicating an increase in unit cell volume. This would be consistent with a decrease in packing density and the lattice energy of the nonadecane in the applied field and would account for the extra time required for crystallisation.

The effects of a solvent in nonadecane crystallisation in an applied field was studied for heptane and nonadecane mixtures. The results showed that in addition to any effects of the applied field, both nonadecane concentration and temperature can have an affect.

In static experiments on (20g nonadecane in 5ml heptane mixtures) at 25^0C showed a statistically significant increase in time to crystallise of the nonadecane for all fields studied.

In static experiments in solutions containing the saturation level of nonadecane (15g nonadecane in 5ml of heptane mixtures) at 20^0C a statistically significant increase in time to crystallise for the nonadecane in the 500G, 2500G permanent magnetic fields, pulsed field and a 12V DC electromagnetic field was found. The time to crystallise was, however, found to decrease for the AC and 6V DC electromagnetic fields. To check this observation experiments were carried out with nonadecane present below the saturation level. (10g nonadecane in 5ml of heptane at 20^0C). The 6V DC fields again showed a decrease in time to crystallise.

In static experiments in solutions containing the saturation level of nonadecane (5g of nonadecane in 5 ml of heptane) at 15^0C a statistically significant increase in time to crystallise for the nonadecane in the 2500G permanent magnetic field, pulsed field, the 6V DC and 12V DC electromagnetic fields were found.

Experiments in dynamic systems showed that there were differences between flowing and non flowing systems in that only the pulsed field consistently showed a significant increase in time to crystallise for all nonadecane and heptane mixtures at

25 and 20^{0}C. The only fields which resulted in a decrease in the time to crystallisation was the AC and DC electromagnetic fields.

Dynamic experiments on (20g nonadecane:5ml heptane mixtures) at 25^{0}C showed a statistically significant increase in time to crystallise of the nonadecane for 2500G permanent magnetic fields, pulsed field and the AC electromagnetic field. The time to crystallise decreases for the 6V DC and 12V DC electromagnetic fields.

Dynamic experiments in the saturation level of nonadecane (15g nonadecane in 5ml of heptane mixtures) at 20^{0}C showed a statistically significant increase in time to crystallise for the nonadecane in the pulsed field and 12V DC electromagnetic field. The time to crystallise however decreased for the AC and 6V DC electromagnetic fields. To check this observation experiments were carried out with nonadecane present below the saturation level. (10g nonadecane in 5ml of heptane at 20^{0}C). The pulsed field again showed an increase in time to crystallise.

Dynamic experiments with nonadecane present at the saturation level (5g of nonadecane in 5 ml of heptane) at 15^{0}C a statistically significant decrease in time to crystallise was found for the nonadecane in the AC field.

The effects of a mixed solid hydrocarbon system were studied for the nonadecane-heneicosane system and for crude oil samples. In only one system was a decrease in time to crystallise observed and that system was for the static nonadecane-heneicosane mixture in the absence of a solvent at 10^{0}C and in an AC applied field. All other significant changes in theses systems were increases in the following systems listed below:

In static experiments with equal amounts of nonadecane and heneicosane at 10^{0}C a statistically significant increase in time to crystallise the hydrocarbons was found in a pulsed field.

In dynamic experiments with equal amounts of nonadecane and heneicosane at 10^{0}C a statistically significant increase in time to crystallise for the hydrocarbons was

found for the 2500G permanent magnetic field, pulsed field, AC, 6V DC and 12V DC electromagnetic fields.

In static experiments with equal amounts of nonadecane and heneicosane in heptane at 10^0C a statistically significant increase in time to crystallise the hydrocarbons in heptane was found for the 2500G permanent magnetic field, pulsed field, and AC, 6V DC and 12V DC electromagnetic fields.

In dynamic experiments with equal amounts of nonadecane and heneicosane in heptane at 10^0C a statistically significant increase in time to crystallise for the hydrocarbons in heptane was found for the 2500G permanent magnetic field, pulsed field, and the AC, 6V DC and 12V DC electromagnetic fields.

In static experiments for a mixture of crude oil and nonadecane at 22.5^0C statistically significant increases in time to crystallise for the nonadecane and crude oil was found for the 2500G permanent magnetic field, pulsed field, 6V DC and 12VDC electromagnetic fields.

In dynamic experiments for a mixture of crude oil and nonadecane at 22.5^0C statistically significant increases in time to crystallise for the nonadecane and crude oil was found for the 2500G permanent magnetic field, pulsed field, AC, 6V DC and 12V DC electromagnetic fields.
Again the pulsed field always caused an increase in the time of crystallisation.

4.7 Interpretation of Results

The static and dynamic experimental studies for nonadecane at 25^0C showed one of the greatest effects from exposure to applied fields. The effect most commonly observed was that of an increase in crystallisation time. At this temperature it is possible that the individual nonadecane chains were elongated in the applied field. This in turn would increase the time to crystallise, as the nonadecane unit cells would be larger. The X-ray data confirmed that there were small changes in the unit cell, of nonadecane, that had been subjected to applied fields.
The static and dynamic experimental studies for heptane and nonadecane showed two effects from exposure to an applied field. The first was an increase in

crystallisation time for all concentrations. The second was a decrease in crystallisation time. The permanent magnetic field did affect the crystallisation of nonadecane at the higher concentrations. However as the concentration and the temperature decreased the most noticeable changes were found in samples treated by the pulsed AC, 6V DC and 12V DC electromagnetic fields. The possible explanation for the reduction in crystallisation time is the shortening of the nonadecane chain within the unit cell. The solvent which is a shorter chain alkane at certain concentrations will help to retard the crystallisation process whereas at other concentrations will facilitate the crystallisation process thus enabling it to occur more rapidly.

The static and dynamic mixed hydrocarbon studies showed an increase in crystallisation time. This may due to the two different hydrocarbons with different unit cell dimensions crystallising within the same space at slightly different rates. The heneicosane has a higher melting point temperature, 40-42^{0}C compared to the nonadecane, which melts at between 32-34^{0}C. The static system also showed a decrease in crystallisation time for the AC field. This may be due to the effects of an electric field with alternating current on the bond angles within the unit cell. The static and dynamic mixed hydrocarbons in heptane also showed an increase in crystallisation times. However these increases are not as pronounced as the nonadecane set of results, this may be due to the action of the solvent on this system. There are two possible reasons as to why the crystallisation rate was retarded. The first is that in the mixed system the dipole charges could affect the angles in the different chains, therefore causing a miss match between the molecules on every occasion. The second is that the mixture forms a solid solution, this would also cause a miss match, as the different components would crystallise at differing rates. The static and dynamic nonadecane and crude oil studies also showed one of the greatest increases in crystallisation times. This may be due to the nonadecane part, being affected by the various applied fields. The crude oil sample studied, was amorphous and therefore had a poor crystalline structure as compared to the nonadecane. The addition of nonadecane to the crude oil may have increased its potential to crystallise in the presence of an applied field.

5.0 INTERPRETATION OF RESULTS

The interpretation results obtained from the experimental studies and described in previous chapters is discussed. To do this it is necessary to refer to studies previously carried out by the Brunel group to show how applied fields affect the behaviour of charged species in fluids. The concepts developed in the previous work are extended here to the effects of applied fields on soft solids (molecular crystals).

5.1 Effects of Applied Fields on Charged Species in Fluids

Magnetic fields can have a profound effect on the behaviour of charged species. The species that can be affected include ion-pairs, free radicals, small particles with high surface charges and the nuclei or pre nuclear clusters of growing crystals and precipitating systems. Although the important effects in terms of the work described in this thesis are associated with small particles, crystal nucleation and precipitation, some examples of the effects on other types of charged species are given here.

The interaction between a charged particle and a magnetic field can be on two types, viz. (a) direct field-charge interactions that affect the entire charged particle and (b) magnetokinetic energy level modification in which the observed effects arise because interactions between the magnetic field and specific energy levels. Magnetokinetic energy level modification is important in free radical reactions and involves the use of weak magnetic fields[103] (strength 10-100G). Work at Brunel has shown that applied fields can increase the rate of destruction of pollutant organic species by free radical oxidation in the presence of an applied field. Direct field charge interactions require somewhat stronger fields (greater than 500G) and depend upon the nature of the charged species and the strength of the applied field. An example also taken from work at Brunel University[103] shows that the rate of polymerisation of acrylonitrile can be increased by magnetic interactions. This is an example of a direct field-charge interaction in which ion pairs in the fluid are affected by a field of about 1000G. In the process the magnetic field weakens the interaction between the positive and negative parts of the ion-pairs by attempting to set them in helical motion in opposite directions. This, in turn, makes the catalyst active species more available, and speeds up the action, as described in the following paragraph. The polymerisation of acrylonitrile to polyacrylonitrile is an

exothermic reaction providing a means of studying the rate of reaction by thermometric titrimetry. Application of a magnetic field results in an increase in the rate of polymerisation as indicated by an increase in heat output. The active catalyst species in the polymerisation is the propan-2-oxide ion (OR^-) which is added to the monomer solution as a solution of potassium hydroxide in propan-2-oxide. A disadvantage of adding the catalyst in this way is that the activity of the propan-2-oxide ion as a catalyst is reduced by the formation of an ion-pair with potassium ions. The magnetic field on acting to prevent the formation of RO....K+ ion pairs thus releases the active catalytic species and favours the polymerisation reaction. [103]

The use of applied magnetic and electric fields on fuels has been shown to alter the combustion properties of the fuels. The results show that there is an increase in flame temperature, a decrease in flame length and a decrease in the amount of soot formed in the applied field situation. Digital photographs of the flames from both gas and liquid combustion in applied magnetic field show that the flames are different from those in a zero field situation. The flames are more brilliant and the flame surface area is decreased with increasing magnetic field strength. The effects of applied magnetic fields on soot particle sizes from the combustion of acetylene, methane paraffin and a mixture of paraffin and benzene have been compared with the zero field situation. Combustion in a magnetic field results in a major reduction in the amount of soot formed with the particles of soot that are formed being smaller with a longer chain length than for the zero field situation. [102]

Magnetic fields have also been shown to affect the vaporisation rates of liquid fuels. As the magnetic field increases in strength the vapourisation rates decreased thus allowing more of the fuel to be utilised by the flame.

5.1.1 Effects of Applied Fields on Crystal Growth, Precipitation and Small Particles.

The work described in this thesis is concerned with their effects on crystallisation on molecular solids. This section deals with known effects on the crystallisation of mainly inorganic solids

Particle size In the case of calcium carbonate scale [103]it has been shown that the particle size of the precipitates obtained from hard water increases when the water is passed through a magnetic field. An increase in particle size in this case can have

two beneficial effects: (1) the large crystals will not adhere together to form scale in the same way as smaller crystals which have higher surface charges, (2) the presence of larger crystals will upset the equilibrium between the fluid and any existing scale because, in general, smaller particles have higher solubility and hence for larger particles local concentration in solution will be lower. The function of the magnetic units is to alter the nature of precipitation of calcium carbonate from solution in such a way that scale formation is prevented. The descaling action, therefore, arises as a consequence of this effect and of the resulting changes in scale/fluid equilibria. The increase in particle size of calcium carbonate precipitates on magnetic treatment has been confirmed by both electron microscopy and laser scattering particle size measurement.

Crystallinity associated with changes in crystal size, in some systems, are changes in the crystallinity of the precipitates obtained. The precipitation of an amino acid, DL valine, for example [103], shows how the magnetic field can alter the crystallinity. In the presence of an applied magnetic field the DL-valine crystals are large and well formed hexagonal platelets while the crystals obtained under the same conditions, but in a zero field are much smaller and less well formed.

Morphology the external faces seen on a crystal are those of the slowest growing faces in the development of the crystal. It is well known that the addition of a chemical can change the growth on one set of crystal planes relative to other planes and hence the morphology (habit) [103]. Any factor that affects the relative rates of growth of crystals on the various planes, could alter the crystal habit. An ability to change the crystal habit can be important in determining the nature of precipitation scale formation and scale prevention. Among the factors that are known to change the morphology of growing crystals under specific circumstances are rate of cooling, nature of solvent, pH, impurities present and degree of supersaturation[103]. There is considerable evidence that the effect of the magnetic field on the growing crystals in magnetically treated fluids also changes the relative growth rates of the possible external faces of the crystals precipitated. Changes in the relative intensities of the two strongest lines in the X-ray diffraction powder pattern for calcium sulphate dihydrate on magnetic treatment are consistent with a change in morphology of the crystals. In the case of anthranilic acid the crystals obtained in the zero field are very large, thin acicular plates, which contrast markedly with the

small well formed, three dimensional rhombic crystals deposited on magnetic treatment.

Crystal Phase when hydrated sodium carbonate is crystallised from aqueous solution the phase obtained depends upon the temperature. Under normal conditions it is necessary to carry out crystalliations at temperatures above 45 degrees to obtain sodium carbonate monohydrate ($Na_2CO_3.H_2O$). At temperatures below 35 degrees the crystals deposited are pure sodium carbonate decahydrate ($Na_2CO_3.10H_2O$). Between 35 and 45 degrees the product is a mixture of monohydrate, decahydrate and heptahydrate ($Na_2CO_3.7H_2O$). When the sodium carbonate is crystallised in a magnetic field, however, the phase obtained at temperatures of less than 35 degrees is the pure monohydrate not the decahydrate. The thermal analytical data confirm that the low temperature product crystallised in a field is the monohydrate and that the material precipitated under the same conditions in zero field is a mixture of the three hydrates.

Solubility there is a considerable amount of evidence from the zinc phosphate experiments carried out both in industry and in the Brunel laboratories to suggest that treatment of fluids containing zinc phosphate leads to an increase in the solubility or the level of supersaturation of the zinc phosphate in the fluid.[104]

From the preceding examples there are three possible explanations as to why magnetic fields can affect ionic substances. The first could be turbulence because the flow of liquid through a magnetic unit is very turbulent. However the same effects are not observed with the dummy units and this shows that the observed effects are due to the applied fields and not simply to turbulence. The second possible explanation of the effects seen could be the Lorentz effect. The Lorentz effect is the combined effects of an applied field, a charged species, the induced magnetic field on the charged species and the rate of flow of the fluid. It is possible to produce energy that could act downstream altering the crystallisation process, but the energy produced in this process for typical crystallisation systems, is very small and would in many cases be dissipated by normal collision processes when the fluid leaves the field. It is possible that such small energies could contribute to the overall process, but they could not fully explain all of the phenomena observed.

5.1.2 Conclusion of Affects on Precipitation and Crystallisation

The third and favoured explanation is that magnetic and other applied fields interact directly with the surface charges of growing nuclei affecting their behaviour. Three components of a simple precipitation solution will be affected by the field: (a) the charged surface of the growth nuclei (b) the anions and (c) the cations. The individual anions and cations may increase their available energy by the Lorentz effect as they pass through the field. This extra energy will only be of value if it is dissipated by collision with a growing crystal, which must be a rare occurrence in comparison with normal inter-ionic collisions and collisions between ions and water molecules. It is therefore at the solid/fluid interface region that explanations of the effects of the magnetic treatment of fluids must be sought. It is also possible that major processes in the direct-field charged species interactions could occur with pre nuclear clusters because they are even smaller and will have even larger surface charges than growing nuclei. All of the data obtained on the effects of applied fields on crystallisation and precipitation reactions are consistent with direct interactions between the applied field and the surface charges on growing crystals and crystal nuclei and pre-nuclear clusters. These direct field charge interactions are significant because they occur at the charged layers at the solid-liquid interface.

Work previously carried out at the university has shown that applied fields can have an effect on dispersions. In the case of aluminium hydroxide [103], differences were noted between applied fields and zero field conditions. Under applied and magnetic field conditions the settling rate of the flocs were increased as compared to a zero field.

From the above descriptions it can be seen:

- That applied magnetic fields can have a profound effect on the behaviour of charged species in fluids.
- The interactions between applied fields and highly charged materials such as fine precipitates crystal nuclei and prenuclear structures do change their subsequent behaviour including their growth and aggregation patterns and
- That the scale prevention results achieved with magnetic devices are part of this general phenomenon- the magnetic treatment of fluids.
- That scale prevention properties of applied fields are not unique to calcium carbonate scale prevention (the most common application)

- The magnetic interactions can alter the crystallisation patterns of any type of crystal and are not restricted to scale forming precipitates and
- That these crystal growth mechanisms, including scale prevention are part of a general field charged species phenomenon. [103]

5. 2 Applied Fields on Organic species

The Brunel group have carried out a number of studies in the effects of applied fields on organic molecules [105].

5.2.1 Dyes and Applied Field Effects

Experiments with methylene blue [104] showed that magnetic fields affect the intensity of the dye. This experiment showed that, as the time of exposure of a magnetic field increased, the intensity of the light absorption of the dye decreased. Further studies on a series of Maxilon dyes, blue, red and yellow, also showed that in the presence of a weak magnetic field the intensity of the visible light absorption of the dye solution decreased with time.

Further investigation showed that the addition of varying salts to differing dye solutions could also alter the absorption intensity of the dyes.

In the case of methylene blue when aliquots at 10%(w/v) of KCl were added the intensity of the colour decreases because of increased dye $-Cl^-$ interaction. But this trend is reversed in the presence of an applied field. [104]

5.2.2 Cocoa Butter and Palm Oil

Studies performed on the solidification of cocoa butter have shown that applied fields can affect the onset of solidification. The time taken for the material to begin solidification is delayed in an applied field[105].

As cocoa butter cools from the melt it undergoes phase changes. There are six phase transitions possible for cocoa butter fat. Theoretically, in the absence of any external affects, phase type 1 is the final product at room temperature. In the chocolate industry the desired phase is the Type V polymorph. The affect of the applied field on the crystallisation is a decrease in time required to achieve the maximum torque during temping. The use of a DC electromagnetic field produced both Type V and type VI phases. In experiments where a constant field was applied the product precipitated was a 100% of type VI. It has been found that cocoa butter

solidifies in six different polymorphic forms, under differing conditions. Studies on tripalmaltin and oleopalmatin in magnetic and other applied field conditions imply that the crystallisation of palm oil is altered by the fields. These changes can be determined due to the alterations in the solid fat content and plasticity of the palm oil. This can be seen because and increase in the free fatty acids and the diglyceride content decreases the solid fat content, i.e. the part containing the crystals. There is also an increase in the plasticity of the palm oil. [105]

5.2.3 Sugar

The effects of applied fields on sucrose crystallisation were studied by the Brunel group [105]. It has been shown that the applied field affects the crystallisation process of sucrose in both static and dynamic conditions across a varying grades of sucrose. Specifically the changes that occurred in the sucrose growing in an applied field were:

- Changes in the particle size, the crystals in the treated material were larger
- Changes in the crystallinity, the crystals in the treated material were much more regular and distinct microcrystallites were formed.
- Changes in morphology, the crystal shape under high magnification was shown to be altered.
- Changes in phase, under applied field conditions a hydrated sucrose is crystallised out from the solution.
- Changes in levels of supersaturation, hydrated crystals were precipitated from a lower supersaturated solution.

The sucrose studies showed that there were more pronounced field effects in the presence of a DC electromagnetic field as compared to the pulsed, permanent and AC electromagnetic field. The results showed that the magnetic field effects are dominant and superimposed on any effects resulting from impurities or residence time but that low residence times could reduce the overall effect of the field. It was also shown that the purer the sucrose grade and the longer the residence time in the field, the more pronounced were the effects on the crystallisation process.

The crystallisation of sucrose in magnetic field is dependent upon:

- The type of applied field
- The purity of the sucrose solution
- The residence time of the solution in the applied field [105]

5.3 Molecular Solids

The purpose of the work described in this thesis is to determine whether the effects of magnetic fields at the solid solution interface also apply to molecular solids. Molecular solids consist of molecules held together by weak intermolecular forces. These molecules differ from other solids, in that they are comprised of discrete molecules unlike ionic solids, which are held together by strong long range columbic forces, a molecular solid is held together by intermolecular forces, which are weaker and short range in their effect. The structure of a molecular crystal can be affected by these intramolecular forces as they have an influence on molecular shape. Molecular solids are more complicated than ionic solids because they are made up of repeating segments of polymer chains, often with several segments in a unit cell.

The work contained in this thesis, is concerned with the effect of applied and magnetic fields on weak electrostatic forces.

Weak electrostatic forces consist of:

- Ion-dipole
- Hydrogen Bonding
- Ion- induced dipole
- Dipole- Dipole
- Dipole induced- dipole
- Van der Waals forces

Ion-dipole – is the attraction between an ion i.e. Na^+ and a dipole (e.g. H_2O). A permanent dipole moment exists in a molecule that has charges distributed in an unsymmetrical manner, such as H_2O. Ion-dipole forces exist between an ion and partial charge on a polar molecule. Therefore when an ionic substance dissolves in a polar solvent (that is, a solvent whose molecules have a permanent dipole moment) the majority of the solvent molecules orient themselves with the oppositely charged end of the solvent molecule near an ion. This attraction between the ions and the solvent molecules can win out over the attraction of the ions to each other, allowing the substance to stay in solution. Therefore the ion-dipole increases, as the charge on the ion or dipole in the molecule increases. Ion - dipole forces are responsible for the dissolution of ionic substances in water.

Hydrogen Bonding- Hydrogen bonding is a unique type of intermolecular attraction. There are two requirements:

- The first is that there is a covalent bond between an H atom and either F, O, or N.

- The second is that there is an interaction of the H atom in this kind of polar bond with a lone pair of electrons on a nearby atom of F, O, or N

Hydrogen bonds form only between a limited number of elements bonded in a specific sequence. If -A-H is part of one molecule and B- is part of a second molecule (or another portion of the first molecule), a hydrogen bond will form only if A and B are small, electronegative atoms i.e.(N, O or F). The hydrogen bond involves the lone pairs on atom B.

If a hydrogen bond can form between a pair of molecules it will be stronger than other intermolecular forces between the molecules. Hydrogen bonding is responsible for the unexpectedly high boiling point of water, the lower density of ice compared to liquid water. The normal boiling point for water is 100 degrees Celsius the observed boiling point is high compared to the expected value. The predicted boiling point from the trend of boiling points for H_2Te, H_2Se, H_2S and H_2O is very low. If the trend continued the predicted boiling point would be below -62 °C. The "anomalous" boiling point for water is the result of hydrogen bonding between water molecules.

Ion-Induced dipole- occurs when a charge near a molecule causes the electron distribution of the molecule to become distorted from its original distribution. The molecule may or may not have a permanent dipole moment. Molecules such as O_2 or benzene do not have a permanent dipole moment and a charge can come near and induce an unsymmetrical charge distribution with a resulting instantaneous dipole moment. Once the instantaneous dipole moment is induced, there can then be an ion-induced dipole interaction. The process of inducing a dipole is called polarization and different atoms and molecules have different polarizabilities (ability to be polarized)

Dipole-Dipole- interactions exist between molecules that are polar. If two neutral molecules, each having a permanent dipole moment, come together such that their oppositely charged ends align, they will be attracted to each other. In a liquid or solid these alignments are favoured over those where like-charged ends of the molecules are close together and hence repel each other. One reason why CH_3F has a higher boiling point (-84 °C) than CF_4 (-128 °C) is that CF_3H has a permanent dipole moment, while CF_4 does not. The forces become weaker with increasing

distance, conversely the force increases with increasing size and molar mass. The dipole-dipole force is 1% as strong as covalent and ionic bonds. Therefore compared to a covalent bond this intermolecular force is weak. However the dipole-dipole interaction is one of the stronger intermolecular attractions.

Dipole induced dipole-. Is where the dipole rather than a charge induces the instantaneous dipole moment. An example is the attraction that is known to exist between O_2 and water. Oxygen is slightly soluble in water, and for that solubility to exist there must be an attraction between water and oxygen. Oxygen is a symmetrical molecule so it does not have a permanent dipole moment. However, the water dipole can cause the charges on oxygen to become unsymmetrical with a resulting instantaneous dipole moment.

Van der Waals Forces- Dispersion forces or London forces, arise from the temporary variations in electron density around atoms and molecules and are the weakest of all intermolecular forces. These forces form an instantaneous dipole and can exist between all molecules. Non-polar molecules have a certain minimum symmetry to their average shape and electron distribution. These forces result from temporary charge imbalances. The temporary charges exist because the electrons in a molecule or ion move randomly in the structure. The nucleus of one atom attracts electrons from the neighbouring atom. At the same time, the electrons in one particle repel the electrons in the neighbour and create a short-lived charge imbalance. These temporary charges in one molecule or atom attract opposite charges in nearby molecules or atoms. A local slight positive charge δ^+ in one molecule will be attracted to a temporary slight δ^-negative charge in a neighbouring molecule. The temporary separations of charge that lead to the London force attractions are what attract one non-polar organic molecule to its neighbours. The possibilities for these interactions go up with increasing molecular size and surface. The larger surface area increases the chances for the "induced" charge separations. If the molecules are linear they have more surface area than if they are folded into a sphere. The linear molecules have higher melting and boiling points because of the increased attraction.

The work carried out so far on crystallisation has been concerned with ionic forces and molecular forces, including Hydrogen bonding, ion-dipole, ion-induced dipole, dipole-induced dipole and dipole-dipole interactions. This is due to the stronger attractive forces present in these systems.

5.3.1 Affect of Field Affects on Van der Waals Forces

In a molecular crystal the secondary forces are weak electrostatic forces such as Hydrogen bonding, Dipole-Dipole, dipole-induced-dipole, ion-dipole, dispersion forces and Van der Waals forces. Molecules which have orientations which maximise the dipole-dipole or dipole-induced-dipole interactions can lead to the formation of chains of molecules with strong attractions between opposite ends of the molecules. The chains pack efficiently into layers with the molecular dipoles all in the same direction in a given layer and in opposite directions in successive layers Hydrogen bonds are formed between hydrogen atoms and for example the oxygen atoms of one alcohol molecule and the hydroxy hydrogen atom of another molecule. Hydrogen bonds are longer and weaker than covalent bonds. Hydrogen-bonded molecular crystals frequently have rather open structures, which optimise the dipolar hydrogen bonding interactions [107].

Work that been performed to date on soft solids has shown that they possess molecular crystals with strong covalent intermolecular bonding are held together in solids by weak electrostatic interactions, including Van der Waals forces and hydrogen bonding. Studies carried out show that magnetic and other applied fields can alter the behaviours of molecular solids held together by the relatively strong forces arising from hydrogen bonding. [106-108]

All of the work on molecular solids described by the Brunel group in earlier work has been concerned with relatively strong intermolecular forces made up of ion-dipole attractions and hydrogen-bonding. The purpose of the work described in this thesis is to determine whether magnetic fields can have an effect on the bonding of molecular solids even when the force holding the molecules in the solid are the weakest possible i.e. Van der Waals forces.

5.4 Hydrocarbon Studies: Nonadecane

Nonadecane is a hydrocarbon held together in the solid only by Van der Waals Forces. From the nonadecane studies described in this work it can be seen that an applied field or magnetic field can affect crystallisation times and in general the time taken for the onset crystallisation is delayed by applied magnetic fields compared to that for a zero field.

Nonadecane has a rhombic structure made up of nonadecane chains.

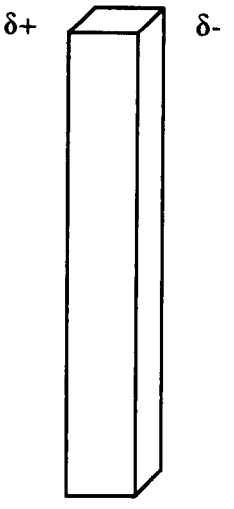

Figure 5.1. Nonadecane: The unit cell rhombic structure comprised of nonadecane chains

The chains are alkanes consisting of nineteen carbons. An alkane has

- No ions
- No dipoles
- No Hydrogen bonding

This means that any effects on crystallisation caused by magnetic applied fields must be interactions with the Van der Waals forces that hold the solid material in a lattice as it is growing.

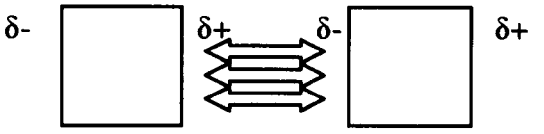

Figure 5.2 The interaction of Van der Waals forces with the nonadecane molecules

Since the effects of applied fields must be due to direct applied field – charged system interactions, the importance of the observations made in this work is that effects can be seen in crystallisation from a molten alkane system even when the charges at the solid – melt interface are very small charges that would arise from dipole-induced – dipole-induced interactions.

5.4.1 Nonadecane and Heptane Studies

The effects of the solvent heptane on the crystallisation of nonadecane were also studied to determine whether there was a difference between the applied-field – charged surface interactions at the surface of the growing crystal between a nonadecane melt nonadecane growing from a hydrocarbon solvent system. Significant differences in the time to crystallise nonadecane were found for a number of static and dynamic solution systems with a different types of applied field showing that applied fields can interact with the surface charges of growing nonadecane crystals at the solid – heptane solvent interface. The interaction could effect, either or both of the following factors:

The interactions between neighbouring molecules forming the lattice

The level of supersaturation of the nonadecane in heptane

Both of these effects have been observed in the crystallisation of ionic solids and non-alkane organic molecules.

5.4.2 Mixed Solid Systems

Work carried out with mixed alkane systems, especially in the presence of a solvent, confirmed that the effects seen for nonadecane alone can also be seen in mixed systems.

5.4.3 Crude Oil and Nonadecane

The results of this work are of commercial importance in petroleum recovery where the deposition of waxes from the crude oil can lead to blockage of delivery pipework. In studies of the crystallisation of nonadecane from crude oil in this work, it was found that applied field effects did lead to significant increases in the time to crystallise out nonadecane. These results are consistent with the use of magnetic field devices in the field to prevent wax deposition.

5.5. Conclusion

Applied magnetic and other fields are known to affect the behaviour of charged particles in fluids including the charged surfaces on crystal nuclei and growing crystals. Previous work has demonstrated that these charged surfaces can arise from the strong electrostatic forces in the crystallisation of ionic solids and the weaker electrostatic interactions in molecular crystals arising from the presence of permanent dipoles and hydrogen bonding. The importance of the work described in this thesis is that is that it has now been shown that applied fields can alter the crystallisation behaviour of molecular solids even if the surface charges involved arise only from Van der Waals dipole-induced – dipole-induced interactions.

REFERENCES

102. J. Donaldson et al, *Paper to be submitted*, 2000

103. J. Donaldson, *Waterline*, 1995 75-84

104. M. Wei, *Final Report*, 1987

105. M. Miller, *Ph.D. Thesis*, Brunel University London, 2000

106. R. Haines, *www.chem..unsw.edu.au*, 2002

107. L. Combs, *erkki-kerresaw.edu*, 2002

108. Anon, *www.scvs.nevada.edu*, 2002